



Miljø- og
Fødevareministeriet
Miljøstyrelsen

Udvikling af bedre og mere energieffektive renseanlæg med næringsstoffs fjernelse

MUDP-rapport

Juni 2018

Udgiver: Miljøstyrelsen

Redaktion: Gertsen & Olufsen A/S

ISBN: 978-87-93710-47-4

Miljøstyrelsen offentliggør rapporter og indlæg vedrørende forsknings- og udviklingsprojekter inden for miljøsektoren, som er finansieret af Miljøstyrelsen. Det skal bemærkes, at en sådan offentliggørelse ikke nødvendigvis betyder, at det pågældende indlæg giver udtryk for Miljøstyrelsens synspunkter. Offentliggørelsen betyder imidlertid, at Miljøstyrelsen finder, at indholdet udgør et væsentligt indlæg i debatten omkring den danske miljøpolitik.

Må citeres med kildeangivelse

Indhold

1.	Projektets formål	4
1.1	Projektets tidsplan	4
1.2	Projektets organisation	4
1.3	Projektets hovedaktiviteter og tidsplan	5
2.	Fase 1. Analyse af projektet	5
3.	Fase 2. Fastlæggelse af koncept	5
3.1	Det eksisterende renseanlæg, biologisk fixfilmanlæg	5
3.2	Det nye renseanlæg, biologisk MBR anlæg med mulighed for næringssaltsfjernelse	6
4.	Fase 3: Produktion	6
4.1.1	I perioden 15/8-15 til 1/9-15 blev følgende væsentlige test udført:	7
4.1.2	I perioden fra den 1/9-15 til 1/11-15 blev følgende væsentlige test udført:	8
4.1.3	I perioden fra 1/11-15 til 1/5-16 blev følgende væsentlige test udført:	9
5.	Fase 4. Test og certificering	11
5.1	Test af El-skab, Udført af DELTA, en del af Force Institute.	11
5.1.1	Konklusion af DELTA test	14
5.2	Test af konstruktionens styrke, udført af SDA-engineering GmbH	14
5.2.1	Konklusion af chok-test	14
5.2.2	Konklusion af tiltningstest	15
5.3	Test af funktionalitet, PIA, Prüfinstitut für Abwassertechnik GmbH	15
5.3.1	Fase 2: Test for certificering af anlæg for kulstoffjernelse	16
5.3.2	Fase 3: Test for certificering af anlæg for kulstof, kvælstof og fosforfjernelse	16
5.3.3	Konklusion af funktionalitetstest	17
6.	Officiel modtagelse af certifikater	18
Bilag 1		19
Bilag 2		20

1. Projektets formål

Formålet med projektet er at undersøge markedet for avanceret spildevandsrensning off-shore og bringe ny teknologi ind i det nuværende Gertsen og Olufsen produkt til off-shore spildevandsrensning, for derigennem at kunne opfylde de skærpede krav til spildevandsrensning, som træder i kraft fra 2016. De nye krav vil, foruden de eksisterende krav til organiskstof og mikroorganismer, også stille krav til næringssaltsfjernelse.

1.1 Projektets tidsplan

Projektet blev påbegyndt den 1. april 2014. I forbindelse med projektafviklingen har der været et stort tidsforbrug til såvel produktion fasen som test- og certificeringsfasen.

Det ekstra tidsforbrug til produktion fasen er forankret i, at det blev fundet nødvendig at teste et præliminært anlægsdesign over en længere periode, for at sikre robustheden i det nye procesdesign.

Det ekstra tidsforbrug til test og certificering, er dels forankret i den præliminære testperiode, og dels forankret i at certificeringskravene til såvel IMO som USCG krævede uforudsete tidskrævende specialtest.

1.2 Projektets organisation

Projektet er afviklet med følgende organisation.

Gertsen og Olufsen A/S har dannet en projektgruppe bestående af følgende nøglepersoner:

Teknisk ansvarlig	CTO Klaus Vium Andersen *)	kva@g-o.dk
Proces og projektledelse	Civ.ing. Niels Henrik Johansen *)	
Salgs Direktør	Thomas Højbo Hansen	thh@g-o.dk
Projekt ing.	Bjørn Ørum Ryhding	bjr@g-o.dk
Projekt ing.	Christian Glud	chg@g-o.dk
Test & certificering	CTO Ronni Palmqvist	rp@g-o.dk

Gertsen og Olufsen A/S er i projektperioden blevet sammenlagt med Pres-Vac, Heco og Atlas incinerators A/S, og er nu en del af G&O Maritime Group. Dette har medført, at der gennem projektperioden har været udskiftning af CEO posten, hvorfor tidligere CEO Jakob Kjelstrup i dag er erstattet med CEO John Åge Lazar, som øverst ansvarlig for projektet.

Kontaktperson fra NST er:

Specialkonsulent Jóannes J. Gaard *) jojga@nst.dk

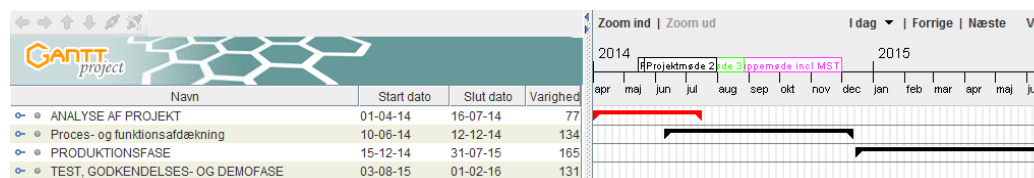
Navne mærket med *) = Projektets følgegruppe.

Der har været afholdt 2 møder i følgegruppen:

- 17/07-2014: Gennemgang af "Statusrapport 17/07-2014"
- 23/09-2015: Præsentation af funktionalitet for nyt design af renseanlæg.

1.3 Projektets hovedaktiviteter og tidsplan

Projektet er opdelt i 4 hovedaktiviteter med nedenstående tidsplan.



Figur 1. Overordnet tidsplan for de 4 faser.

Fase 1 og 2 er blevet aflagt i tidligere fremsendt rapport "Statusrapport 1. halvår – 2014".

Fase 3 og fase 4 er begge blevet forlænget med 6 måneder, jf afsnit 1.1.

Nærværende rapport indeholder en opsummering af ovennævnte rapport som en aflagting af den resterende del af projektet.

2. Fase 1. Analyse af projektet

Der er udført en analyse af G&O's eksisterende renseanlæg, hvor de enkelte enhedsprocesser er gennemregnet med det formål at identificere såvel procesekniske, maskintekniske og driftstekniske forhold for derigennem at afdække styrker og svagheder.

Dette skal sikre, at allerede eksisterende samt forudsigelige problemstillinger bliver adresseret i selve designfasen af det nye renseanlæg.

3. Fase 2. Fastlæggelse af koncept

3.1 Det eksisterende renseanlæg, biologisk fixfilmanlæg

Det eksisterende renseanlæg er et biologisk fixfilm anlæg designet for fjernelse af organisk-stof. Anlægget er udstyret med et UV-anlæg for inaktivering af mikroorganismer inden udledning til recipient.

3.2 Det nye renseanlæg, biologisk MBR anlæg med mulighed for næringssaltsfjernelse

Det nye renseanlæg er en kombination en ren MBR proces, med kombineret ANOX & buffer tank.

Det valgte anlægsdesign medførte at der i samarbejde med udvalgte leverandører skulle udarbejdes nye systemløsninger.

Der er udført en præliminær konkurrentanalyse, hvor lignende produkter, med henblik på identifikation af teknologivalg, dimensionering og prisforhold.

4. Fase 3: Produktion

Projektgruppen har valgt at bygge et præliminært testanlæg, "Testanlæg-DK", hvor den nye teknologi kunne afprøves over længere tid, for at sikre robusthed i en kommende procesteknisk løsning, samt afprøve og justere nyudviklet teknologier og nye komponenter.

Anlægget var opstillet på Usserød Renseanlæg, og belastet med råspildevand fra den nærliggende tilløbspumpestation.



Figur 2. Præliminært testanlæg, Testanlæg-DK opstillet på Usserød Rensemønsteranlæg

"Testanlæg-DK" blev opstillet medio august 2015.

4.1.1 I perioden 15/8-15 til 1/9-15 blev følgende væsentlige test udført:

- Test af styring og regulering.
 - o Auto niveaustyring
 - o Auto flowstyring
- Test af nyudviklet enkelt komponenter.
 - o Stress test MBR-filter
 - o Test af macerator
- Test at omrøringseffektivitet
- Test af DeOx anordning mellem OX-tank og AN-tank



Figur 3. Undersøgelse af MBR filter efter stresstest. T.h. ses DeOx anordning.



Figur 4. Test af styring og regulering



Figur 5. Test af maceratorpumpe. Opstillet filter undersøger at partikkelstørrelse er < 2 mm.

4.1.2 I perioden fra den 1/9-15 til 1/11-15 blev følgende væsentlige test udført:

- Test af omrører
- Test af permeat-pumpe system
- Test af backflush system
- Test af COD reduktion effektivitet
- Test af nitrifikations effektivitet
- Test af denitrifikations effektivitet
- Præliminær test af fosforfjernelse



Figur 5. Præliminær test af fosforfjernelse. (PAX)

Enhed	Tilløb	Afløb	Rensegrad	Krav
COD	mg/l	550	30-40	< 125
N-tot	mg/l	70	5-15	< 20/70%
NH4-N	mg/l	50	0,1-0,5	
NO3-N	mg/l	0	5-15	
P-tot	mg/l	8,0	1,0	< 1,0/80%
pH		7,5	7,5	
e-Coli	pr 100 ml		1	<100

Figur 7. Foreløbige testresultater, frem-lagt på følgegruppemøde den 23/9-2015



Figur 8. Test og optimering af permeat-pumpe

4.1.3 I perioden fra 1/11-15 til 1/5-16 blev følgende væsentlige test udført:

- Test af recirkulationsgrad
- Optimering af beluftning
- Optimering af volumenudnyttelse
 - o Stresstest af belastning
- Stresstest af vakuum pumpe til MBR-filter
- Test af fosforgjernelses effektivitet



Figur 9. Stresstest af belastning.



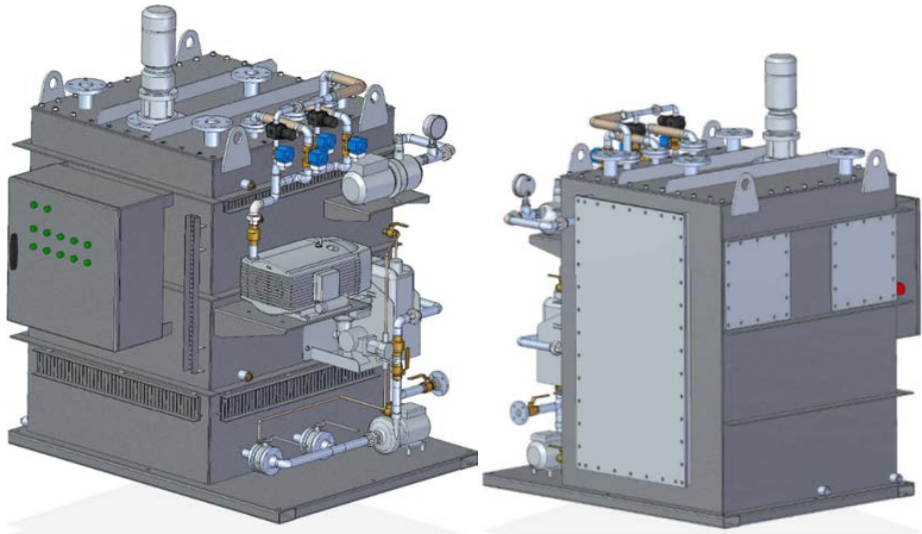
Figur 10. Optimering af beluftning



Figur 11. Test af forsforfjernel-seseffektivitet (PIX-113)

Afprøvninger og test på det præliminære testanlæg-DK blev afsluttet i juni 2016.

Det har i forbindelse med udviklingen af det nye renseanlæg, været en uvurderlig hjælp, at såvel ny teknologi, som designgrundlag har kunne afprøves og optimeres på "Testanlæg-DK", inden det endelige design blev fastlåst og sendt til produktion. Dette har betydet, at det endelige testanlæg, "Testanlæg-PIA" som certificeringen er udført på, er blevet optimeret, både hvad angår funktionalitet og økonomi.



Figur 12. Det endelige design, som blev sendt til PIA, (Prüfinstitut für Abwassertechnik GmbH) for test til certificering.

Produktion af "Testanlæg-PIA", det anlæg der blev testes hos PIA, Prüfinstitut für Abwassertechnik GmbH, blev udført i november til december 2015. Den elektriske tavle, ankom primo januar 2016, medens selve renseanlægget ankom primo marts 2016.



Figur 13. Teatanlæg-PIA, klar til fremsendelse.



Figur 14. El-tavle sendt til certificering hos DELTA

5. Fase 4. Test og certificering

5.1 Test af El-skab, Udført af DELTA, en del af Force Institute.

Elskabet er testet i hht USCG 33 CFR, m.v.; IMO resolution MEPC 227/(64) og IMO resolution MEPC 107/(49) hvor der er udført følgende test:

Lav temperatur test: Udført ved 0°C i 16 timer

Tør varme test: Udført ved 60°C i 16 timer, Luftfugtighed < 50% RH

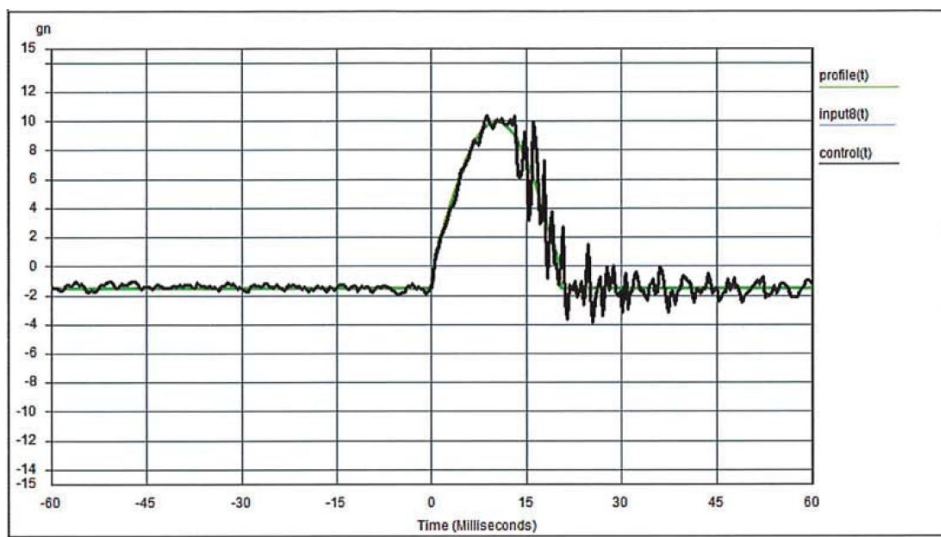
Fugtighedstest: 2 cyklusser bestående af 25°C ved 95-100% RH i 12 timer,
efterfulgt af 55°C ved 90-96% RH i 12 timer.



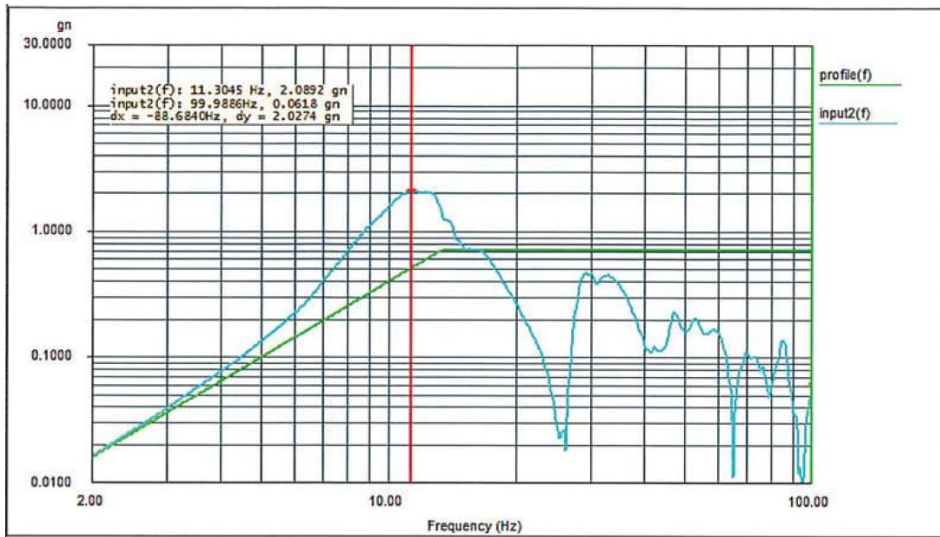
Figur 15. Opstilling for temperatur og fugtighedstest.



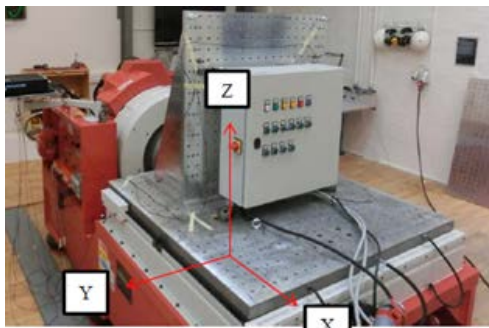
Figur 16. Opstilling for choktest.



Figur 17. Kurve fra choktest. 1000 chok i 20 ms med en G-påvirkning på 10 i vertikal retning



Figur 18. Viborationstest af strømforsyning.



Figur 19. Opstilling for viborationstest

5.1.1 Konklusion af DELTA test

Konklusionen af de udførte 5 test er aflagt i bilag 1, afsnit 4.1 hvorfra det fremgår at alle test er bestået.

Test	Test object
Low temperature test	OK
Dry heat test	OK
Humidity test	OK
Shock test	OK
Vibration test	OK

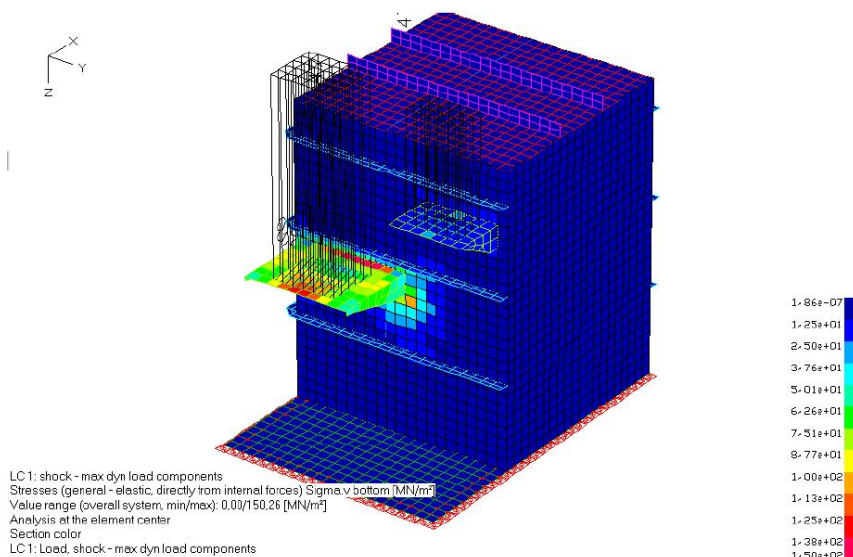
Figur 20. Uddrag fra test

5.2 Test af konstruktionens styrke, udført af SDA-engineering GmbH

Denne test undersøger og kontrol testanlæg-PIA, vedrørende chok-test og rulle-test på et numerisk/analytisk grundlag som alternativ til den eksperimentelle testprocedure på 33 CFR §159.105 og §159.107.

5.2.1 Konklusion af chok-test

Det blev bevist, at de resulterende spændinger på grund af chok lastning er mindre end de tilladte spændinger (se afsnit 3.3.2). Det blev endvidere bekræftet, at forekommende belastninger på de påsvejsede hylderne sikkert overføres til beholderen, forudsat at hylderne er svejset til skallen med en kontinuerlig svejsning på mindst 3 mm på begge sider af hylderne (se bilag 2, afsnit 0).



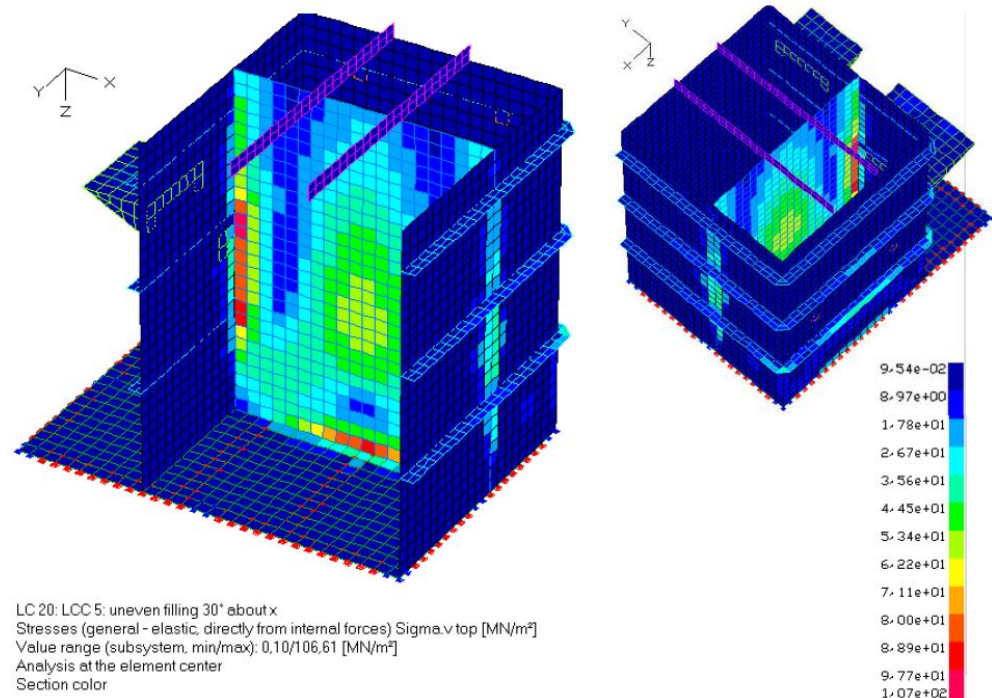
Figur 6. Chok-test af hylde.

5.2.2 Konklusion af tiltingstest

Der blev udført 5 belastnings senarer; 30° og 0° tiltning i x-aksen, 30° og 0° tiltning i y-aksen samt ujævn fyldning (den en tank tom) ved 30° tiltning i x-aksen.

Det blev bevist, at spændinger som følge af tiltning er mindre end den tilladte belastninger (se bilag 2, afsnit 4.5.2). Den maksimale belastning af forankringen af enheden blev bestemt for alle lasttilfælde og skal sikkert overføres til jorden/skib ved tilstrækkeligt dimensioneret og stramt fastgjorte skruer.

Udover kravene i CFR 33 §59.107 blev sikkerheden mod foldning bevist af lineære buckling analyser (se bilag 2, afsnit 4.5.4).



Figur 22. Tiltning ved 30° - kun én tank

5.3 Test af funktionalitet, PIA, Prüfinstitut für Abwassertechnik GmbH

Test hos PIA, Prüfinstitut für Abwassertechnik GmbH, var opdelt i 3 faser:

Fase 1: Indkøring, oparbejdelse af biokultur.

- 31/5-16 til 31/7-16

Fase 2: Test for certificering af anlæg for kulstoffs fjernelse

- 1/8-16 til den 11/8-16: "Funktionalitetstest bestået"

Fase 3: Test for certificering af anlæg for Kulstof, kvælstof og fosforfjernelse.

- 8/9-16 til den 17/9-16: "Funktionalitetstest bestået"

5.3.1 Fase 2: Test for certificering af anlæg for kulstoffjernelse

For at opfylde funktionalitetstesten iht MECP 227 og USCG, skal "Testanlæg-PIA" overholde de betingede randbetegnelser i 10 døgn i træk, hvoraf anlægget i ét af døgnene skal være tiltet til en vinkel på mindst 22,5°.

Design hydraulisk belastning:	3,3 m ³ /d
Design organisk belastning:	2,21 kgBOD/d
Anvendt reaktorvolumen:	1,14 m ³

Testen blev afviklet med en slambelastning på mellem 8-10 kg/m³.

Resultatet af testen var yderst tilfredsstillende, og viser at det valgte procesdesign, kan opfylde såvel krav til organiskstoffjernelse som krav til reduktion af coliforme bakterier. Samtidig viser resultaterne at der yderligere kapacitet, som dermed giver anlægget en robusthed for variationer i belastningen.

5.3.2 Fase 3: Test for certificering af anlæg for kulstof, kvælstof og fosforfjernelse

For at opfylde funktionalitetstesten iht MECP 227, skal testanlægget overholde de betingede randbetegnelser i 10 døgn i træk, hvoraf anlægget i ét af døgnene skal være tiltet til en vinkel på mindst 22,5°.

Design hydraulisk belastning:	2,2 m ³ /d
Design organisk belastning:	1,05 kgBOD/d
Anvendt reaktorvolumen:	1,14 m ³

Testen blev afviklet med en slambelastning på mellem 10-12 kg/m³.

Resultatet af testen var yderst tilfredsstillende, og viser at det valgte procesdesign, kan opfylde såvel krav til organiskstof, kvælstof og fosforfjernelse, samt krav til reduktion af coliforme bakterier. Samtidig viser resultaterne at der yderligere kapacitet, som dermed giver anlægget en robusthed for variationer i belastningen.



Figur 7. Testanlæg-PIA opstillet hos PIA. Tiltet

5.3.3 Konklusion af funktionalitetstest

Iht. de udførte test konkluderer PIA at testanlægget fra Gertsen & Olufsen opfylder krav for test af renseanlæg iht til "International Maritime Organization resolution MECP.227(64) to meet the operational requirements referred in regulations 9.1.1 of MARPOL Annex IV of the international Convention for the Prevention of Pollution from Ships, 1973, as modified by the 1978 and 1997 protocols."

6. Officiel modtagelse af certifikater

Gertsen og Olufsen har fremsendt ansøgning til DNV-GL om MED og IMO flagstatsgodkendelse, og forventer at modtage disse certifikater om 2-4 måneder.

Bilag 1

EC-TYPE EXAMINATION CERTIFICATE (MODULE B)

Application of: Directive 2014/90/EU of 23 July 2014 on marine equipment (MED), issued as "Forskrift om Skipsutstyr" by the Norwegian Maritime Authority. This Certificate is issued by DNV GL AS under the authority of the Government of the Kingdom of Norway.

This is to certify:

That the Sewage systems

with type designation(s)

**NX10-C/N, NX20-C/N, NX25-C/N, NX30-C/N, NX35-C/N, NX40-C/N, NX45-C/N, NX50-C/N,
NX55-C/N, NX60-C/N, NX65-C/N, NX70-C/N, NX75-C/N, NX80-C/N, NX90-C/N**

Issued to

Gertsen & Olufsen AS

Allerød, Denmark

is found to comply with the requirements in the following Regulations/Standards:

Regulation **(EU) 2015/559**,

NX-C:

Annex A.1, item No. A.1/2.6 and Annex B, Module B in the Directive. Marpol 73/78 as amended, Annex IV Regulation 9, IMO Res. MEPC.227(64) with the exception of Section 4.2.

NX-N:

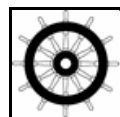
Annex A.1, item No. A.1/2.6 and Annex B, Module B in the Directive. Marpol 73/78 as amended, Annex IV Regulation 9, IMO Res. MEPC.227(64)

Further details of the equipment and conditions for certification are given overleaf.

This Certificate is valid until **2022-03-06**.

Issued at **Høvik** on **2017-03-07**

DNV GL local station:
Copenhagen



for **DNV GL AS**

Approval Engineer:
Pål Evang Nundal

Notified Body
No.: **0575**

Vidar Dolonen
Head of Notified Body

The mark of conformity may only be affixed to the above type approved equipment and a Manufacturer's Declaration of Conformity issued when the production-surveillance module (D, E or F) of Annex B of the MED is fully complied with and controlled by a written inspection agreement with a Notified Body. The product liability rests with the manufacturer or his representative in accordance with Directive 2014/90/EU.

This certificate is valid for equipment, which is conform to the approved type. The manufacturer shall inform DNV GL AS of any changes to the approved equipment. This certificate remains valid unless suspended, withdrawn, recalled or cancelled. Should the specified regulations or standards be amended during the validity of this certificate, the product is to be re-approved before being placed on board a vessel to which the amended regulations or standards apply.



Product description

The equipment is intended for installation onboard ships to provide sewage treatment for the protection of the marine environment.

The sewage treatment plant is a membrane bioreactor (MBR) type, which combines biological treatment with membrane filtration.

The sewage treatment plant can be delivered with two different configurations.

- **NX-C:** According to MEPC.227(64) excluding section 4.2.
- **NX-N:** According to MEPC.227(64) including section 4.2.

Application/Limitation

Model	NX-C		NX-N				
	Design Hydraulic load (m ³ /day)	Organic load (BOD kg/day)	Model	Design Hydraulic load (m ³ /day)	Organic load (BOD kg/day)	Max. Nitrogen (kg TOT- N/day)	Max. Phosphorus (kg TOT- P/day)
NX10-C	1,7	0,6	NX10-N	-	-	-	-
NX20-C	3,3	1,17	NX20-N	1,16	0,56	0,11	0,02
NX25-C	6,6	2,34	NX25-N	2,54	1,22	0,24	0,04
NX30-C	9,9	3,51	NX30-N	3,9	1,87	0,37	0,05
NX35-C	13,2	4,69	NX35-N	5,08	2,44	0,49	0,07
NX40-C	16,5	5,86	NX40-N	6,45	3,09	0,62	0,09
NX45-C	19,8	7,03	NX45-N	7,6	3,64	0,73	0,11
NX50-C	26,4	9,37	NX50-N	10,12	4,85	0,97	0,14
NX55-C	39,6	14,06	NX55-N	15,2	7,29	1,46	0,21
NX60-C	52,8	18,74	NX60-N	20,06	9,62	1,92	0,28
NX65-C	79,2	28,12	NX65-N	30,18	14,47	2,89	0,42
NX70-C	118,8	42,17	NX70-N	45,17	21,66	4,33	0,63
NX75-C	264	93,72	NX75-N	100,26	48,07	9,61	1,39
NX80-C	495	175,73	NX80-N	187,89	90,09	18,02	2,61
NX90-C	990	351,45	NX90-N	375,75	180,17	36,03	5,22

The Administration confirms that the sewage treatment plant can operate at angles of inclination of 30° in any plane from the normal operating position.

Control system:

The environmental test was performed on the components below:

Gertsen & Olufsen control cabinet: TFCTEH

Mitsubishi inverter HW type: FR-D740-SC

Mitsubishi PLC HW Type: FX3G

If other components are used they shall carry a certificate of successful environmental testing according to part 3 of MEPC.107(49), performed at an accredited lab.

Type Examination documentation

Drawing No.:	Date:	Revision:	Title:
1502-135-5	23.02.2017	5	P&ID without N&P (NX-C)
1502-135-5	23.02.2017	5	P&ID Full (NX-P)
191-1502-GA-01	29.05.2016	-	General arrangement drawing
x,y,z, Size-00	23.02.2017	0	Size overview
1502-Equipment-00	23.02.2017	0	Equipment location
1910134	15.02.2016	0	Nameplate
NX10	23.02.2017	0	Proces volume
NX20	23.02.2017	0	Proces volume
NX25	23.02.2017	0	Proces volume
NX30	23.02.2017	0	Proces volume
NX35	23.02.2017	0	Proces volume
NX40	23.02.2017	0	Proces volume
NX45	23.02.2017	0	Proces volume
NX50	23.02.2017	0	Proces volume
NX55	23.02.2017	0	Proces volume
NX60	23.02.2017	0	Proces volume
NX65	23.02.2017	0	Proces volume
NX70	23.02.2017	0	Proces volume
NX75	23.02.2017	0	Proces volume
NX80	23.02.2017	0	Proces volume
NX90	23.02.2017	0	Proces volume
0000E201	01.03.2017	1	NX test plant (electrical drawings)

Instruction manual NX-C:

Operation & Maintenance Manual for Gertsen & Olufsen AS Sewage Treatment Plant NX series - Carbon Reduction

Instruction manual NX-N:

Operation & Maintenance Manual for Gertsen & Olufsen AS Sewage Treatment Plant NX series - Carbon and nutrient reduction

Tests carried out

Performance test of type NX-C, according to MEPC.227(64) excluding section. 4.2:

Prüfinstitut für Abwassertechnik GmbH (PIA), *Test of a Marine Sanitation Device of Gertsen & Olufsen*, Report No.: PIA2016-AT1602-10121-03 – Version 3, Dated 2016-12-20.

Performance test of type NX-N, according to MEPC.227(64) including section. 4.2:

Prüfinstitut für Abwassertechnik GmbH (PIA), *Test of a Marine Sanitation Device of Gertsen & Olufsen*, Report No.: PIA2016-AT1602-10122-02 – Version 2, Dated 2016-12-20.

Environmental test according to MEPC.107(49):

Delta, *Test for Marine Type Approval of control cabinet for sewage treatment system, type TFCTEH*, Report No.: DANAK-19/16866, Dated 2016-09-13.

Marking of product

For traceability to this type approval, each unit is to be marked with;

- Manufacturer's name or trade mark
- Type designation (including suffix "-C" or "-N")
- Serial No.
- Capacity
- Mark of Conformity

APPENDIX I – test data for NX-C

Test results and details of tests conducted on samples from the sewage treatment plant in accordance with resolution MEPC.227(64) excluding section 4.2:

<u>Sewage treatment plant, Type</u>	<u>NX-C</u>
<u>Manufactured by</u>	<u>Gertsen & Olufsen</u>
<u>Organization conducting the test</u>	<u>PIA</u>
<u>Designed hydraulic loading</u>	<u>3,30 m³/day</u>
<u>Designed organic loading</u>	<u>2,21 kg/day BOD</u>
<u>Number of effluent samples tested</u>	<u>40</u>
<u>Number of influent samples tested</u>	<u>40</u>
<u>Total suspended solids influent quality</u>	<u>515 mg/l</u>
<u>BOD5 without nitrification influent quality</u>	<u>341 mg/l</u>
<u>Maximum hydraulic loading</u>	<u>7,92 m³/day</u>
<u>Minimum hydraulic loading</u>	<u>0,24 m³/day</u>
<u>Average hydraulic loading (Q_i)</u>	<u>3,30 m³/day</u>
<u>Effluent flow (Q_e)</u>	<u>3,30 m³/day</u>
<u>Dilution compensation factor (Q_i/Q_e)</u>	<u>1</u>
<u>Geometric mean of total suspended solids</u>	<u>3 mg/l</u>
<u>Geometric mean of the thermotolerant coliform count</u>	<u>4 coliforms/100 ml</u>
<u>Geometric mean of BOD5 without nitrification</u>	<u>1,6 mg/l</u>
<u>Geometric mean of COD</u>	<u>21,5 mg/l</u>
<u>Maximum pH:</u>	<u>7,6</u>
<u>Minimum pH:</u>	<u>6,9</u>
<u>Type of disinfectant used</u>	<u>None</u>
<u>Was the sewage treatment plant tested with:</u>	
<u>Fresh water flushing?</u>	<u>No</u>
<u>Salt water flushing?</u>	<u>No</u>
<u>Fresh and salt water flushing?</u>	<u>No</u>
<u>Grey water added?</u>	<u>No</u>
<u>Was the sewage treatment plant tested against the environmental conditions specified in section 5.9 of resolution MEPC.227(64):</u>	
<u>Temperature</u>	<u>Yes</u>
<u>Humidity</u>	<u>Yes</u>
<u>Inclination</u>	<u>Yes</u>
<u>Vibration</u>	<u>Yes</u>
<u>Reliability of Electrical and Electronic Equipment</u>	<u>Yes</u>

APPENDIX II – test data for NX-N

Test results and details of tests conducted on samples from the sewage treatment plant in accordance with resolution MEPC.227(64) including section 4.2:

<u>Sewage treatment plant, Type</u>	<u>NX-N</u>
<u>Manufactured by</u>	<u>Gertsen & Olufsen</u>
<u>Organization conducting the test</u>	<u>PIA</u>
<u>Designed hydraulic loading</u>	<u>2,20 m³/day</u>
<u>Designed organic loading</u>	<u>1,05 kg/day BOD</u>
<u>Number of effluent samples tested</u>	<u>40</u>
<u>Number of influent samples tested</u>	<u>40</u>
<u>Total suspended solids influent quality</u>	<u>605 mg/l</u>
<u>Total nitrogen influent quality</u>	<u>96 mg/l as nitrogen</u>
<u>Total phosphorus influent quality</u>	<u>14 mg/l as phosphorus</u>
<u>BOD5 without nitrification influent quality</u>	<u>425 mg/l</u>
<u>Maximum hydraulic loading</u>	<u>5,28 m³/day</u>
<u>Minimum hydraulic loading</u>	<u>0,24 m³/day</u>
<u>Average hydraulic loading (Q_i)</u>	<u>2,2 m³/day</u>
<u>Effluent flow (Q_e)</u>	<u>2,2 m³/day</u>
<u>Dilution compensation factor (Q_i/Q_e)</u>	<u>1</u>
<u>Geometric mean of total suspended solids</u>	<u>2,8 mg/l</u>
<u>Geometric mean of the thermotolerant coliform count</u>	<u>2,7 coliforms/100 ml</u>
<u>Geometric mean of BOD5 without nitrification</u>	<u>1,6 mg/l</u>
<u>Geometric mean of COD</u>	<u>17,4 mg/l</u>
<u>Geometric mean of total nitrogen</u>	<u>21 mg/l, 77,1 % reduction</u>
<u>Geometric mean of total phosphorus</u>	<u>0,98 mg/l, 92,8 % reduction</u>
<u>Maximum pH:</u>	<u>7,4</u>
<u>Minimum pH:</u>	<u>6,9</u>
<u>Type of disinfectant used</u>	<u>None</u>

Was the sewage treatment plant tested with:

<u>Fresh water flushing?</u>	<u>No</u>
<u>Salt water flushing?</u>	<u>No</u>
<u>Fresh and salt water flushing?</u>	<u>No</u>
<u>Grey water added?</u>	<u>No</u>

Was the sewage treatment plant tested against the environmental conditions specified in section 5.9 of resolution MEPC.227(64):

<u>Temperature</u>	<u>Yes</u>
<u>Humidity</u>	<u>Yes</u>
<u>Inclination</u>	<u>Yes</u>
<u>Vibration</u>	<u>Yes</u>
<u>Reliability of Electrical and Electronic Equipment</u>	<u>Yes</u>

QS - CERTIFICATE OF ASSESSMENT - EC (MODULE E)

Application of: Directive 2014/90/EU of 23 July 2014 on marine equipment (MED), issued as "Forskrift om Skipstyr" by the Norwegian Maritime Authority. This Certificate is issued by DNV GL AS under the authority of the Government of the Kingdom of Norway.

This is to certify:

That the Quality System for the products

with type designation(s) as specified in the Appendix to this Certificate

Issued to

Gertsen & Olufsen AS
Allerød, Denmark

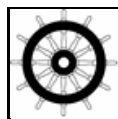
is found to comply with the applicable requirements.

The quality system has been assessed with respect to the procedure of conformity assessment described in Annex II, Module E in the directive 2014/90/EU and regulation (EU) 2017/306.

This Certificate is valid until **2022-08-28**.

Issued at **Høvik** on **2017-08-29**

DNV GL local station:
Copenhagen

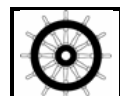


for **DNV GL AS**

Approval Engineer:
Pål Evang Nundal

Notified Body
No.: **0575**

Vidar Dolonen
Head of Notified Body



0575/yyyy

0575: Notified Body number undertaking quality surveillance
yyyy: The year in which the mark is affixed

The product liability rests with the manufacturer or his representative in accordance with Directive 2014/90/EU.
This certificate authorizes the manufacturer in conjunction with the valid EC Type Examination (Module B) Certificate(s) of the equipment listed before to affix the Mark of Conformity (wheelmark) to the product described herein.

This certificate loses its validity if the manufacturer makes any changes to the approved quality system which have not been notified to and agreed with the notified body named on this certificate.

This certificate remains valid unless suspended, withdrawn, recalled or cancelled.

The Manufacturer has to apply for periodical audits to verify the maintenance and application of the quality system every 12 months.



Form code: MED 221.NOR

Revision: 2017-02

www.dnvg.com

Page 1 of 2

© DNV GL 2014. DNV GL and the Horizon Graphic are trademarks of DNV GL AS.

APPENDIX

Item no. MED/2.6 Sewage systems

Type designation	EC Type-Examination Certificate No.	Expiry date	Notified Body No.	USCG approval number
NX10-C/N, NX20-C/N, NX25-C/N, NX30-C/N, NX35-C/N, NX40-C/N, NX45-C/N, NX50-C/N, NX55-C/N, NX60-C/N, NX65-C/N, NX70-C/N, NX75-C/N, NX80-C/N, NX90-C/N ¹	MEDB000017N	2022-03-06	0575	N/A
G&O Bioreactor, Models; BR 014800, BR 018500, BR 023125, BR 027750, BR 037000, BR 046250, BR 055500, BR 064750, BR 074000 ¹	MEDB00001ST	2020-05-29	0575	N/A
G&O Bioreactor, Models; BR 1850BG, BR 3700BG, BR 5550BG, BR 7400BG, BR 9250BG, BR 11100BG ¹	MEDB00002ZC	2020-05-29	0575	N/A

Places of production

1.KSM Poland Sp. z o.o., ul. Złotoryjska 194, Legnica, Poland

Bilag 2

SDA-engineering GmbH



Kaiserstr. 100, TPH III

D – 52134 Herzogenrath

Fon +49 - (0) 24 07 – 56 848 -0

Fax +49 - (0) 24 07 - 56 848 -29

e-mail: info@sda-engineering.de

web: www.sda-engineering.de

Report

Analysis of a marine sanitation device according to 33 CFR, §159.105 and §159.107

Project 16-1003.01

Client: Gertsen & Olufsen A/S
Savsvinget 4
DK-2970 Hørsholm
phone: +45 45763600
Fax: +45 45761773

Contractor: SDA-engineering GmbH
Kaiserstr. 100, TPH III
52134 Herzogenrath
phone: +49 (0)2407-56848 0
fax: +49 (0)2407-56848 29

Editors: Dr.-Ing. Britta Holtschoppen
Prof. Dr.-Ing. Christoph Butenweg

Preparation Date: 15.06.2016

Revision: R-0

Number of Pages: 46

Table of Contents

CODES AND LITERATURE	4
TECHNICAL DOCUMENTS ON THE DEVICE.....	4
SOFTWARE	4
1. INTRODUCTION	5
2. SYSTEM / DEVICE.....	5
3. SHOCK TEST.....	7
3.1 General calculation method.....	7
3.2 Calculations on SDof systems.....	9
3.2.1 Material properties	9
3.2.2 Stiffness of the SDof-system.....	9
3.2.3 Eigenperiod of the SDof-system	10
3.2.4 Detailed calculations for the compressor shelf.....	11
3.2.5 Detailed calculations for the permat pump shelf.....	13
3.2.6 Detailed calculations for the dosing pump	14
3.2.7 Detailed calculations for the electrical cabinet.....	14
3.3 Verifications	15
3.3.1 Numerical model.....	16
3.3.2 Verification of the tank shell and the shelf plates.....	17
3.3.3 Verification of welds.....	19
4. ROLLING TEST.....	20
4.1 General calculation method.....	21
4.2 Impulsive rigid response – tangential and radial acceleration due to rolling .	22
4.2.1 Liquid pressure due to resulting acceleration	24
4.2.2 Point loads due to resulting acceleration.....	28
4.3 Numerical model.....	29
4.4 Load cases and load case combinations	29
4.4.1 Load case combination 1: Rolling about x-axis, $\theta = 30^\circ$	30

SDA-engineering GmbH



Kaiserstr. 100, TPH III

D – 52134 Herzogenrath

Fon +49 - (0) 24 07 – 56 848 -0

Fax +49 - (0) 24 07 - 56 848 -29

e-mail: info@sda-engineering.de

web: www.sda-engineering.de

4.4.2 Load case combination 2: Rolling about x-axis, $\theta = 0^\circ$	30
4.4.3 Load case combination 3: Rolling about y-axis, $\theta = 30^\circ$	31
4.4.4 Load case combination 4: Rolling about y-axis, $\theta = 0^\circ$	32
4.5 Results and verifications	33
4.5.1 Equivalent stresses.....	35
5. SUMMARY	45

Codes and Literature

- [1] Code of Federal Regulation (CFR) 33, Chapter I – Coast Guard, Department of Homeland Security, Subchapter O - Pollution, Part 159 - Marine Sanitation Devices; Jan. 30, 1975 with editorial notes of June 19, 2008 = edition valid on April 1, 2016; source: U.S. Government Publishing Office www.ecfr.gov
- [2] Department of Transportation, United States Coast Guard: MSD Laboratory Technical Information Sheet no. 8: Calculations submitted in lieu of Rolling Test; reference: 33 CFR 159.107; 28.03.1978
- [3] Department of Transportation, United States Coast Guard: MSD Laboratory Technical Information Sheet no. 5: Development of Large Equipment Certification Programs; reference: 33 CFR 159.19; 12.04.1976
- [4] DIN EN 1993-1-8; Eurocode 3: Bemessung und Konstruktion von Stahlbauten – Teil 1-8: Bemessung von Anschlüssen; Dez. 2010
- [5] A. K. Chopra: Dynamics of Structures, Prentice Hall, ISBN: 0-13-156174-X, 2007
- [6] K. Meskouris: Structural Dynamics, Ernst & Sohn, ISBN: 3-433-01327-6, 2000

Technical documents on the device

- [7] Isometric view on CAD drawing 1502-001
- [8] Isometric view on CAD drawing 1502-002
- [9] Drawing of the device including plate arrangement; drawing no. 1502-Platearrangement-01
- [10] Drawing of the device including overall dimensions; drawing no. 1502-STATIKMODEL-01
- [11] Three dimensional model of the device as .stp-file; file 1502-STATIKMODEL-01.stp

Software

- [12] InfoCAD, Version 14.50, InfoGraph GmbH, Aachen/Germany

1. Introduction

The code of Federal Regulation (CFR) no. 33 [1] lists requirements for the Certification, Design, Construction and Testing of Marine Sanitation Devices. According to 33 CFR several tests must be performed on each newly developed device type. However, the MSD Laboratory Technical Information Sheet no. 8 [3] describes alternatives to the experimental tests described in 33 CFR §159.103 through §159.131 which may be acceptable to the Coast Guard under 33 CFR §159.19 – Testing equivalency.

The scope of this report is the investigation and verification of the PIA test plant produced by Gertsen & Olufsen, Hørsholm, Denmark regarding shock test and rolling test on a numerical/analytical basis as alternative to the experimental test procedure of 33 CFR § 159.105 and § 159.107.

2. System / Device

The considered device is a rectangular steel tank of dimensions width/depth/height = 1051 / 1006 / 1356 mm with externally attached components (Figure 2-1). Three tank sides and the tank top are stiffened by steel stiffeners of 50 and 60 mm width respectively. The external components are supported by steel shelf constructions that are welded to the tank side (Figure 2-2).

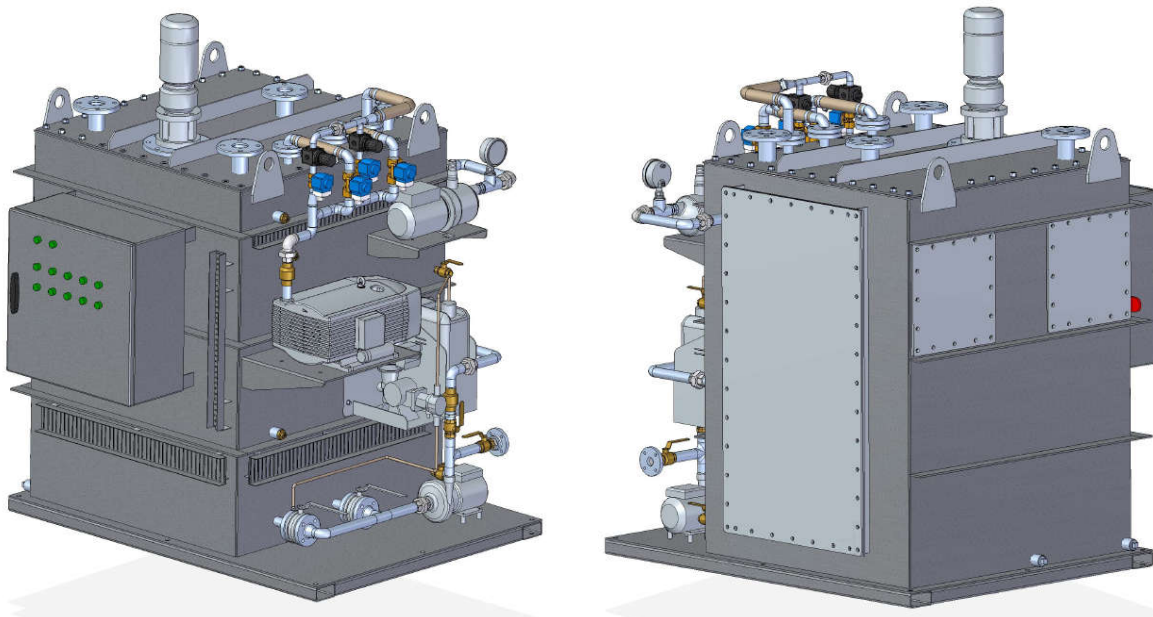


Figure 2-1: CAD drawings of the investigated device [7], [8]

SDA-engineering GmbH



Kaiserstr. 100, TPH III

D – 52134 Herzogenrath

Fon +49 - (0) 24 07 – 56 848 -0

Fax +49 - (0) 24 07 - 56 848 -29

e-mail: info@sda-engineering.de

web: www.sda-engineering.de

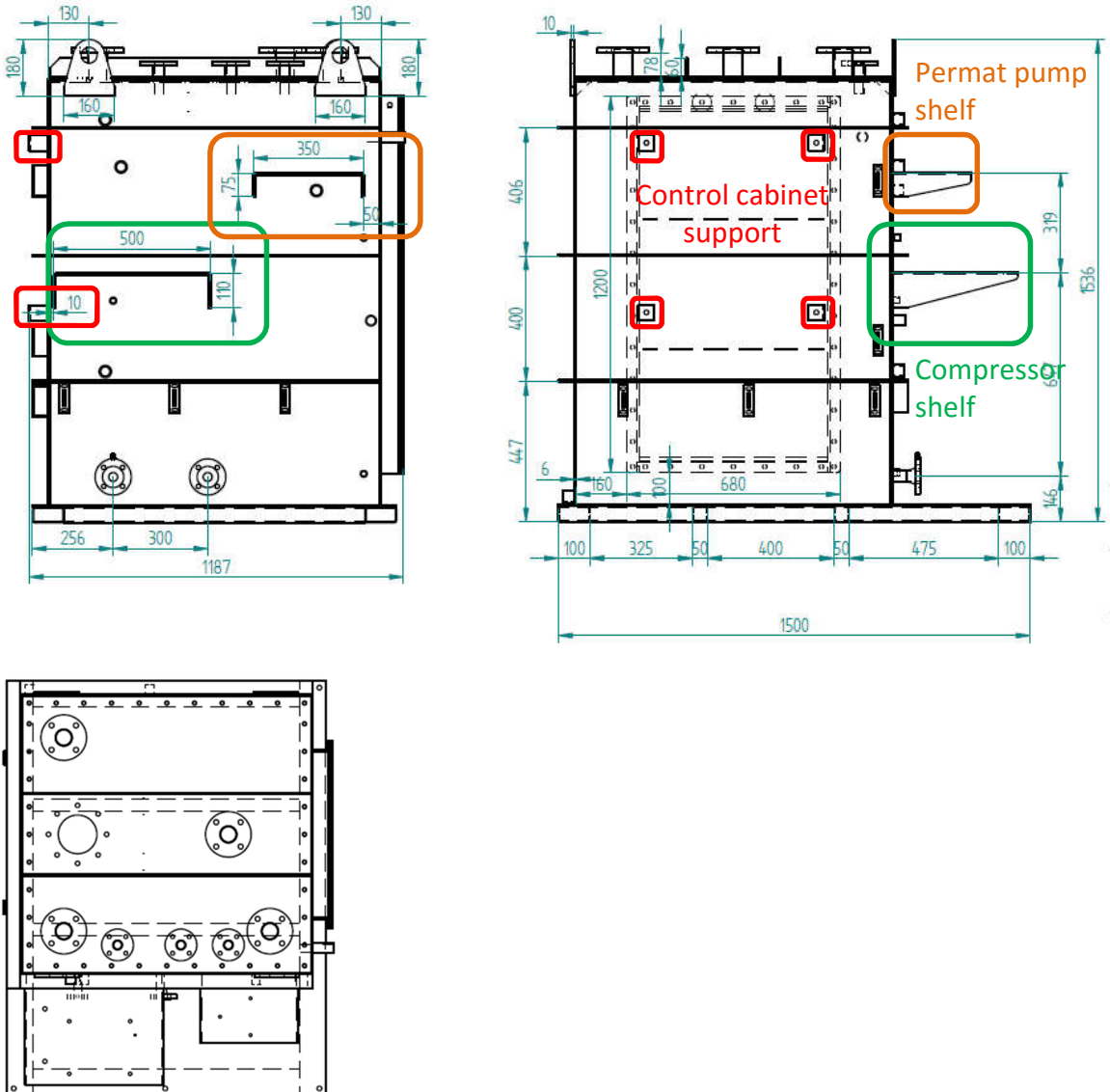


Figure 2-2: Dimensions of the device and auxiliary structural parts [10]

3. Shock test

3.1 General calculation method

In the present investigation the external components depict single degree of freedom systems whose stiffness is given by the shelf structures. Thus, shock spectra can be used to determine the maximum possible dynamic deflection of the shelf and the resulting additional loading to the tank shell.

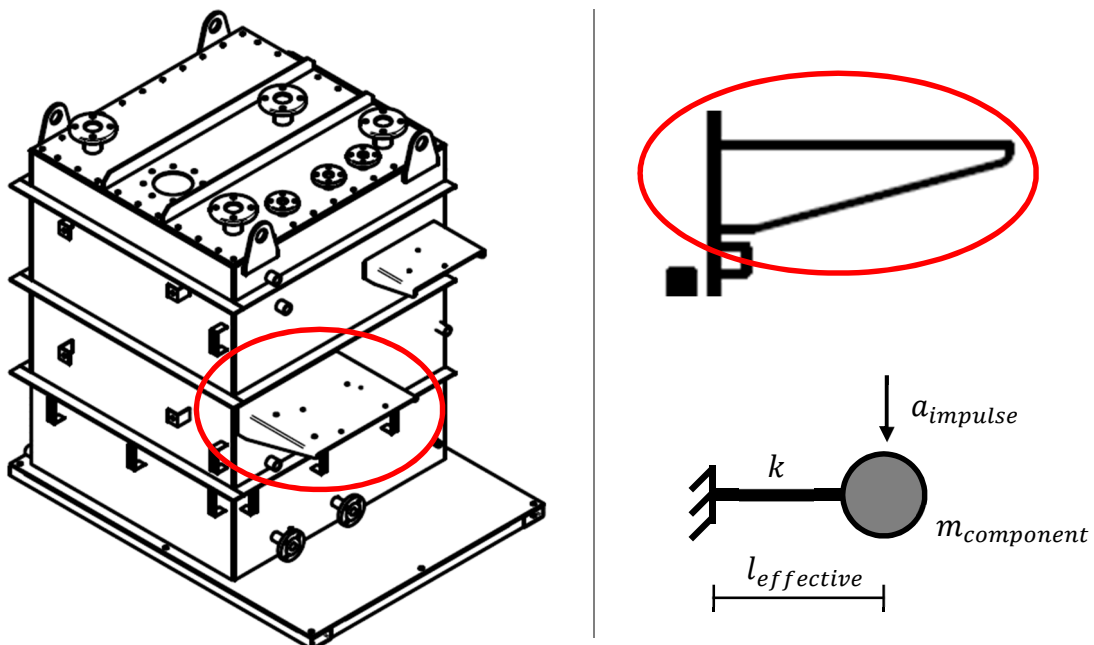


Figure 3-1: Single-degree-of-freedom representation of shelf-structures

Shock spectra depict the amplification in deformation for undamped single-degree-of-freedom systems for typical pulse loads. Depending on the relation between the impulse duration and the eigenperiod of the SDof-system the maximum possible response can be easily read off from the diagram. Figure 3-2 (c) shows the shock spectrum for a half-cycle sine pulse. It is the envelope of the response of the forced vibration phase (Figure 3-2 (a)) and the free vibration phase (Figure 3-2 (b)).

Note: Despite of the substitute analytical verification of the integrity of the device and its components, the operability of the electrical control panel itself must be verified by the shock test procedure described in 33 CFR §159.105 (see [3]) and is, thus, not part of the verifications of this report.

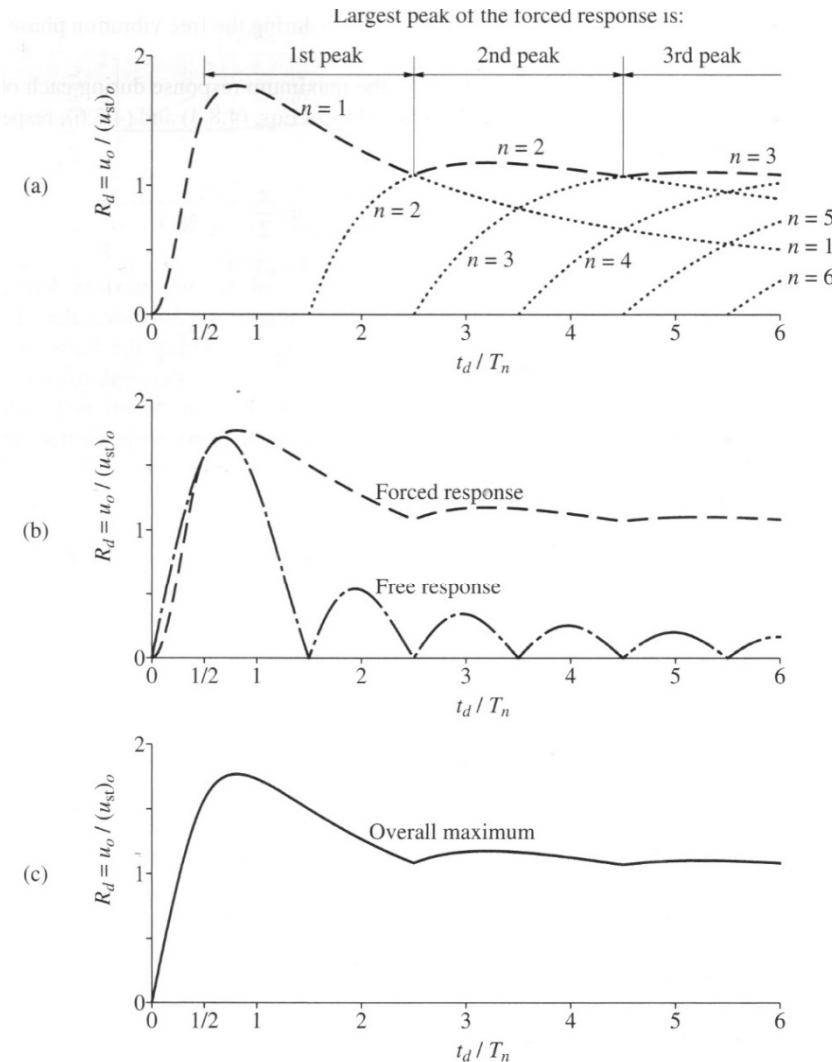


Figure 4.8.3 Response to half-cycle sine pulse force: (a) response maxima during forced vibration phase; (b) maximum responses during each of forced vibration and free vibration phases; (c) shock spectrum.

Figure 3-2: Shock spectrum for a half-cycle sine pulse force [5]

According to 33 CFR §159.105 [1] and MSD Laboratory Technical Information Sheet no. 8 [3] a pulse load (vertical acceleration) of maximum 10 g represented by a half-cycle sine of a duration of 25 milliseconds (Figure 3-3 left) was taken as basis for the calculations regarding the shock test.

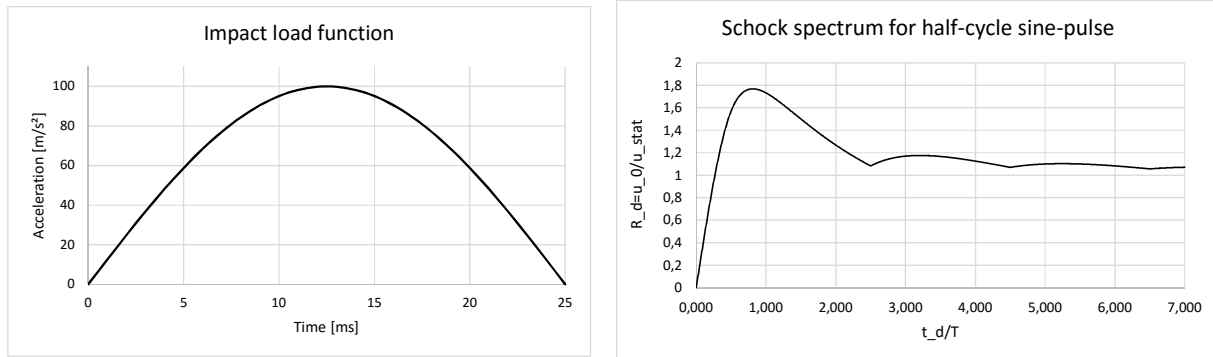


Figure 3-3: left: Half-cycle sine pulse load for shock test
right: Analytically determined shock spectrum for half-cycle sine pulse

In the present study the shock spectrum for the half-cycle sine pulse was set up analytically in order to pick up the exact amplification factor in reference to the calculated period ratio. Figure 3-3 right shows the shock spectrum used for further calculations.

3.2 Calculations on SDof systems

As stated above, the external components and their bearing systems are represented by Single-degree-of-freedom systems. Their parameters (stiffness, eigenperiod) were determined with the help of an auxiliary numerical model because of the complex three-sided bearing behaviour of the shelf plate (see Figure 3-4).

Figure 3-1 serves as reference for the naming of parameters.

3.2.1 Material properties

The shelves as well as the tank itself are made of stainless steel SS316L as stated by Gertsen&Olufson. The corresponding material properties considered in numerical analyses are given as

Material	SS316L
Density	7.9 t/m ³
Elastic modulus	193 000 MN/m ²
Tensile strength	485 MN/m ²
Yield strength @ 0.2%	172 MN/m ²

3.2.2 Stiffness of the SDof-system

In order to determine the stiffness of the equivalent SDof system a 1 N = 0.001 kN vertical load was applied to the shelf beneath the center of mass of the component (Figure 3-4). The resulting vertical deformation δ at the point of load was then employed to calculate the stiffness of the SDof system in terms of $k = 1/\delta$.

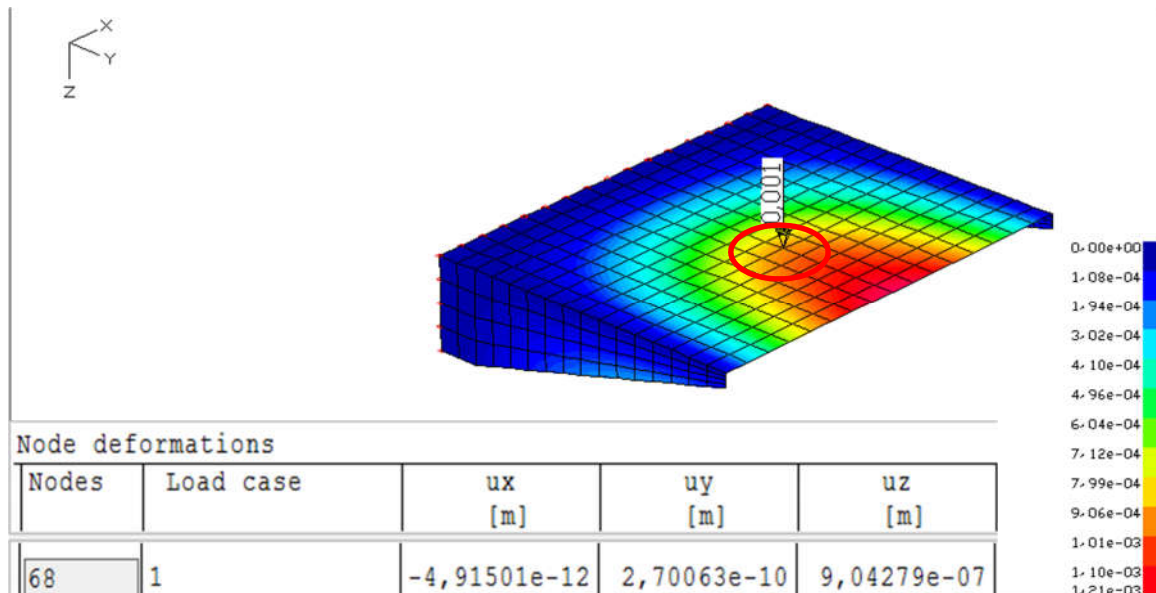


Figure 3-4: Shelf deformation of the compressor unit due to “1”-load beneath center of mass of the unit

3.2.3 Eigenperiod of the SDof-system

The eigenperiod of the system was determined by a modal analysis of the shelf structure including a point mass beneath the center of mass of the component representing the mass of the unit (Figure 3-5). Hand calculations based on the equivalent stiffness k of the SDof-system and the approximate effective mass (including the mass of the component and the vibration effective part of mass of the shelf) resulted in equivalent eigenperiods (see sections 3.2.4 and 3.2.5) verifying the numerical approach.

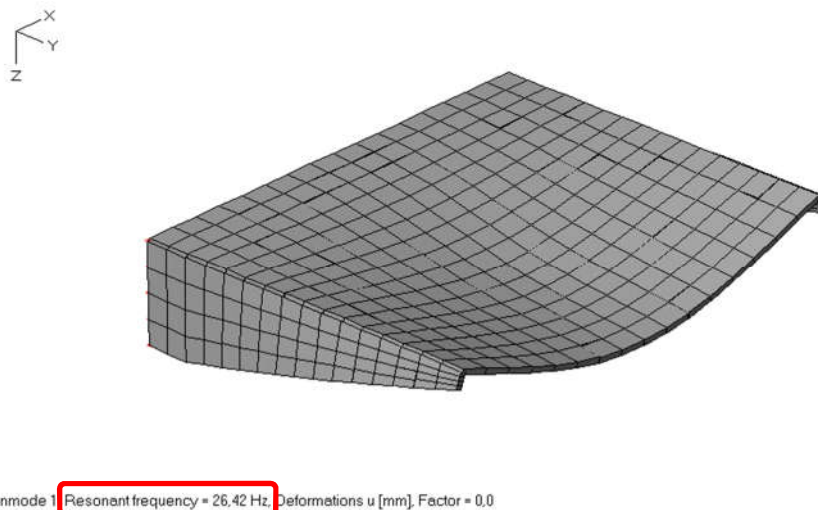


Figure 3-5: 1st eigenform of the compressor shelf and corresponding eigenfrequency

3.2.4 Detailed calculations for the compressor shelf

Evaluation of a half-cycle acceleration sine pulse		
component:	compressor unit	
gravity	g	9,81 m/s ²
SDoF-system		
mass compressor unit given by G&O	m_unit	37 kg
mass of shelf (dead load calculation)	m_shelf	12,33 kg
vibration effective mass of shelf	m_shelf_eff ≈ 1/4*m_shelf	3,08 kg
mass SDoF-system	m = m_unit+m_shelf_eff	40,08 kg
effective length of equiv. SDoF-system	I_eff = distance component - support	0,265 m
calculated deformation due to "1"-load	delta	9,04E-07 m
stiffness of SDoF-system	k = 1/delta	1.105.853 N/m
circular eigenfrequency ("hand calculation")	$\omega = \sqrt{\frac{k}{m}}$	166,10 rad/s
eigenfrequency (from modal analysis of shelf model with unit as point mass)	f	26,42 Hz
circ. eigenfreq. (compare to ω above)	$\omega = 2\pi \cdot f$	166,00 rad/s
Eigenperiod	$T = \frac{1}{f}$	0,0379 s
Pulse load		
duration	t_d [ms]	25 ms
	[s] = t_d [ms] /1000	0,0250 s
max. amplitude	a_max [g]	10 g
	[m/s ²] = a_max [g]*9,81 m/s ²	98,1 m/s ²

SDA-engineering GmbH



Kaiserstr. 100, TPH III

D – 52134 Herzogenrath

Fon +49 - (0) 24 07 – 56 848 -0

Fax +49 - (0) 24 07 - 56 848 -29

e-mail: info@sda-engineering.de

web: www.sda-engineering.de

Evaluation of shock spectrum		
Period ratio	t_d/T	0,6605 [-]
Deformation ratio (from shock spectrum of half-sine pulse)	$R_d = \frac{u_0}{u_{stat,0}} = \text{function of } \left(\frac{t_d}{T} \right)$	1,7320 [-]
static load due to max acc.	$P_{stat} = m \cdot a_{max}$	3932,20 N
calculated deformation due to "1"-load (see above)	delta	9,04E-07 m
static deflection due to P_{stat} (linear material behaviour assumed)	$u_{stat,0} = \frac{\text{delta}}{1N} \cdot P_{stat}$	3,56E-03 m
maximum dynamic deflection	$u_{0,dyn} = R_d \cdot u_{stat,0}$	0,0062 m
Equivalent dynamic load (vertical)		
	$P_{dyn} = R_d \cdot P_{stat}$	6.810,74 N
width footprint compressor unit in model	b_unit	0,25 m
length footprint compressor unit in model	l_unit	0,4 m
footprint compressor unit in model	A_unit	0,1 m ²
maximum dynamic pressure (vertical)	$p_{dyn} = P_{dyn}/A_{unit}$	68.107,38 N/m²

3.2.5 Detailed calculations for the permat pump shelf

Evaluation of a half-cycle acceleration sine pulse		
component:	permat pump unit	
gravity	g	9,81 m/s ²
SDoF-system		
mass permat pump unit given by G&O	m_unit	9,6 kg
mass of shelf (dead load calculation)	m_shelf	5,71 kg
vibration effective mass of shelf	m_shelf_eff ≈ 1/4*m_shelf	1,43 kg
mass SDoF-system	m = m_unit+m_shelf_eff	11,03 kg
effective length of equiv. SDoF-system	l_eff = distance component - support	0,1535 m
calculated deformation due to "1"-load	delta	3,40E-07 m
stiffness of SDoF-system	k = 1/delta	2.937.997 N/m
circular eigenfrequency ("hand calculation")	$\omega = \sqrt{\frac{k}{m}}$	516,17 rad/s
eigenfrequency (from modal analysis of shelf model with unit as point mass)	f	81,40 Hz
circ. eigenfreq. (compare to ω above)	$\omega = 2\pi \cdot f$	511,45 rad/s
Eigenperiod	$T = \frac{1}{f}$	0,0123 s
Pulse load		
duration	t_d [ms]	25 ms
	[s] = t_d [ms] /1000	0,0250 s
max. amplitude	a_max [g]	10 g
	[m/s ²] = a_max [g]*9,81 m/s ²	98,1 m/s ²

Evaluation of shock spectrum		
Period ratio	t_d/T	2,0350 [-]
Deformation ratio (from shock spectrum of half-sine pulse)	$R_d = \frac{u_0}{u_{stat,0}} = \text{function of } \left(\frac{t_d}{T} \right)$	1,7500 [-]
static load due to max acc.	$P_{stat} = m \cdot a_{max}$	1081,76 N
calculated deformation due to "1"-load (see above)	delta	3,40E-07 m
static deflection due to P_{stat} (linear material behaviour assumed)	$u_{stat,0} = \frac{\text{delta}}{1N} \cdot P_{stat}$	3,68E-04 m
maximum dynamic deflection	$u_{0,dyn} = R_d \cdot u_{stat,0}$	0,0006 m
Equivalent dynamic load (vertical)	$P_{dyn} = R_d \cdot P_{stat}$	1893,08 N
width permat pump unit in model	b_unit	0,15 m
length permat pump unit in model	l_unit	0,25 m
footprint permat pump unit in model	A_unit	0,0375 m ²
maximum dynamic pressure (vertical)	$p_{dyn} = P_{dyn}/A_{unit}$	50.482,13 N/m ²

3.2.6 Detailed calculations for the dosing pump

Since the mass of the dosing pump plus adjacent chemical can is way smaller than the mass of the compressor unit (8+5=13 kg < 38 kg) detailed calculations for the dosing pump and its shelf are not necessary.

It must be assured, however, that the shelf for the dosing pump and the chemical can is constructed similarly to the compressor unit shelf (two vertical webs at the shelf sides welded to the tank attachment plate) and that both, the pump and the can are tightly fastened to the shelf construction. The shelf itself (or its tank attachment plate respectively) must be welded to the tank shell with the boundary conditions given in section 0.

3.2.7 Detailed calculations for the electrical cabinet

The electrical cabinet (dimensions 600 x 600 mm; mass: 38 kg) is mounted on four steel brackets. Due to its configuration it can be regarded as stiff. Thus, the maximum dynamic vertical load due to acceleration impulse is equal to the mass times an acceleration of 10 g. The vertical load must be transferred to the tank shell by the four steel brackets. Additionally, a horizontal force at the upper (tension) and lower (pressure) brackets results from the bending moment due to the eccentric installation.

SDoF-system		
mass electrical cabinet given by G&O	m_unit	38 kg
connection to tank		stiff
Pulse load		
max. amplitude	a_max [g]	10 g
	[m/s ²] = a_max [g]*9,81 m/s ²	98,1 m/s ²
Maximum dynamic vertical load		
maximum total vertical load	F_v = m_unit * a_max	3.727,8 N
maximum vertical load per support	F_v,s = 1/4 * F_v	932,0 N
maximum vertical load per node	F_v,n = 1/2 * F_v,s	466,0 N
maximum total horizontal load		
lever arm (approximately)	d = d_support + 1/2 d_cabinet	160 mm
bending moment due to max. vert. load	M = F_v * d	596.448,00 Nmm
height of cabinet	h_cabinet	600 mm
tot. horiz. support force due to bend. mom.	F_h = M/h_cabinet	994,08 N
horizontal force per support	F_h,s = total support force / 2	497,04 N
horizontal force per node	F_h,n = force per support / 2	248,52 N

3.3 Verifications

The maximum dynamic pressure due to acceleration impulse, which were determined in sections 3.2.4 and 3.2.5 were applied to a model of the tank structure (Figure 3-6) in order to identify the maximum resulting stresses in the tank shell and the maximum internal forces for a verification of the welds of the shelves.

3.3.1 Numerical model

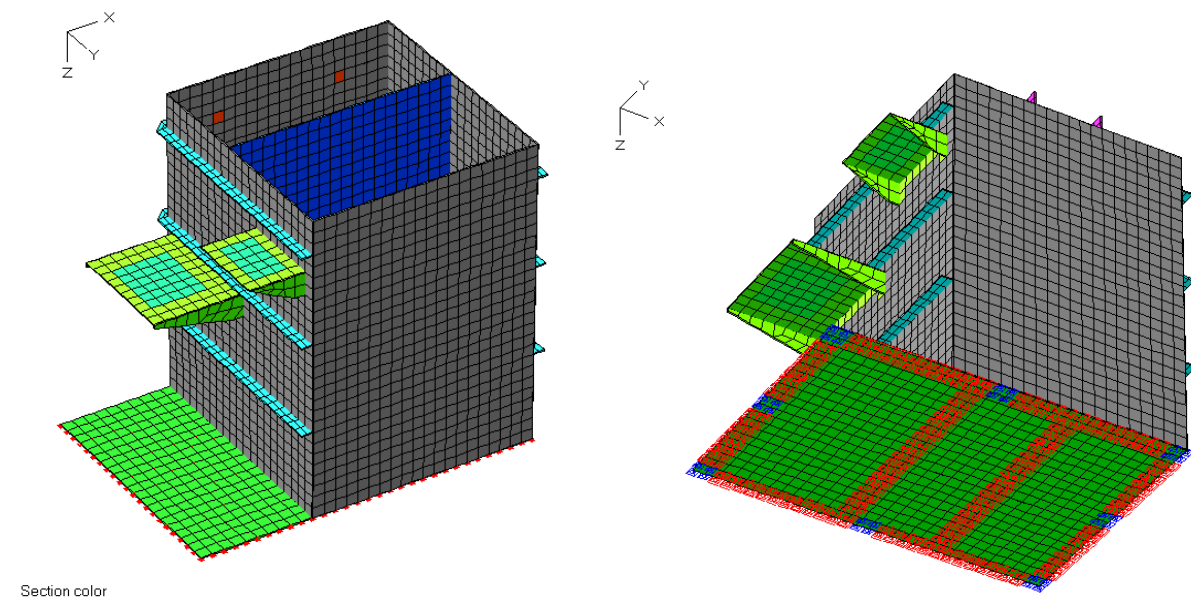


Figure 3-6: FE-model with supports of bottom plate

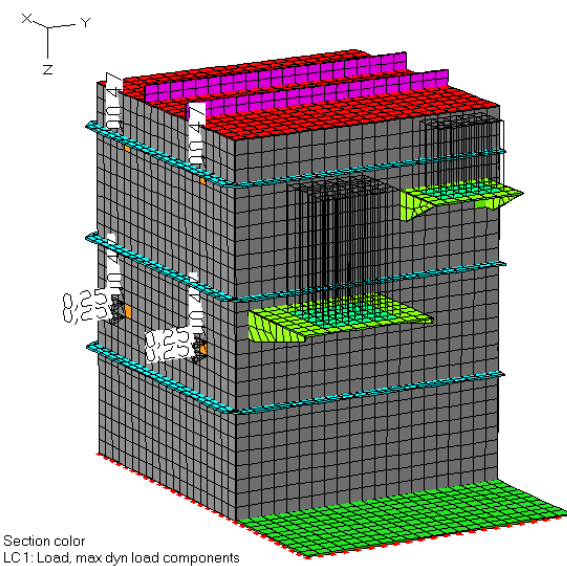


Figure 3-7: FE-model with maximum dynamic loading of components due to sine acceleration impulse

The simulation was done with the FE Software InfoCAD [12] in terms of a static finite element calculation since the dynamic effects are already included in the shock spectra.

The tank shell (sides, top and bottom) and the stiffeners were modelled as 4-node shell elements of 6 mm thickness with nearly quadratic geometry and an element width of approximately 5 cm (elements of stiffeners: rectangular).

Anchorage of the tank was considered by vertical supports (pressure only) at the locations of hollow sections underneath the bottom steel plate (red supports in Figure 3-6 right) and by translational supports in all three directions at the location of bore holes in the bottom steel plate (blue supports in Figure 3-6 right).

The material properties of tank shell and stiffeners are identical to those of the component shelves already given in section 3.2.1 according to Gertsen&Olufson.

3.3.2 Verification of the tank shell and the shelf plates

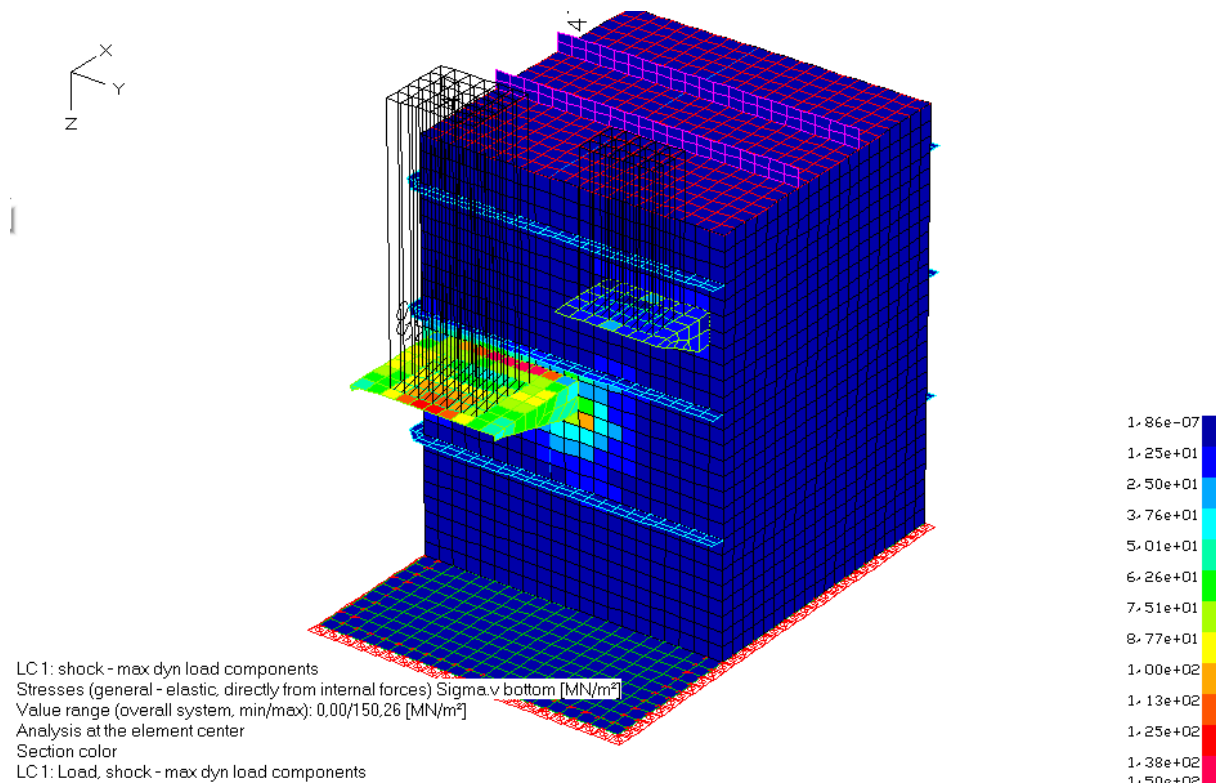


Figure 3-8: Equivalent stresses due to shock load on shelf components 150 MN/m² < 172 MN/m² ✓

The maximum equivalent stresses due to shock load are 150.3 MN/m² which is less than the maximum yield strength of 172 MN/m².

According to DIN EN 1993 the partial safety factor γ_{M0} for the capacity of sections is equal to 1.0, so the yield strength does not have to be reduced.

$$\text{The limit value for shell stresses are met as } \sigma_{v,Ed} = 150 \frac{\text{MN}}{\text{m}^2} < 17 \cdot 2 \frac{\text{MN}}{\text{m}^2} = \frac{f_y}{\gamma_{M0}}$$

The stress values due to the acceleration of the electrical cabinet are much smaller than that ($14,5 \text{ MN/m}^2$) and thus not relevant for design of the shell.

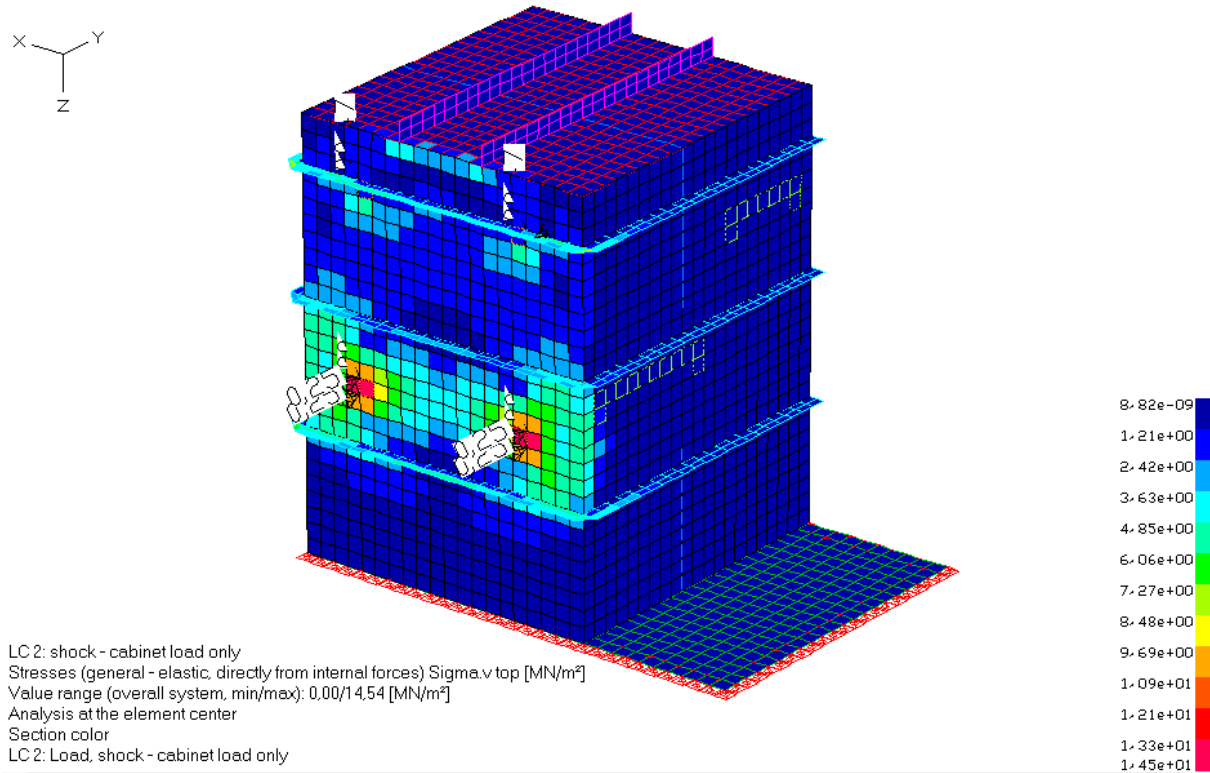


Figure 3-9: Equivalent stresses due to acceleration of electrical cabinet $14,5 \text{ MN/m}^2 < 172 \text{ MN/m}^2 \checkmark$

3.3.3 Verification of welds

As both shelves are connected to the tank shell with identical welds only the highest loading is considered for weld verification, i.e. the shelf of the compressor unit. The verifications are carried out in accordance with DIN EN 1993-1-8 [4].

Dynamic maximum support reactions		
Vertical force at shelf connection	$F_v = k \cdot u_{0,dyn} = P_{dyn}$	6.810,74 N
Bending moment at shelf connection	$M = F_v \cdot d_{eff}$	1.804,85 Nm
Shear force to be taken up by vertical welds	= F_v	6.810,74 N
lever arm for bending moment	= height of shelf	0,11 m
Tension force to be taken up by horiz. weld	= $M/\text{height of shelf}$	16.407,69 N
weld verification according to DIN EN 1993-1-8		
weld type		fillet weld
shelf thickness	t_{shelf}	6 mm
shell thickness	t_{shell}	6 mm
maximum steel thickness	t_{max}	6 mm
minimum weld thickness	$a_{min} = \max(\sqrt{t_{max}} - 0,5; 3 \text{ mm})$	3,0 mm
chosen weld thickness (assumed)	a	3,0 mm
partial safety factor (material) for connect.	$\gamma_M 2$	1,25 -
correlation factor	β_w	0,8 -
min. tensile strength of the connected parts	f_u	485 N/mm ²
Design value of shear capacity of the weld	$f_{vw,d} = \frac{f_u / \sqrt{3}}{\beta_w \cdot \gamma_M 2}$	280 N/mm ²
horizontal weld (takes up on horizontal (tension) force due to bending moment)		
shelf length	l_{shelf}	500 mm
minimum effective weld length	$l_{eff} \geq 6 \cdot a \text{ and } l_{eff} \geq 30 \text{ mm}$	18 mm
effective weld length	$l_{eff} = 2 * (l_{shelf} - 2 * t_{shelf})$	976 mm
effective weld area	$A_w = a * l_{eff}$	2928 mm ²
tension force per unit weld length	$F_{w,Ed} = \text{Tension force} / l_{eff}$	16,81 N/mm
capacity of the weld	$F_{w,Rd} = f_{vw,d} * a$	840,04 N/mm²
safety factor	$F_{w,Rd} / F_{w,Ed}$	49,97 > 1 ok
vertical weld (takes up on shear force due to vertical load)		
shelf height (see above)	h_{shelf}	110 mm
minimum effective weld length	$l_{eff} \geq 6 \cdot a \text{ and } l_{eff} \geq 30 \text{ mm}$	18 mm
effective weld length	$l_{eff} = 4 * (h_{shelf} - 1 * t_{shelf})$	368 mm
effective weld area	$A_w = a * l_{eff}$	1104 mm ²
shear force per unit weld length	$F_{w,Ed} = \text{Shear force} / h_{eff}$	61,92 N/mm
capacity of the weld	$F_{w,Rd} = f_{vw,d} * a$	840,04 N/mm²
safety factor	$F_{w,Rd} / F_{w,Ed}$	13,57 > 1 ok

4. Rolling test

The MSD Laboratory Technical Information Sheet no. 5 [2] outlines design aspects of marine sanitation devices that should be considered in performing theoretical analyses for submission in lieu of the actual experimental rolling test required by 33 CFR § 159.107.

The Coast Guard's main interests in the rolling test are the system's processing capability (including the prevention of spillover from the device into work spaces or from one chamber into another) and the proof of structural integrity of the device under roll-induced loads.

The following conditions apply:

- The axis of roll should be in the plane of the base of the device and offset from the centerline by $r=1.22$ m.
- The period of the roll should be $T=4$ seconds.
- The angle θ_{max} used should be the maximum for which the device is to be certified.
- The forces to be considered are the weight of the tank and its contents as well as the tangential force due to rolling.
- Stresses should be calculated for the supports, bottom plating, side- and end plating.
- Additionally, if any heavy components are supported by the tank top or sides, the load on the tank plating due to the component's weight and developed tangential force should be considered.

MAXIMUM TANGENTIAL FORCE F_t IS
GIVEN BY

$$F_t = \frac{4\pi^2 r \theta_0 W}{g T^2}$$

WHERE

r = distance from axis to CG

θ_0 = max. roll angle

W = weight of tank and contents

T = period of roll

g = acceleration due to gravity

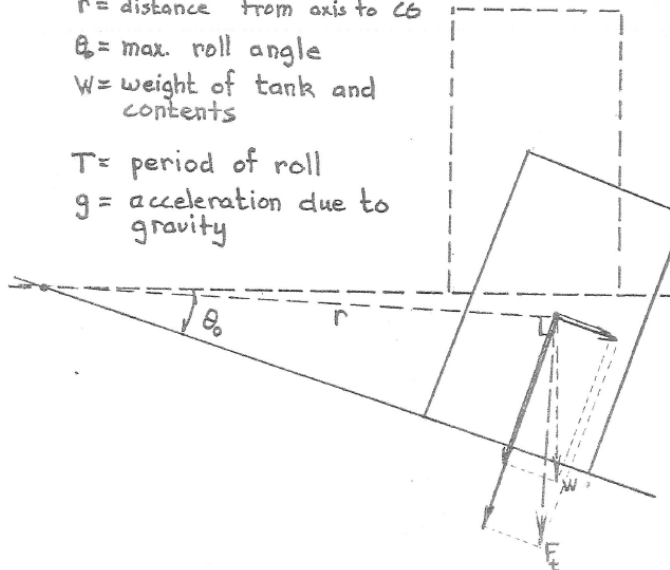


Figure 4-1: Test conditions to be assumed according to MSD Laboratory Technical Information Sheet no. 5 [2]

4.1 General calculation method

Generally, a liquid filled container is exposed to different response components when loaded dynamically:

- The impulsive rigid load component results from a rigid body movement of the liquid together with the tank. **It is pictured by a constant acceleration value that is determined in accordance with the harmonic rolling of the container (see section 4.2).**
- The impulsive flexible load component results from the interaction of the liquid with the deforming thin tank shell. **This is not relevant for the considered case of a sanitation device since the tank is braced by stiffeners and can be regarded as non-deforming when calculating the liquid response.**
- The convective load component results from the sloshing of the liquid. **The additional pressure due to sloshing is very small compared to the impulsive rigid pressure component and can be neglected due to sufficient capacity of the tank. The sloshing height, however, should be taken into account when evaluating the risk of spill over.**

In the following sections the loads to rolling are determined and applied to a numerical model of the device. The resulting stresses in the bottom, side and end plates are calculated and compared to the allowable stresses.

As the sanitation device can be mounted on the ship in either direction, two possible rolling axes are considered in calculation. This is in accordance with the regulations of CFR 33 §159.107 (a) [1].

4.2 Impulsive rigid response due to rolling

4.2.1 Tangential and radial acceleration due to rolling

The impulsive rigid response depends on the rolling angle of the container and leads to a maximum tangential acceleration (at maximum rolling angle) or a maximum radial acceleration (at zero rolling angle). Both are calculated in the following; the maximum tangential acceleration is equal to the value given in MSD Laboratory Technical Information Sheet no. 5 [2]. The direction of action of both accelerations is shown in Figure 4-2.

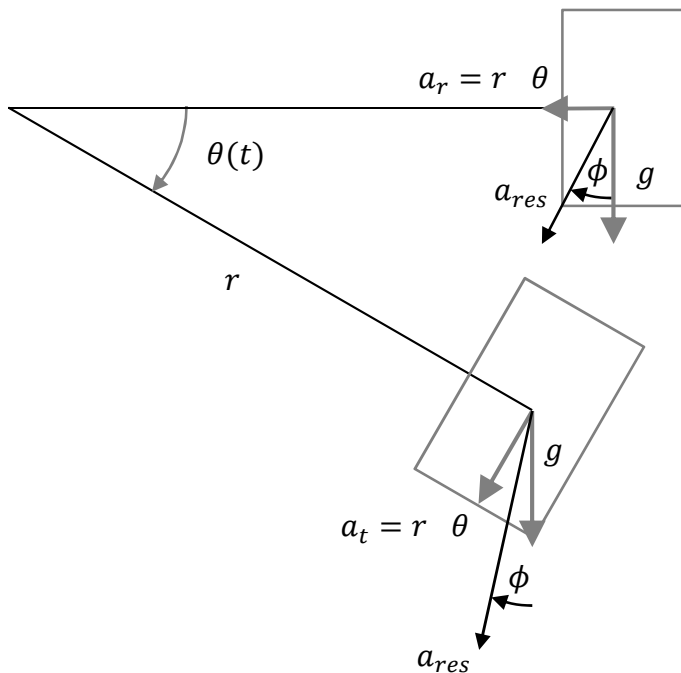


Figure 4-2: Definition of tangential, radial and resulting acceleration

Derivation of maximum acceleration due to rolling:

Circular rolling frequency

$$\omega = \frac{2\pi}{T} = \frac{2\pi}{4s} = 1.571 \frac{\text{rad}}{\text{s}}$$

Maximum rolling angle

$$\theta_{max} = 30^\circ = \pi/6$$

Considered rolling radius

$$r = 1.22 \text{ m}$$

Time dependent rolling angle

$$\theta(t) = \theta_{max} \sin(\omega t)$$

Time dependent rolling velocity

$$\theta(t) = \theta_{max} \omega \cos(\omega t)$$

Time dependent rolling acceleration

$$\theta(t) = \theta_{max} \omega^2 \sin(\omega t)$$

If $\theta(t) = \theta_{max}$:

$$\theta(t) = 0$$

$$\theta(t) = \theta_{max} = \theta_{max} \frac{4\pi^2}{T^2}$$

radial acceleration:

$$a_{r,max} = r \theta^2 = 0$$

tangential acceleration:

$$a_{t,max} = r \theta_{max} = \frac{4\pi^2}{(4s)^2} 1.22 \text{ m} \frac{\pi}{6} = 1.58 \text{ m/s}^2$$

If $\theta(t) = 0$:

$$\theta(t) = \theta_{max} = \theta_{max} \frac{2\pi}{T}$$

$$\theta(t) = 0$$

radial acceleration:

$$a_{r,max} = r \theta^2 = 1.22 \text{ m} \left(\frac{\pi}{6} \frac{2\pi}{4s} \right) = 1.0 \text{ m/s}^2$$

tangential acceleration:

$$a_{t,max} = r \theta = 0$$

The tangential and radial acceleration act on both the liquid and the components attached to the container. It can be combined with gravity to determine a resulting global acceleration:

Resulting acceleration on liquid and components and its global direction:

If $\theta(t) = \theta_{max} = 30^\circ$:

$$g = 9.81 \text{ m/s}^2 @ 0^\circ \text{ (= z-direction)}$$

$$a_{t,max} = 1.58 \text{ m/s}^2 @ 150^\circ$$

resulting acceleration:

$$a_{res} = \sqrt{9.81^2 + 1.58^2 - 2 \cdot 9.81 \cdot 1.58 \cos(150^\circ)} \\ = 11.21 \text{ m/s}^2$$

angle of resulting acc.:

$$\phi = \arcsin \left(\frac{a_{t,max} \sin 30^\circ}{a_{res}} \right) = 4.04^\circ \text{ off the vertical}$$

global acceleration in z:

$$a_z = a_{res} \cos \phi = 11.18 \text{ m/s}^2$$

global gravity factor in z:

$$a_{z,factor} = \frac{a_z}{g} = \frac{11.18}{9.81} = 1.14$$

global acceleration in x or y:

$$a_y = a_{res} \sin \phi = 0.80 \text{ m/s}^2$$

global gravity factor in x or y:

$$a_{y,factor} = \frac{a_y}{g} = \frac{0.80}{9.81} = 0.08$$

If $\theta(t) = 0$:	$g = 9.81 \text{ m/s}^2$	@ 0° (= z-direction)
	$a_{r,max} = 1.0 \text{ m/s}^2$	@ 90°
resulting acceleration:	$a_{res} = \sqrt{9.81^2 + 1.0^2} = 9.86 \text{ m/s}^2$	
angle of resulting acc.:	$\phi = \arctan\left(\frac{1.0}{9.81}\right) = 5.82^\circ$ off the vertical	
global acceleration in z:	$g = 9.81 \text{ m/s}^2$	
global gravity factor in z:	$a_{z,factor} = \frac{g}{g} = 1.0$	
global acceleration in x or y:	$a_{r,max} = 1.0 \text{ m/s}^2$	
global gravity factor in x or y:	$a_{y,factor} = \frac{1.0}{g} = 0.1$	

4.2.2 Liquid pressure due to resulting acceleration

The liquid pressure due to the rigid-body acceleration can be determined analogously to the hydrostatic pressure where the gravity component is replaced by the resulting impulsive rigid acceleration (Figure 4-3 and calculation in section 4.2.1). The maximum height h_{liquid} for the calculation of liquid pressure depends on the rolling angle θ and the width of the tank b . It is calculated by

$$h_{liquid} = h_{filling} \cos \theta \pm \frac{b_{tank}}{2} \sin \theta$$

The resulting triangle-shaped pressure is distributed over the wetted surface, which refers to the inclined fluid surface and is calculated by

$$h_{wetted\ surface} = h_{liquid} \pm \frac{b}{2} \tan \theta$$

In the case of maximum radial acceleration (which occurs at an angle of $\theta = 0^\circ$) the values of h_{liquid} and $h_{wetted\ surface}$ are obviously identical and equal to the filling height $h_{filling}$ (Figure 4-3 right).

The maximum filling height was specified by Gertsen&Olufson as $h_{filling} = 1150 \text{ mm}$ for tank 1 and $h_{filling} = 1225 \text{ mm}$ for tank 2.

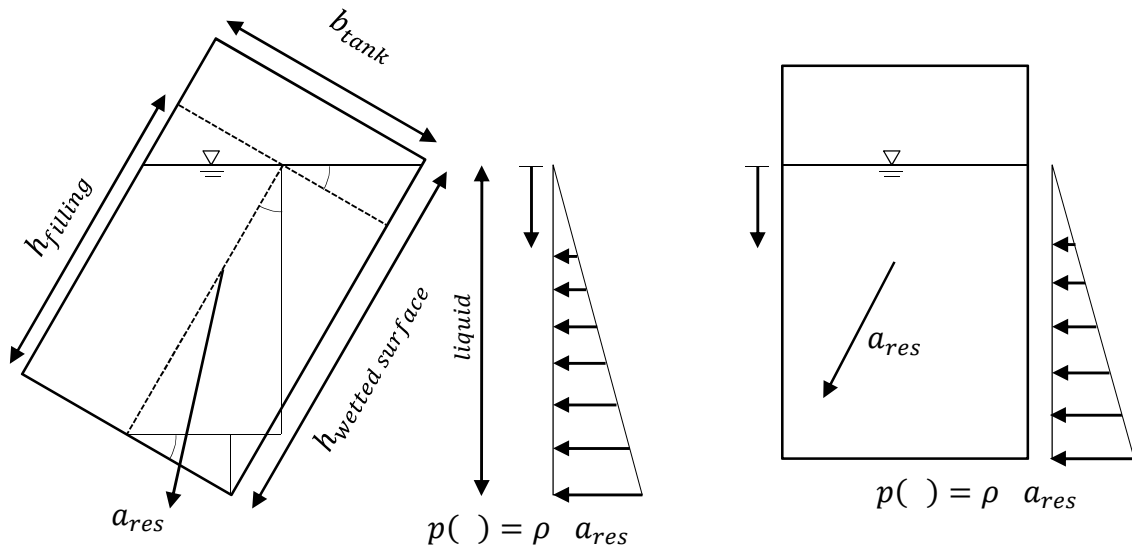


Figure 4-3: Impulsive rigid pressure component at maximum rolling angle (left) and at 0° rolling angle (right)

The following tables summarise the relevant heights and the resulting pressure components for the individual load case combinations. The pressures are calculated with reference to the flat liquid surface at a roll angle of 30°. The effect of sloshing (waves) additional to the surface inclination is not relevant for stress analysis and, thus, not considered in the determination of the liquid pressures.

Please note, though, that in the case of rolling about the y-axis (30° max; LCC 3) the calculative maximum height of the liquid surface will be higher than the height of the tank walls (see underlined values below). That means that the liquid will slosh to the tank top leading to a potential spill over if tank top and walls are not sealed.

Sloshing above the maximum wall height is also expected in the case of rolling about the x-axis (LCC 1) since the values given in the tables below only refer to the flat liquid surface in case of 30° rolling angle. Wave height due to sloshing must be added to these values.

In order to comply with CFR 33 [1], the manufacturer must in particular prevent spill over between the two tanks by sealing the gap between internal wall and tank top. Tank top and outer walls of the device must be tightly bolted together to prevent spill over to the outside.

SDA-engineering GmbH



Kaiserstr. 100, TPH III

D – 52134 Herzogenrath

Fon +49 - (0) 24 07 – 56 848 -0

Fax +49 - (0) 24 07 - 56 848 -29

e-mail: info@sda-engineering.de

web: www.sda-engineering.de

For load case combination 1 ($\theta(t) = \theta_{max} = 30^\circ$, rolling about the x-axis)

tank no.	filling height	width	$h_{min,wet\ sur}$	$h_{liquid,left}$	$h_{max,wet\ sur}$	$h_{liquid,right}$
1 (big)	1150 mm	604 mm	976 mm	845 mm	1324 mm	1147 mm
2 (small)	1225 mm	435 mm	1099 mm	952 mm	<u>1351 mm</u>	1170 mm

$$\text{Specific weight of the water (see 4.2.1): } \rho \quad a_{res} = 1 \frac{t}{m^3} \quad 11.21 \frac{m}{s^2} = 11.21 \frac{kN}{m^3}$$

→ loads on tank 2 (small)

$$\begin{aligned}
 p_{max,left} &= 11.21 \cdot 0.952 = 10.7 \frac{kN}{m^2} \text{ up to 1099 mm} & = 11.21 \cdot 0.845 = 9.5 \frac{kN}{m^2} \text{ up to 976 mm} \\
 p_{max,right} &= 11.21 \cdot 1.170 = 13.1 \frac{kN}{m^2} \text{ up to 1350 mm} & = 11.21 \cdot 1.147 = 12.9 \frac{kN}{m^2} \text{ up to 1324 mm} \\
 p_{min,bottom} &= p_{max,left} = 10.7 \frac{kN}{m^2} & = p_{max,left} = 9.5 \frac{kN}{m^2} \\
 p_{max,bottom} &= p_{max,right} = 13.1 \frac{kN}{m^2} & = p_{max,right} = 12.9 \frac{kN}{m^2}
 \end{aligned}$$

→ loads on tank 1 (big)

For load case combination 2 ($\theta(t) = \theta_{max} = 0^\circ$, rolling about the x-axis)

tank no.	filling height	width	$h_{min,wet\ sur}$	$h_{liquid,left}$	$h_{max,wet\ sur}$	$h_{liquid,right}$
1 (big)	1150 mm	604 mm	1150 mm	1150 mm	1150 mm	1150 mm
2 (small)	1225 mm	435 mm	1225 mm	1225 mm	1225 mm	1225 mm

$$\text{Specific weight of the water (see 4.2.1): } \rho \quad a_{res} = 1 \frac{t}{m^3} \quad 9.86 \frac{m}{s^2} = 9.86 \frac{kN}{m^3}$$

→ loads on tank 2 (small)

$$\begin{aligned}
 p_{max} &= 9.86 \cdot 1.225 = 12.1 \frac{kN}{m^2} \text{ up to 1225 mm} & = 9.86 \cdot 1.15 = 11.3 \frac{kN}{m^2} \text{ up to 1150 mm}
 \end{aligned}$$

→ loads on tank 1 (big)

For load case combination 3 ($\theta(t) = \theta_{max} = 30^\circ$, rolling about the y-axis)

tank no.	filling height	width	$h_{min,wet\ sur}$	$h_{liquid,front}$	$h_{max,wet\ sur}$	$h_{liquid,back}$
1 (big)	1150 mm	1000 mm	861 mm	746 mm	<u>1439 mm</u>	1246 mm
2 (small)	1225 mm	1000 mm	936 mm	811 mm	<u>1514 mm</u>	1311 mm

$$\text{Specific weight of the water (see 4.2.1): } \rho \quad a_{res} = 1 \frac{t}{m^3} \quad 11.21 \frac{m}{s^2} = 11.21 \frac{kN}{m^3}$$

➔ loads on tank 2 (small)

$$p_{max,back} = 11.21 \cdot 0.746 = 8.4 \frac{kN}{m^2} \text{ up to 861 mm} \quad = 11.21 \cdot 0.811 = 9.1 \frac{kN}{m^2} \text{ up to 936 mm}$$

$$p_{max,front} = 11.21 \cdot 1.246 = 14.0 \frac{kN}{m^2} \text{ up to 1350 mm} \quad = 11.21 \cdot 1.311 = 14.7 \frac{kN}{m^2} \text{ up to 1350 mm}$$

$$p_{min,bottom} = p_{max,back} = 8.4 \frac{kN}{m^2} \quad = p_{max,back} = 9.1 \frac{kN}{m^2}$$

$$p_{max,bottom} = p_{max,front} = 14.0 \frac{kN}{m^2} \quad = p_{max,front} = 14.7 \frac{kN}{m^2}$$

The small loading of the top shell is negligible for stress and buckling verifications.

➔ loads on tank 1 (big)

For load case combination 4 ($\theta(t) = \theta_{max} = 0^\circ$, rolling about the y-axis)

➔ Calculation of liquid pressure equal to load case combination 2

$$\text{Specific weight of the water (see 4.2.1): } \rho \quad a_{res} = 1 \frac{t}{m^3} \quad 9.86 \frac{m}{s^2} = 9.86 \frac{kN}{m^3}$$

➔ loads on tank 2 (small)

$$p_{max} = 9.86 \cdot 1.225 = 12.1 \frac{kN}{m^2} \text{ up to 1225 mm} \quad = 9.86 \cdot 1.15 = 11.3 \frac{kN}{m^2} \text{ up to 1150 mm}$$

➔ loads on tank 1 (big)

For load case combination 5 (uneven filling; $\theta(t) = \theta_{max} = 30^\circ$, rolling about the x-axis)

- ➔ Calculation of liquid pressure equal to load case combination 1, but liquid pressure is only considered in the smaller tank (higher maximum filling); the bigger tank is considered empty.

4.2.3 Point loads due to resulting acceleration

The following point loads are applied to the FE-model of the tank representing the external components:

For load case combination 1 ($\theta(t) = \theta_{max} = 30^\circ$, rolling about the x-axis)

- ➔ global acceleration in z: $a_z = 11.18 \text{ m/s}^2$ acceleration factor: 1.14
- ➔ global acceleration in y: $a_y = 0.80 \text{ m/s}^2$ acceleration factor: 0.08

Component	mass	load in z-dir.	load in y-dir.
compressor	37.0 kg	414 N = 4*103.5 N	30 N = 4*7.5 N
permat pump	9.6 kg	107 N = 2*53.5 N	8 N = 2*4.0 N
circulation pump	8.3 kg	not relevant (set on base)	not relevant
dosing pump & chemical can	13.0 kg	145 N = 4*36 N	10 N = 4*2.5 N
electrical cabinet	38.0 kg	425 N = 4*106 N	30 N = 4*7.5 N

For load case combination 2 ($\theta(t) = \theta_{max} = 0^\circ$, rolling about the x-axis)

- ➔ global acceleration in z: $a_z = 9,81 \text{ m/s}^2$ acceleration factor: 1.0
- ➔ global acceleration in y: $a_y = 1,0 \text{ m/s}^2$ acceleration factor: 0.1

Component	mass	load in z-dir.	load in y-dir.
compressor	37.0 kg	363 N = 4*91 N	30 N = 4*9,3 N
permat pump	9.6 kg	94 N = 2*47 N	10 N = 2*5.0 N
circulation pump	8.3 kg	not relevant (set on base)	not relevant
dosing pump & chemical can	13.0 kg	128 N = 4*32 N	13 N = 4*3,3 N
electrical cabinet	38.0 kg	373 N = 4*93.6 N	38 N = 4*10 N

For load case combination 3 ($\theta(t) = \theta_{max} = 30^\circ$, rolling about the y-axis)

- ➔ global acceleration in z: $a_z = 11.18 \text{ m/s}^2$ acceleration factor: 1.14
- ➔ global acceleration in x: $a_x = 0.80 \text{ m/s}^2$ acceleration factor: 0.08

Component	mass	load in z-dir.	load in x-dir.
compressor	37.0 kg	414 N = 4*103.5 N	30 N = 4*7.5 N
permat pump	9.6 kg	107 N = 2*53.5 N	8 N = 2*4.0 N
circulation pump	8.3 kg	not relevant (set on base)	not relevant
dosing pump & chemical can	13.0 kg	145 N = 4*36 N	10 N = 4*2.5 N
electrical cabinet	38.0 kg	425 N = 4*106 N	30 N = 4*7.5 N

For load case combination 4 ($\theta(t) = \theta_{max} = 0^\circ$, rolling about the y-axis)

- ➔ global acceleration in z: $a_z = 9,81 \text{ m/s}^2$ acceleration factor: 1.0
- ➔ global acceleration in x: $a_x = 1,0 \text{ m/s}^2$ acceleration factor: 0.1

Component	mass	load in z-dir.	load in x-dir.
compressor	37.0 kg	363 N = 4*91 N	30 N = 4*9,3 N
permat pump	9.6 kg	94 N = 2*47 N	10 N = 2*5.0 N
circulation pump	8.3 kg	not relevant (set on base)	not relevant
dosing pump & chemical can	13.0 kg	128 N = 4*32 N	13 N = 4*3,3 N
electrical cabinet	38.0 kg	373 N = 4*93.6 N	38 N = 4*10 N

For load case combination 5 (uneven filling; $\theta(t) = \theta_{max} = 30^\circ$, rolling about the x-axis)

- ➔ Dead load of components equal to load case combination 1

4.3 Numerical model

The employed numerical model is described in section 3.3.1.

4.4 Load cases and load case combinations; safety factors

In stress and stability analyses the situation of maximum filling height is relevant for verifications. Thus, the case of half-filled tanks was not considered.

However, the effect of uneven filling of the two tanks was investigated by assuming the smaller tank (higher filling level) fully filled and the bigger tank empty (LCC 5).

In all load case combinations, a safety factor of 1.35 for dead load and of 1.5 for liquid pressure was taken into account.

Five load case combinations were considered for the simulation of the roll test:

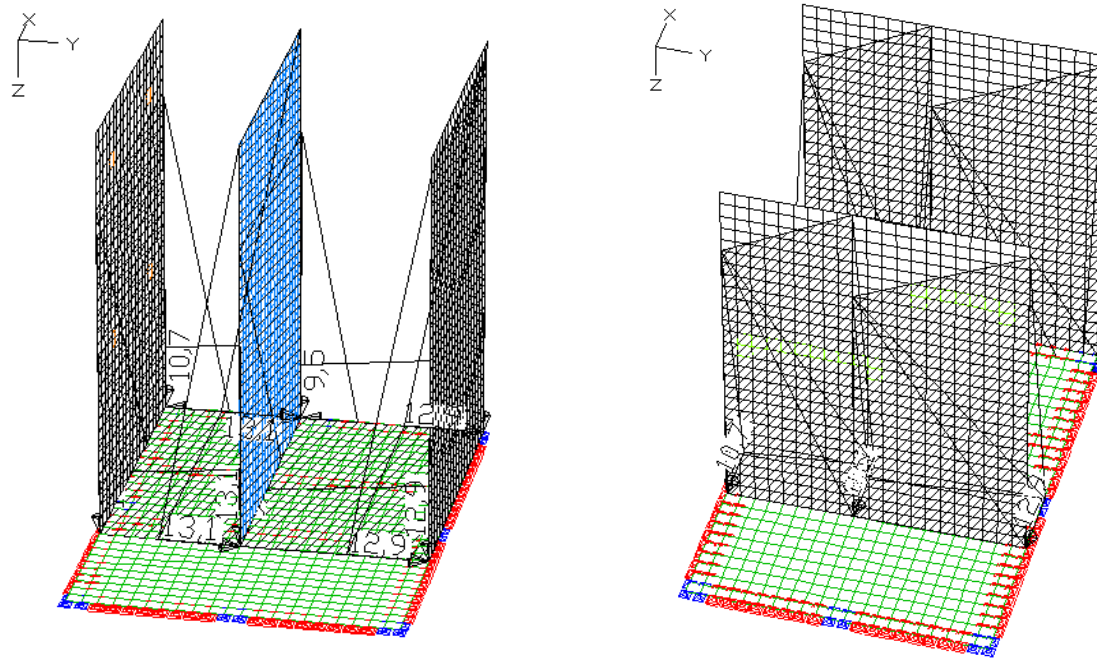
- | | | |
|-------------------------------|----------------------|---------------------|
| LCC 1: maximum filling height | rolling about x-axis | $\theta = 30^\circ$ |
| LCC 2: maximum filling height | Rolling about x-axis | $\theta = 0^\circ$ |
| LCC 3: maximum filling height | Rolling about y-axis | $\theta = 30^\circ$ |
| LCC 4: maximum filling height | Rolling about y-axis | $\theta = 0^\circ$ |
| LCC 5: uneven filling | Rolling about x-axis | $\theta = 30^\circ$ |

For all load case combinations, the resulting deformations and equivalent stresses were determined and a linear buckling analysis was carried out.

4.4.1 Load case combination 1: Rolling about x-axis, $\theta = 30^\circ$

Dead load of components is considered as point loads on the component supports according to section 4.2.3.

Liquid pressure on the tank walls is considered according to section 4.2.2 (see Figure 4-4).



left and right side + internal wall + bottom

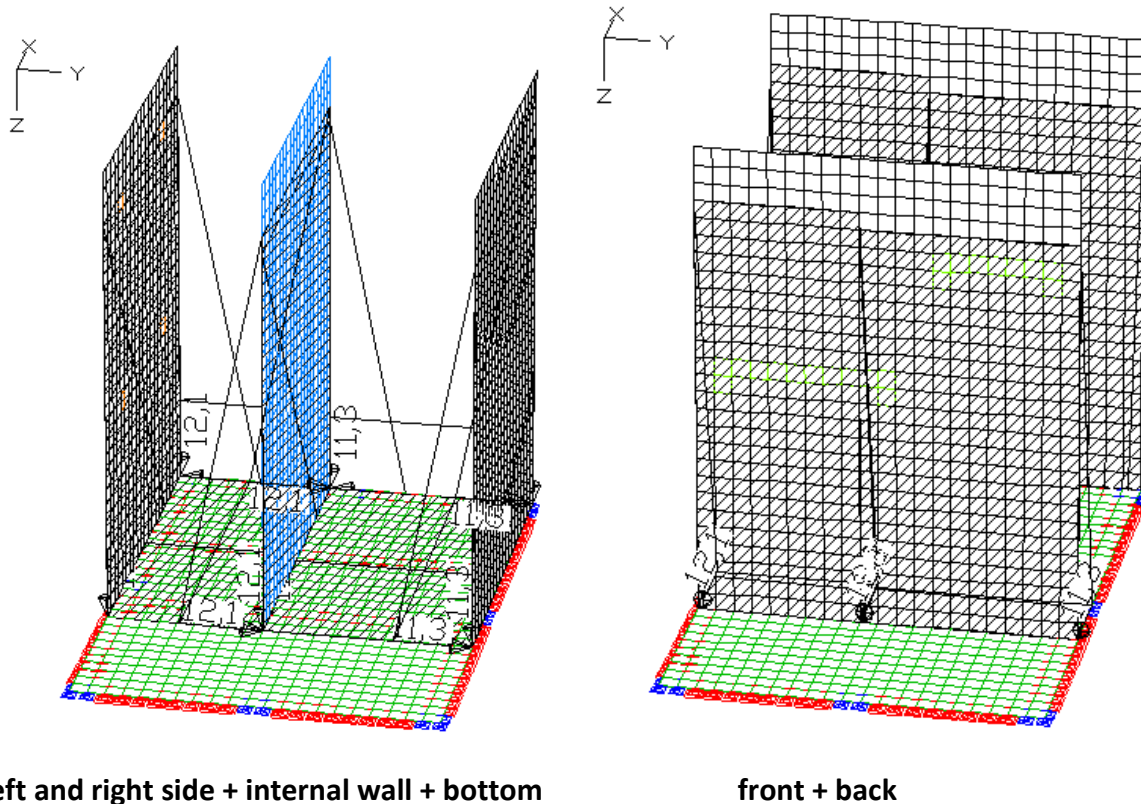
front + back

Figure 4-4: Liquid pressure in load case combination 1

4.4.2 Load case combination 2: Rolling about x-axis, $\theta = 0^\circ$

Dead load of components is considered as point loads on the component supports according to section 4.2.3.

Liquid pressure on the tank walls is considered according to section 4.2.2 (see Figure 4-5).



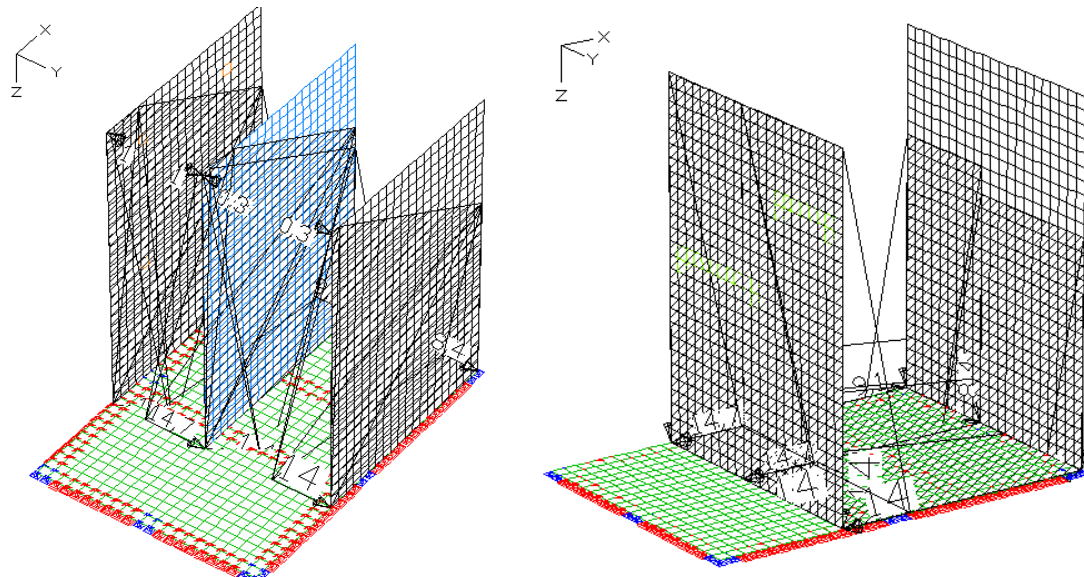
left and right side + internal wall + bottom **front + back**

Figure 4-5: Liquid pressure in load case combination 2

4.4.3 Load case combination 3: Rolling about y-axis, $\theta = 30^\circ$

Dead load of components is considered as point loads on the component supports according to section 4.2.3.

Liquid pressure on the tank walls is considered according to section 4.2.2 (see Figure 4-6). The small liquid pressure on the tank top is not applied to the FE-model as it is not relevant for the stress verifications.



left and right side + internal wall

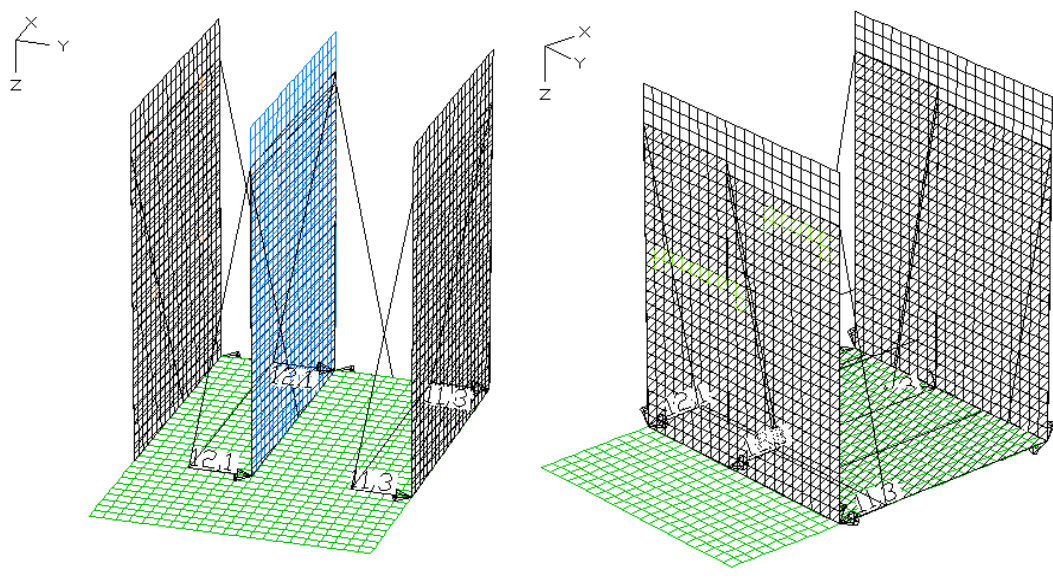
front + back + bottom

Figure 4-6: Liquid pressure in load case combination 3

4.4.4 Load case combination 4: Rolling about y-axis, $\theta = 0^\circ$

Dead load of components is considered according to section 4.2.3.

Liquid pressure on the tank walls is considered according to section 4.2.2 (see Figure 4-7).



left and right side + internal wall

front + back + bottom

Figure 4-7: Liquid pressure in load case combination 4

4.4.5 Load case combination 5: Uneven filling; rolling about x-axis, $\theta = 30^\circ$

Dead load of components is considered according to section 4.2.3.

Liquid pressure on the tank walls is considered according to section 4.2.2 (see Figure 4-8).

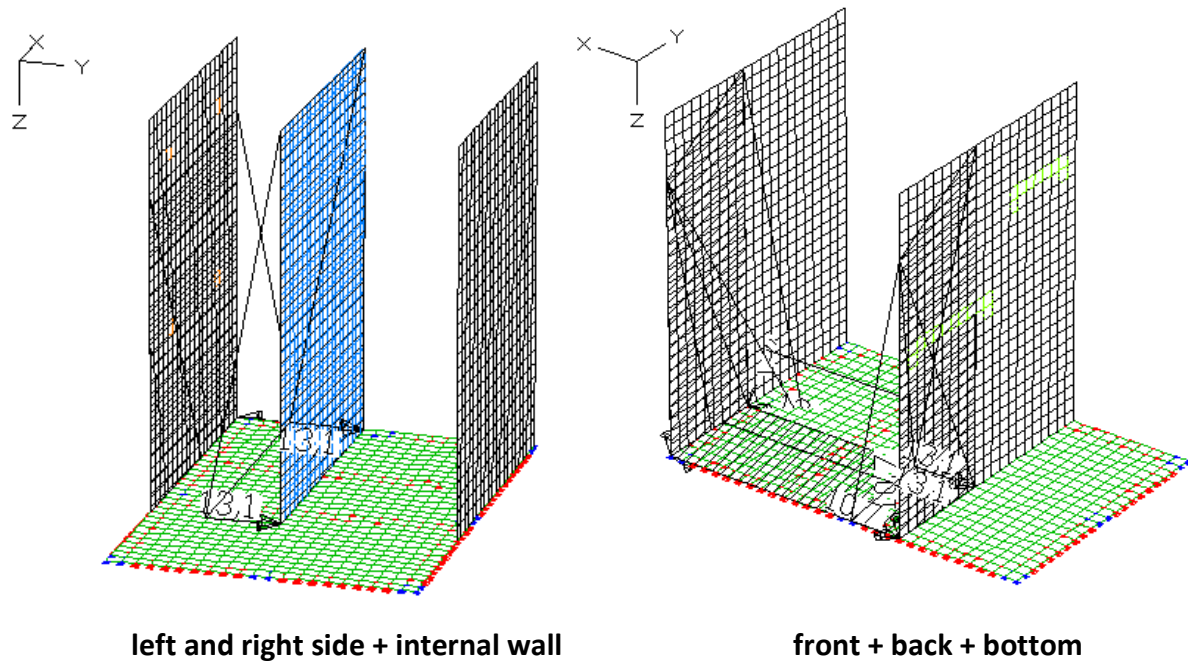


Figure 4-8: Liquid pressure in load case combination 5

4.5 Results and verifications

As expected, the decisive load case combinations are rolling about the x-axis at the maximum roll angle of 30° (LCC 1) and uneven filling of the tanks (LCC 5). The first one leads to a maximum loading of the side shell without stiffeners, the second one to the maximum loading of the internal wall.

Figure 4-9 and Figure 4-10 in section 4.5.1 show the maximum deformations due to LCC 1 and LCC 5 respectively.

Section 4.5.2 highlights the maximum equivalent stresses in all load case combinations.

Section 4.5.3 deals with the anchorage of the device to the ship.

4.5.1 Maximum deformations

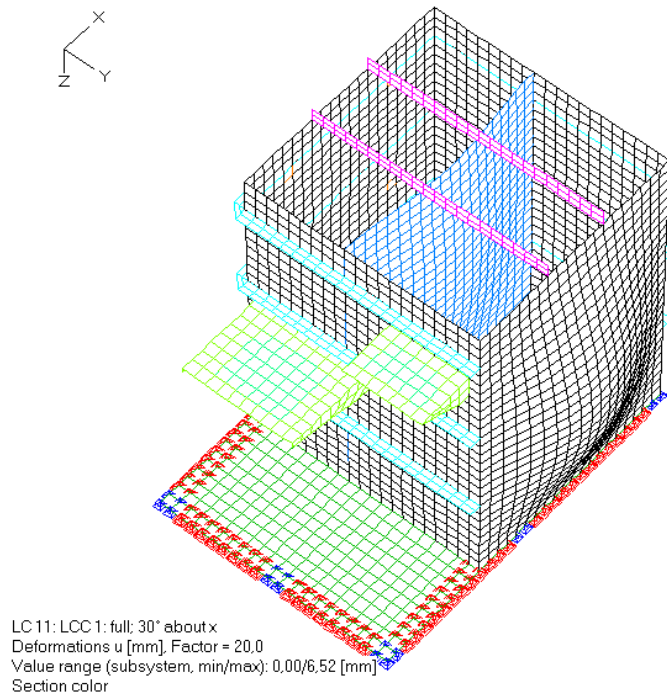


Figure 4-9: Maximum shell deformation due to roll angle 30° about the x-axis: 6,5 mm

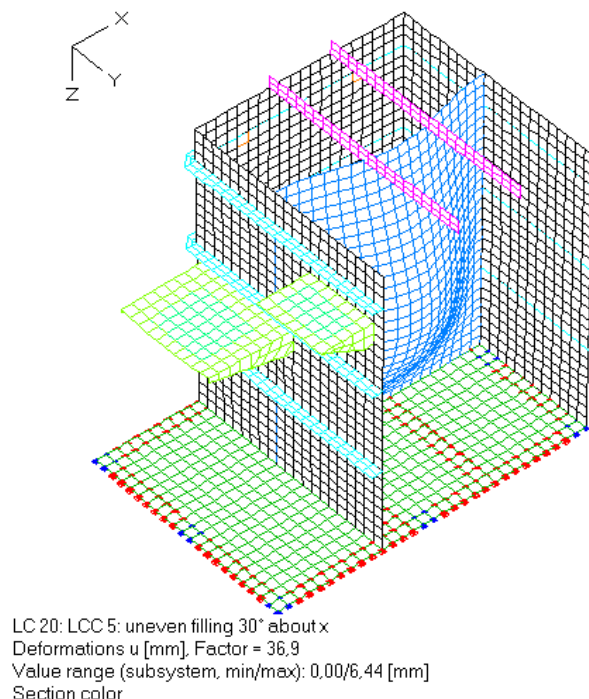


Figure 4-10: Maximum shell deformation due to roll angle 30° about the x-axis at uneven filling of the tanks: 6,4 mm

4.5.2 Equivalent stresses

Due to all load case combinations the maximum allowable stress is met.

Maximum equivalent stresses in a fully filled tank constellation occur on the right side of the device (outer wall of tank 2) at the connections of the right side to the front, back and bottom. It results from the deformation of the non-stiffened outer tank wall (Figure 4-11 to Figure 4-14).

In the unevenly filled situation, maximum equivalent stresses occur on the interior wall at the connections to the front and the back (Figure 4-15).

The effect of tangential acceleration and gravity on the attached component is small compared to the effect of the accelerated liquid.

Equivalent stresses due to all five load case combinations are shown in the following figures.

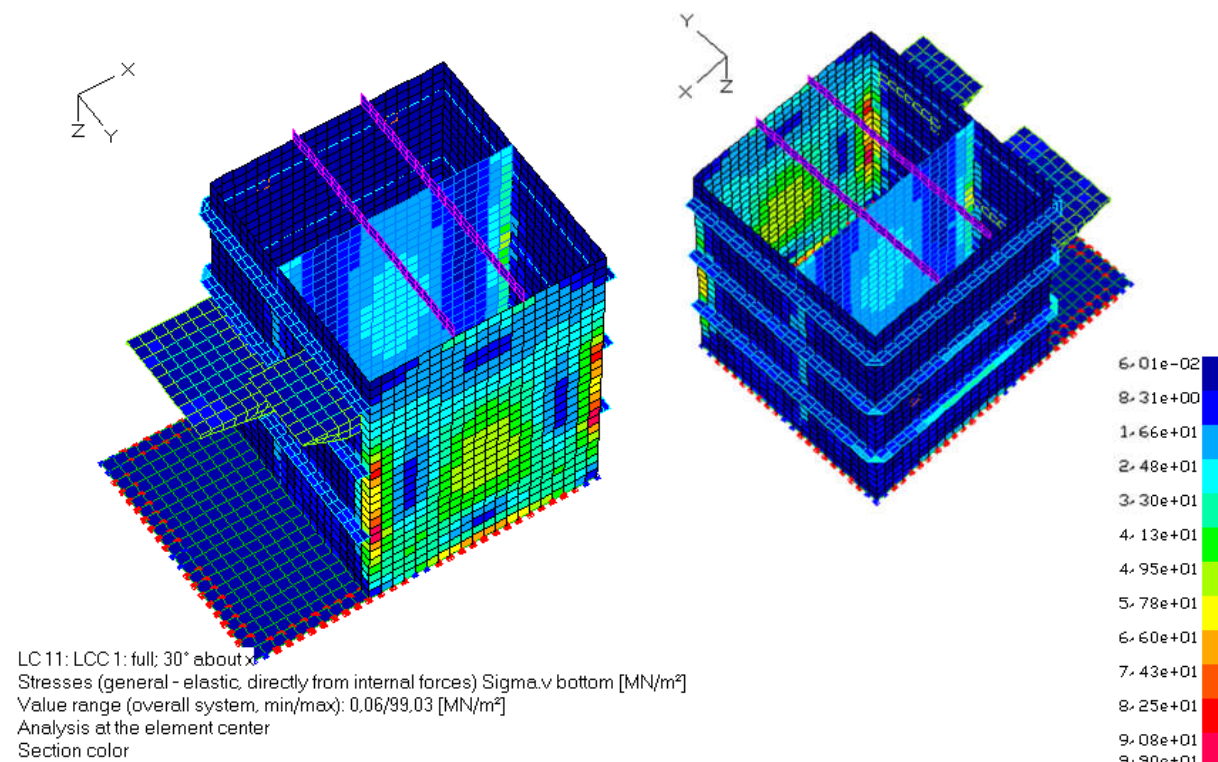
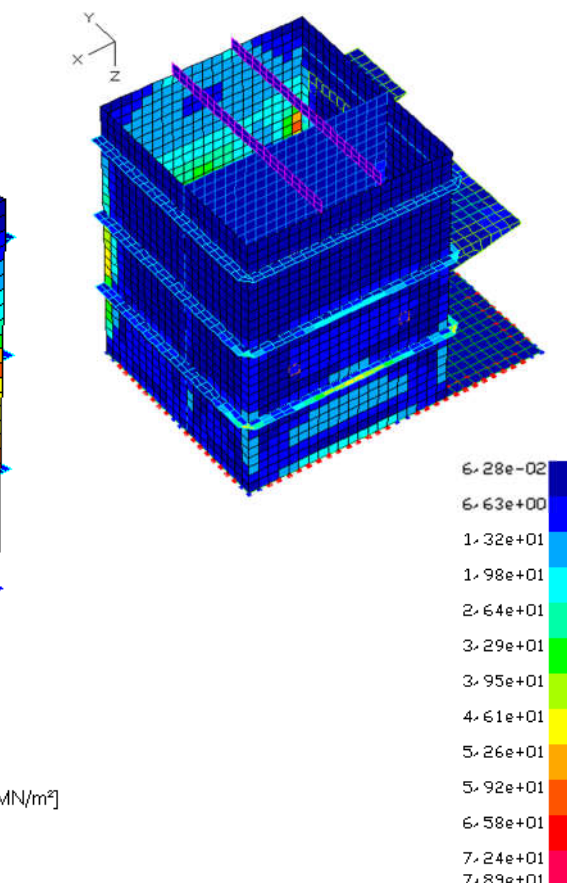


Figure 4-11: LCC 1: Maximum equivalent stresses due to liquid pressure and dead load at roll angle 30° about the x-axis: 99 MN/m² < 172 MN/m² ✓



LC 12: LCC 2: full; 0° about x

Stresses (general - elastic, directly from internal forces) Sigma.v bottom [MN/m²]

Value range (overall system, min/max): 0,06/78,93 [MN/m²]

Analysis at the element center

Section color

Figure 4-12: LCC 2: Maximum equivalent stresses due to liquid pressure and dead load at roll angle 0° about the x-axis: 79 MN/m² < 172 MN/m² ✓

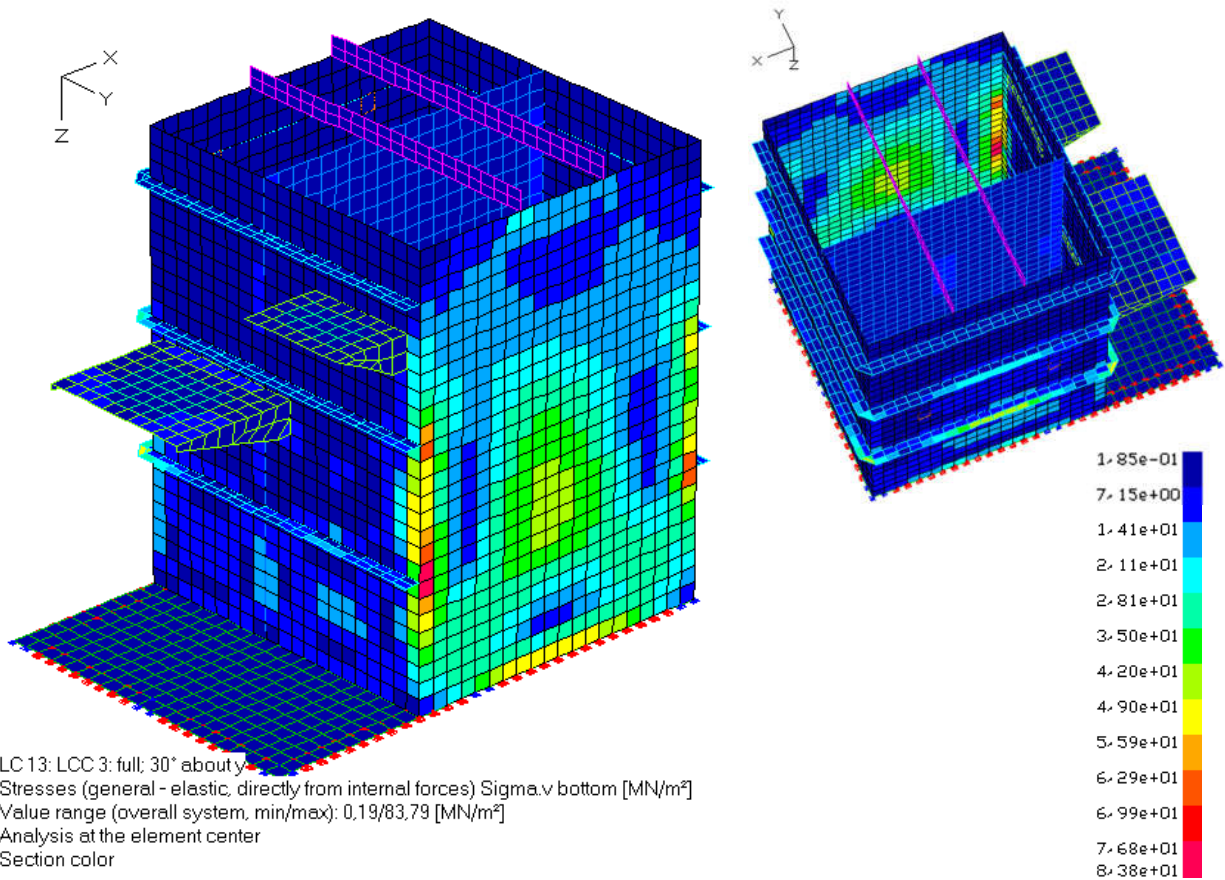


Figure 4-13: LCC 3: Maximum equivalent stresses due to liquid pressure and dead load at roll angle 30° about the y-axis: 84 MN/m² < 172 MN/m² ✓

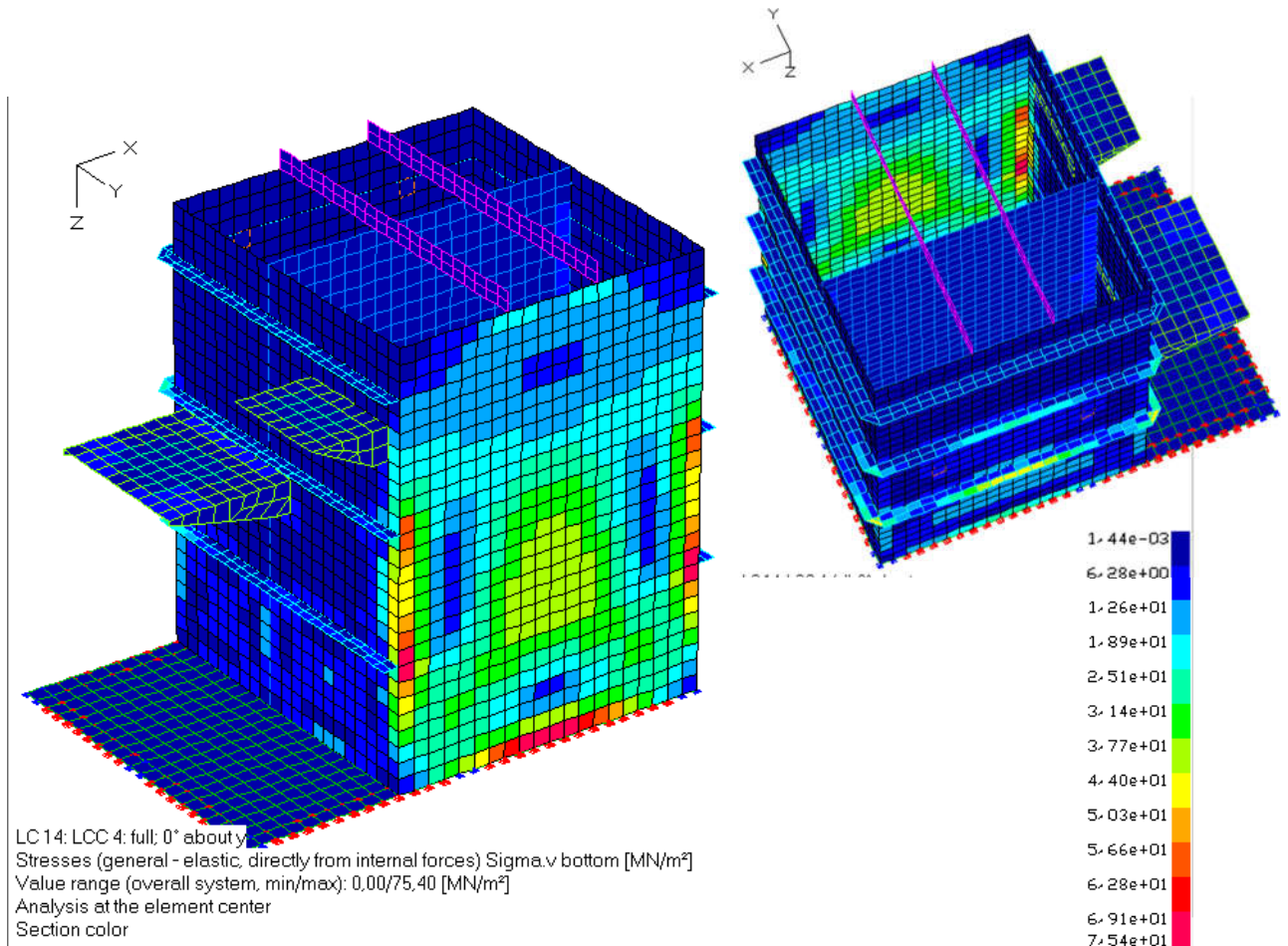


Figure 4-14: LCC 4: Maximum equivalent stresses due to liquid pressure and dead load at roll angle 0° about the y-axis: 78,5 MN/m² < 172 MN/m² ✓

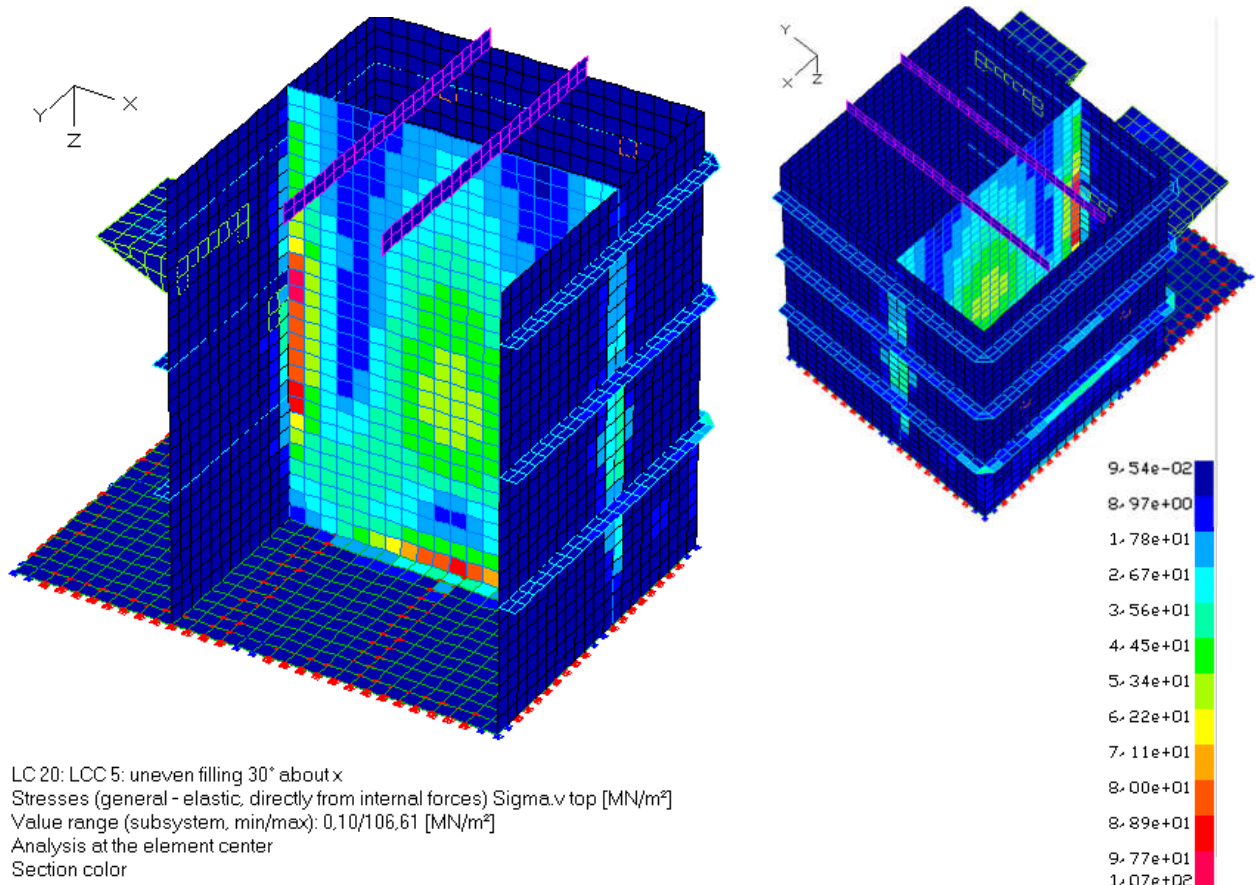
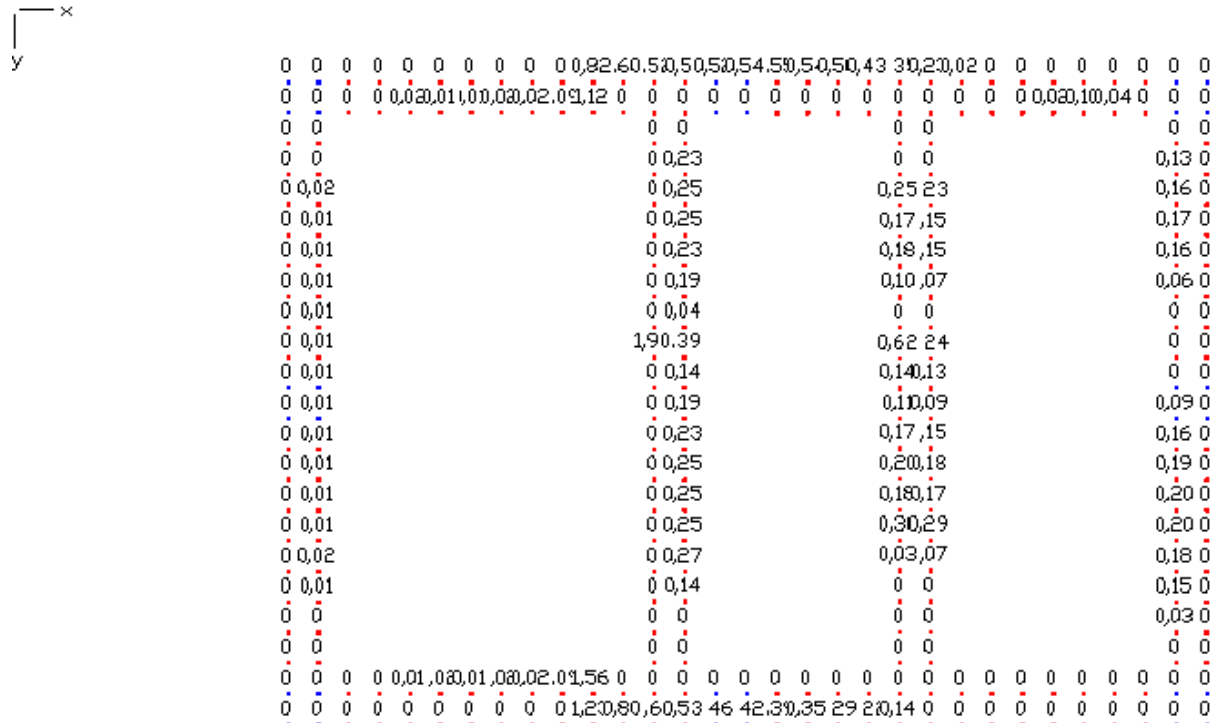


Figure 4-15: LCC 5: Maximum equivalent stresses due to liquid pressure (uneven filling) & dead load at roll angle 30° about the x-axis: 107 MN/m² < 172 MN/m² ✓

4.5.3 Anchorage

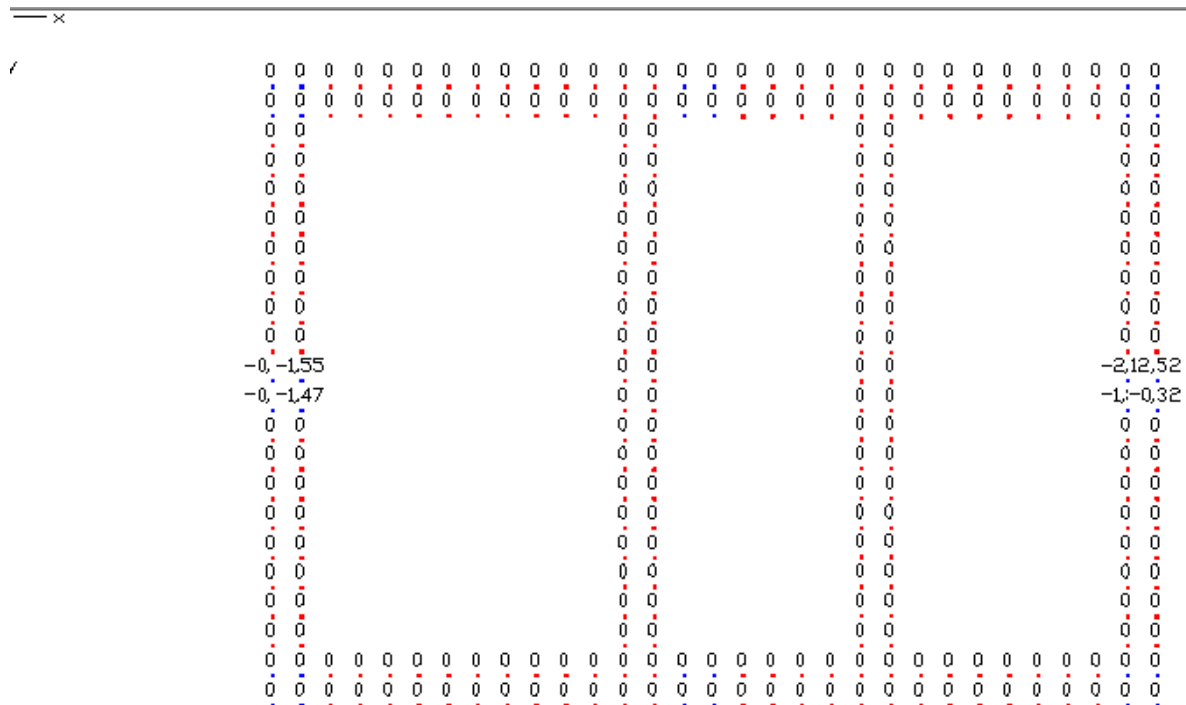


LC 13: LCC 3: full; 30° about y-axis

Support reactions in the local system Rz(l) [kN]

Sum in the global system Rz(g) = 27,42 [kN]

**Figure 4-16: Maximum vertical reaction force
(load case combination 3: full; 30° about y-axis)
No vertical tension forces; this results from vertical (downward) liquid pressure that is higher than the tension force due to overturning moment**

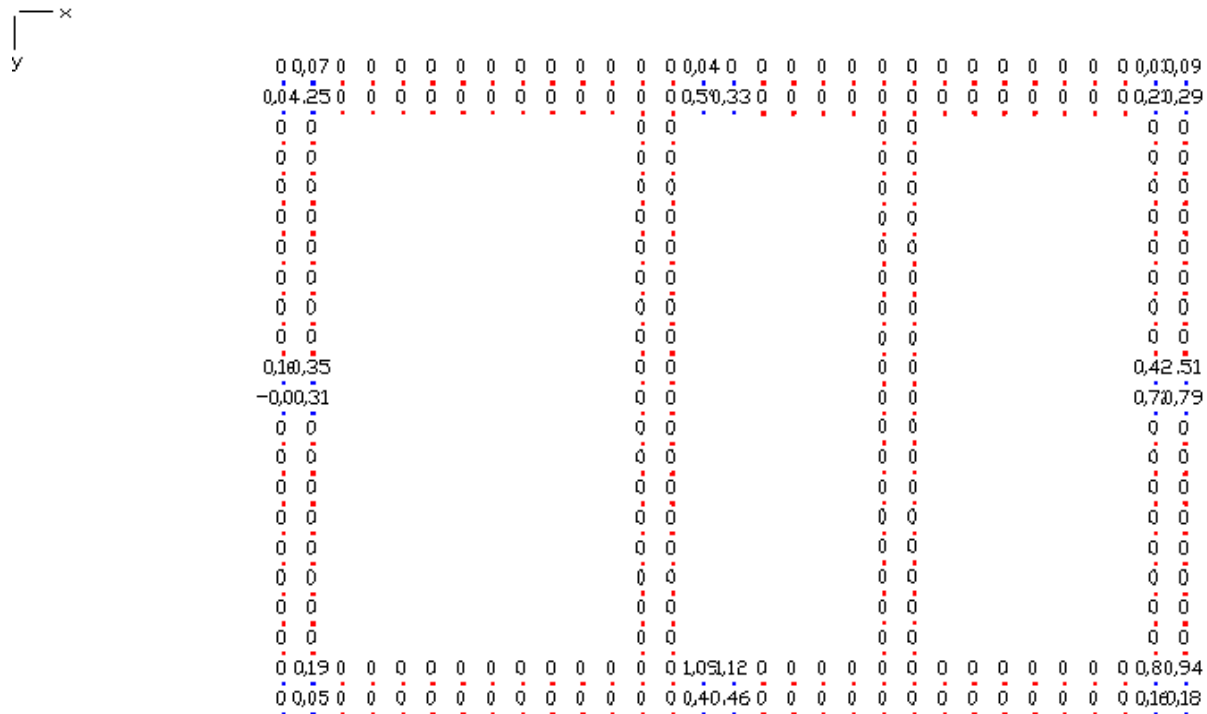


LC13: LCC 3: full; 30° about y

Support reactions in the local system $P_x(l)$ [kN]

Sum in the global system $P_x(g) = -8,52 \text{ [kN]}$

Figure 4-17: Maximum horizontal reaction force in global x-direction
 (load case combination 3: full; 30° about y-axis)
 Maximum horizontal load on screw: 4,8 kN



LC11:LCC1:full; 30° about x

Support reactions in the local system $R_y(l)$ [kN]

Sum in the global system Ry(g) = 10,58 [kN]

Figure 4-18: Maximum horizontal reaction force in global y-direction
 (load case combination 1: full; 30° about x-axis)
 Maximum horizontal load on screw: 2,4 kN

The maximum horizontal (shear) force to be taken on by screw (conservative combination of maximum forces in x- and y-direction regardless of load case combination) results to:

$$F_{h,max} = \sqrt{4,8^2 + 2,4^2} = 5,4 \text{ kN}$$

Additionally, a minimum vertical tension force of 10 kN per screw / bolt should be considered for the dimensioning of the anchorage.

4.5.4 Stability

Additionally to the requirements of CFR 33 §59.107, linear buckling analyses were carried out for all load cases to determine the stability safety of the device. In all cases the buckling load factor was determined to be far beyond the limit value of 1.0. The following figures show the relevant buckling eigenmodes and the corresponding load factors.

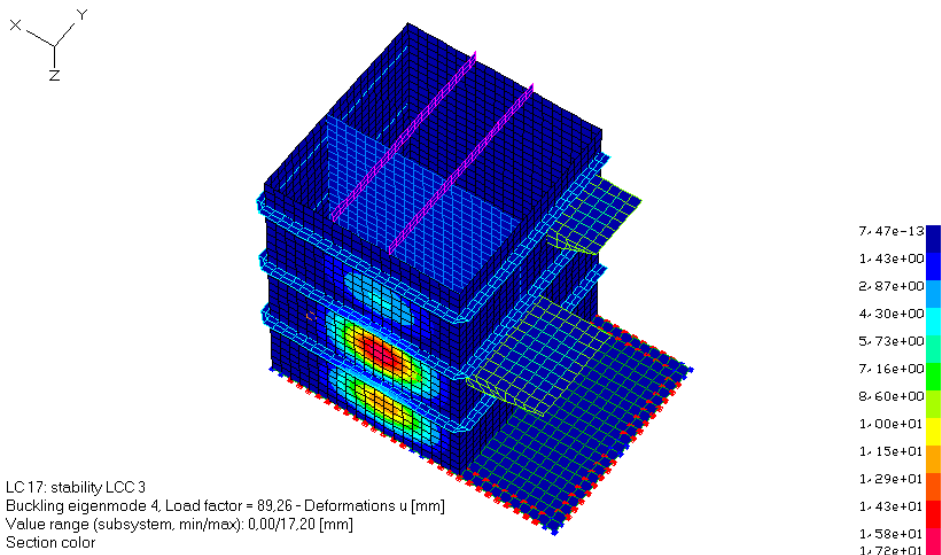


**Figure 4-19: Relevant buckling eigenmode for left wall
loading according to load case combination 3: full; roll 30° about y-axis
load factor 89 > 1 ✓**

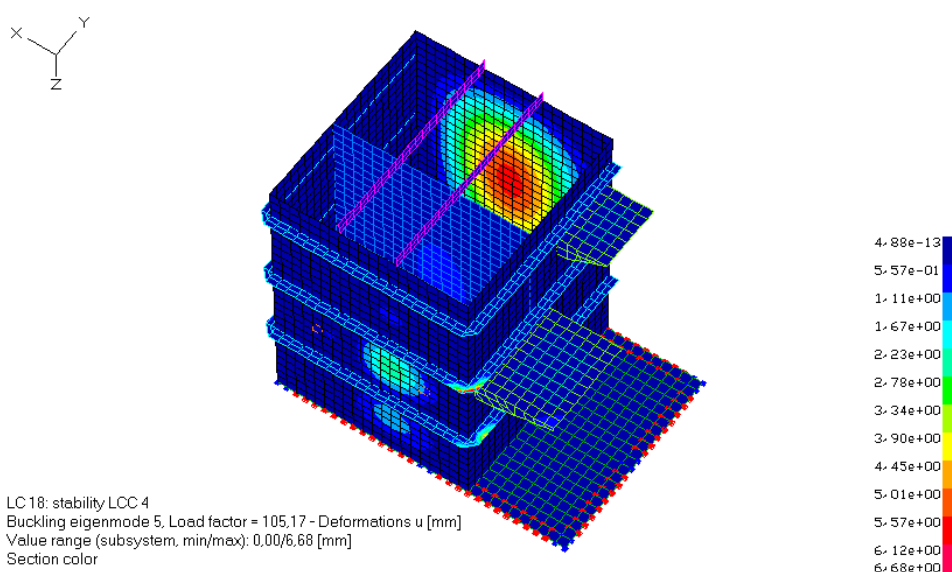


**Figure 4-20: Relevant buckling eigenmode for right wall
loading according to load case combination 4: full; roll 0° about y-axis
load factor 105 > 1 ✓**

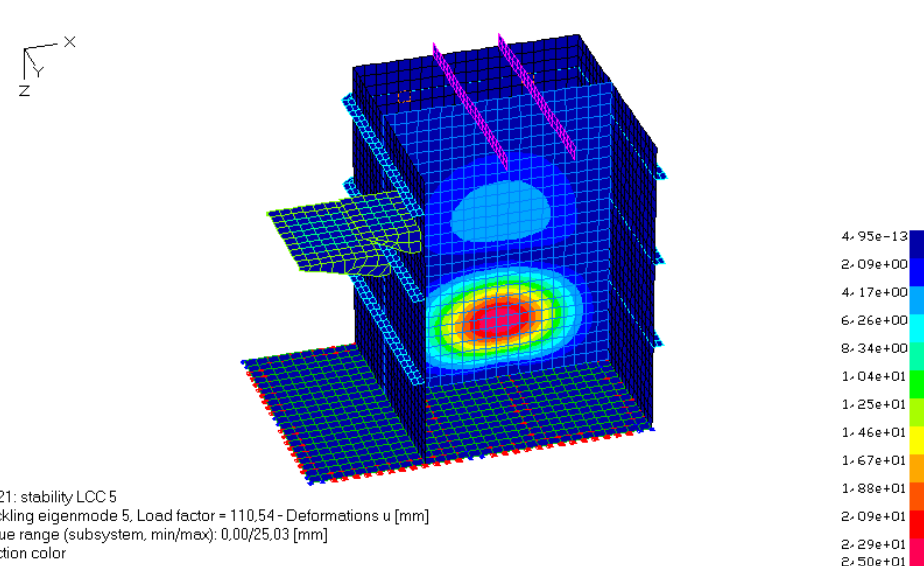


Figure 4-21: Relevant buckling eigenmode for internal wall loading according to load case combination 5: uneven filling; roll 30° about x-axis; load factor 111 > 1 ✓

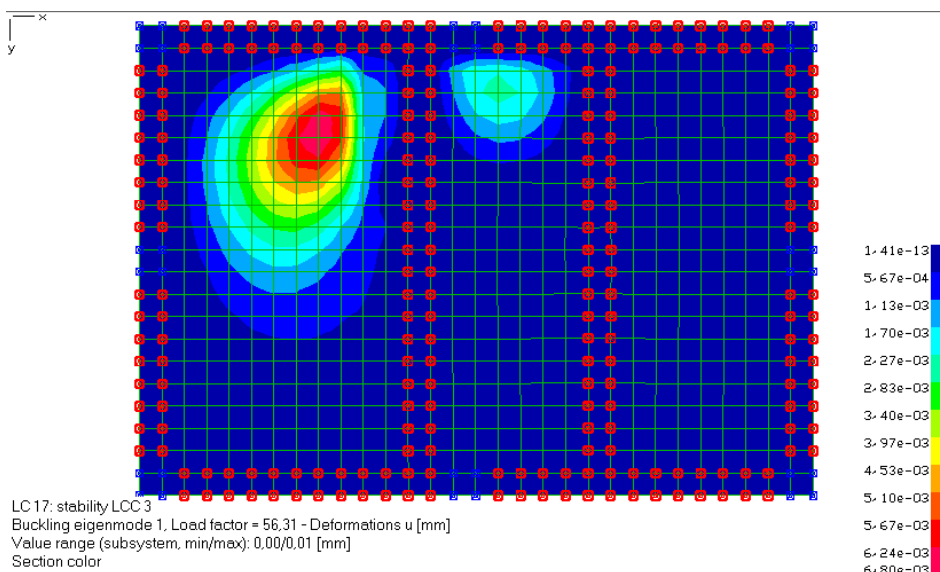


Figure 4-22: Relevant buckling eigenmode for bottom shell loading according to load case combination 3: full; roll 30° about y-axis load factor 56 > 1 ✓

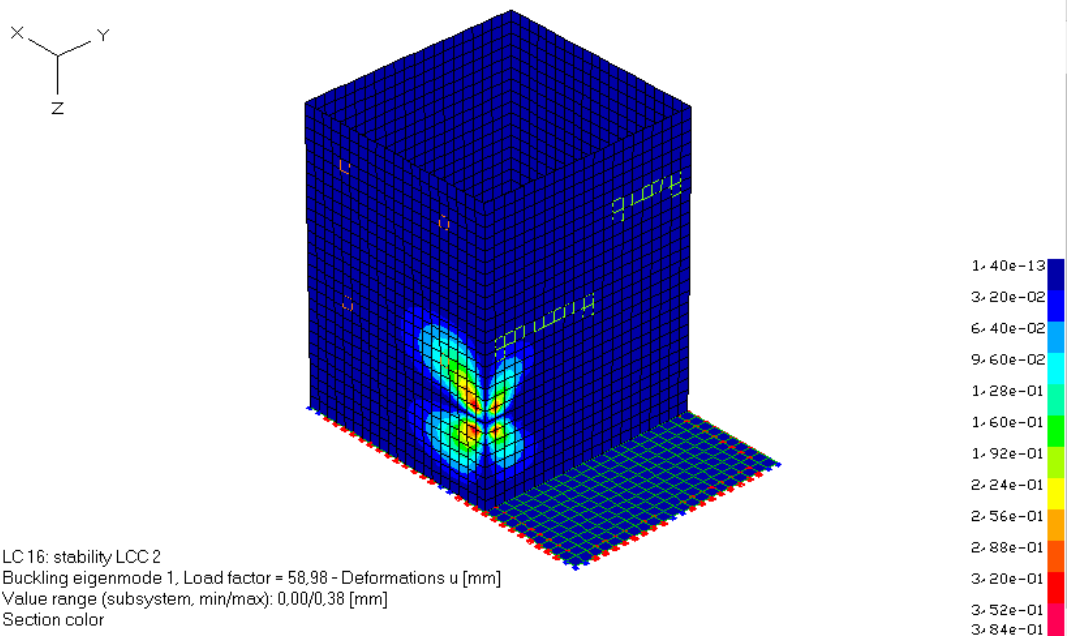


Figure 4-23: Relevant buckling eigenmode for front shell loading according to load case combination 2: full; roll 0° about x-axis load factor 59 > 1 ✓

5. Summary

The scope of this report was the investigation and verification of the PIA test plant produced by Gertsen&Olufsen, Hørsholm, Denmark regarding shock test and rolling test on a numerical/ analytical basis as alternative to the experimental test procedure of 33 CFR §159.105 and §159.107.

Conclusion on shock test

The relevant loading and the equivalent stresses due to a sinusoidal acceleration of 10 g within a duration of 25 ms were determined combining shock spectra analyses on single degree of freedom systems (depicting the externally mounted heavy components) and finite element analyses of the tank shell (see section 3).

It was proven that the resulting equivalent stresses due to shock loading are smaller than the allowable stresses (see section 3.3.2).

Further, it was verified that occurring loads onto the component shelves are safely transferred to the tank shell provided that the shelves are welded to the shell with a continuous weld of at least 3mm on both sides of the shelves (see section 0). The manufacturer is responsible for executing a minimum weld thickness of 3mm on both sides of the shelves.

Conclusion on roll test

The relevant loading and the equivalent stresses due to rolling action of the device were determined based on kinematic considerations and in accordance with the MSD Laboratory Technical Information Sheet no. 5 [2] (see section 4.2).

Five load case combinations were considered to investigate the response to rolling about the x-axis (30° angle + 0° angle) and the y-axis (30° angle + 0° angle) as well as the effect of uneven filling (30° about the x-axis; one tank empty) (see section 4.4).

It was proven that the resulting equivalent stresses due to rolling action are smaller than the allowable stresses (see section 4.5.2).

The maximum loading of the anchorage of the device was determined for all load cases and must be safely transferred to the ground / ship by adequately dimensioned and tightly fastened screws.

Additionally to the requirements of CFR 33 §59.107, the safety against buckling was proven by linear buckling analyses (see section 4.5.4).

General remarks

According to Gertsen&Olufson the internal wall between the two containers is not structurally connected to the top of the tank. In order to assure leak tightness in case of rolling the gap between internal wall and top should be sealed. The maximum horizontal deformation of the upper edge of the internal wall was calculated to 2,35 mm (in load case combination 1 – 30° roll about x-axis). The seal must be able to bear such deformations.

The shelf for the dosing pump and the chemical can was not specified by the manufacturer. It was assumed rigid for the transfer of shock and roll loads. The manufacturer must ensure that the shelf is able to bear and safely transfer shock acceleration of the supported components and that pump and can are tightly attached to the shelf.

The entire device must be safely anchored at the floor / ship. Minimum anchor forces for each screw / bolt are given in section 4.5.3.

Fatigue due to continuous loading was not within the scope of this investigation.

The operability of the electrical control panel itself must be confirmed by the producer of the panel or verified by the shock test procedure described in 33 CFR §159.105 and is not within the scope of this investigation.

Herzogenrath, 15.06.2016



Dr.-Ing. B. Holtschoppen



Prof. Dr.-Ing. C. Butenweg

EC-TYPE EXAMINATION CERTIFICATE (MODULE B)

Application of: Directive 2014/90/EU of 23 July 2014 on marine equipment (MED), issued as "Forskrift om Skipsutstyr" by the Norwegian Maritime Authority. This Certificate is issued by DNV GL AS under the authority of the Government of the Kingdom of Norway.

This is to certify:

That the Sewage systems

with type designation(s)

**NX10-C/N, NX20-C/N, NX25-C/N, NX30-C/N, NX35-C/N, NX40-C/N, NX45-C/N, NX50-C/N,
NX55-C/N, NX60-C/N, NX65-C/N, NX70-C/N, NX75-C/N, NX80-C/N, NX90-C/N**

Issued to

Gertsen & Olufsen AS

Allerød, Denmark

is found to comply with the requirements in the following Regulations/Standards:

Regulation **(EU) 2015/559**,

NX-C:

Annex A.1, item No. A.1/2.6 and Annex B, Module B in the Directive. Marpol 73/78 as amended, Annex IV Regulation 9, IMO Res. MEPC.227(64) with the exception of Section 4.2.

NX-N:

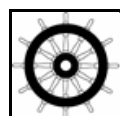
Annex A.1, item No. A.1/2.6 and Annex B, Module B in the Directive. Marpol 73/78 as amended, Annex IV Regulation 9, IMO Res. MEPC.227(64)

Further details of the equipment and conditions for certification are given overleaf.

This Certificate is valid until **2022-03-06**.

Issued at **Høvik** on **2017-03-07**

DNV GL local station:
Copenhagen



for **DNV GL AS**

Approval Engineer:
Pål Evang Nundal

Notified Body
No.: **0575**

Vidar Dolonen
Head of Notified Body

The mark of conformity may only be affixed to the above type approved equipment and a Manufacturer's Declaration of Conformity issued when the production-surveillance module (D, E or F) of Annex B of the MED is fully complied with and controlled by a written inspection agreement with a Notified Body. The product liability rests with the manufacturer or his representative in accordance with Directive 2014/90/EU.

This certificate is valid for equipment, which is conform to the approved type. The manufacturer shall inform DNV GL AS of any changes to the approved equipment. This certificate remains valid unless suspended, withdrawn, recalled or cancelled.

Should the specified regulations or standards be amended during the validity of this certificate, the product is to be re-approved before being placed on board a vessel to which the amended regulations or standards apply.



Form code: MED 201.NOR

Revision: 2016-12

www.dnvg.com

Page 1 of 6

© DNV GL 2014. DNV GL and the Horizon Graphic are trademarks of DNV GL AS.

Product description

The equipment is intended for installation onboard ships to provide sewage treatment for the protection of the marine environment.

The sewage treatment plant is a membrane bioreactor (MBR) type, which combines biological treatment with membrane filtration.

The sewage treatment plant can be delivered with two different configurations.

- **NX-C:** According to MEPC.227(64) excluding section 4.2.
- **NX-N:** According to MEPC.227(64) including section 4.2.

Application/Limitation

Model	NX-C		NX-N				
	Design Hydraulic load (m ³ /day)	Organic load (BOD kg/day)	Model	Design Hydraulic load (m ³ /day)	Organic load (BOD kg/day)	Max. Nitrogen (kg TOT- N/day)	Max. Phosphorus (kg TOT- P/day)
NX10-C	1,7	0,6	NX10-N	-	-	-	-
NX20-C	3,3	1,17	NX20-N	1,16	0,56	0,11	0,02
NX25-C	6,6	2,34	NX25-N	2,54	1,22	0,24	0,04
NX30-C	9,9	3,51	NX30-N	3,9	1,87	0,37	0,05
NX35-C	13,2	4,69	NX35-N	5,08	2,44	0,49	0,07
NX40-C	16,5	5,86	NX40-N	6,45	3,09	0,62	0,09
NX45-C	19,8	7,03	NX45-N	7,6	3,64	0,73	0,11
NX50-C	26,4	9,37	NX50-N	10,12	4,85	0,97	0,14
NX55-C	39,6	14,06	NX55-N	15,2	7,29	1,46	0,21
NX60-C	52,8	18,74	NX60-N	20,06	9,62	1,92	0,28
NX65-C	79,2	28,12	NX65-N	30,18	14,47	2,89	0,42
NX70-C	118,8	42,17	NX70-N	45,17	21,66	4,33	0,63
NX75-C	264	93,72	NX75-N	100,26	48,07	9,61	1,39
NX80-C	495	175,73	NX80-N	187,89	90,09	18,02	2,61
NX90-C	990	351,45	NX90-N	375,75	180,17	36,03	5,22

The Administration confirms that the sewage treatment plant can operate at angles of inclination of 30° in any plane from the normal operating position.

Control system:

The environmental test was performed on the components below:

Gertsen & Olufsen control cabinet: TFCTEH

Mitsubishi inverter HW type: FR-D740-SC

Mitsubishi PLC HW Type: FX3G

If other components are used they shall carry a certificate of successful environmental testing according to part 3 of MEPC.107(49), performed at an accredited lab.

Type Examination documentation

Drawing No.:	Date:	Revision:	Title:
1502-135-5	23.02.2017	5	P&ID without N&P (NX-C)
1502-135-5	23.02.2017	5	P&ID Full (NX-P)
191-1502-GA-01	29.05.2016	-	General arrangement drawing
x,y,z, Size-00	23.02.2017	0	Size overview
1502-Equipment-00	23.02.2017	0	Equipment location
1910134	15.02.2016	0	Nameplate
NX10	23.02.2017	0	Proces volume
NX20	23.02.2017	0	Proces volume
NX25	23.02.2017	0	Proces volume
NX30	23.02.2017	0	Proces volume
NX35	23.02.2017	0	Proces volume
NX40	23.02.2017	0	Proces volume
NX45	23.02.2017	0	Proces volume
NX50	23.02.2017	0	Proces volume
NX55	23.02.2017	0	Proces volume
NX60	23.02.2017	0	Proces volume
NX65	23.02.2017	0	Proces volume
NX70	23.02.2017	0	Proces volume
NX75	23.02.2017	0	Proces volume
NX80	23.02.2017	0	Proces volume
NX90	23.02.2017	0	Proces volume
0000E201	01.03.2017	1	NX test plant (electrical drawings)

Instruction manual NX-C:

Operation & Maintenance Manual for Gertsen & Olufsen AS Sewage Treatment Plant NX series - Carbon Reduction

Instruction manual NX-N:

Operation & Maintenance Manual for Gertsen & Olufsen AS Sewage Treatment Plant NX series - Carbon and nutrient reduction

Tests carried out

Performance test of type NX-C, according to MEPC.227(64) excluding section. 4.2:

Prüfinstitut für Abwassertechnik GmbH (PIA), *Test of a Marine Sanitation Device of Gertsen & Olufsen*, Report No.: PIA2016-AT1602-10121-03 – Version 3, Dated 2016-12-20.

Performance test of type NX-N, according to MEPC.227(64) including section. 4.2:

Prüfinstitut für Abwassertechnik GmbH (PIA), *Test of a Marine Sanitation Device of Gertsen & Olufsen*, Report No.: PIA2016-AT1602-10122-02 – Version 2, Dated 2016-12-20.

Environmental test according to MEPC.107(49):

Delta, *Test for Marine Type Approval of control cabinet for sewage treatment system, type TFCTEH*, Report No.: DANAK-19/16866, Dated 2016-09-13.

Marking of product

For traceability to this type approval, each unit is to be marked with;

- Manufacturer's name or trade mark
- Type designation (including suffix "-C" or "-N")
- Serial No.
- Capacity
- Mark of Conformity

APPENDIX I – test data for NX-C

Test results and details of tests conducted on samples from the sewage treatment plant in accordance with resolution MEPC.227(64) excluding section 4.2:

<u>Sewage treatment plant, Type</u>	<u>NX-C</u>
<u>Manufactured by</u>	<u>Gertsen & Olufsen</u>
<u>Organization conducting the test</u>	<u>PIA</u>
<u>Designed hydraulic loading</u>	<u>3,30 m³/day</u>
<u>Designed organic loading</u>	<u>2,21 kg/day BOD</u>
<u>Number of effluent samples tested</u>	<u>40</u>
<u>Number of influent samples tested</u>	<u>40</u>
<u>Total suspended solids influent quality</u>	<u>515 mg/l</u>
<u>BOD5 without nitrification influent quality</u>	<u>341 mg/l</u>
<u>Maximum hydraulic loading</u>	<u>7,92 m³/day</u>
<u>Minimum hydraulic loading</u>	<u>0,24 m³/day</u>
<u>Average hydraulic loading (Q_i)</u>	<u>3,30 m³/day</u>
<u>Effluent flow (Q_e)</u>	<u>3,30 m³/day</u>
<u>Dilution compensation factor (Q_i/Q_e)</u>	<u>1</u>
<u>Geometric mean of total suspended solids</u>	<u>3 mg/l</u>
<u>Geometric mean of the thermotolerant coliform count</u>	<u>4 coliforms/100 ml</u>
<u>Geometric mean of BOD5 without nitrification</u>	<u>1,6 mg/l</u>
<u>Geometric mean of COD</u>	<u>21,5 mg/l</u>
<u>Maximum pH:</u>	<u>7,6</u>
<u>Minimum pH:</u>	<u>6,9</u>
<u>Type of disinfectant used</u>	<u>None</u>
<u>Was the sewage treatment plant tested with:</u>	
<u>Fresh water flushing?</u>	<u>No</u>
<u>Salt water flushing?</u>	<u>No</u>
<u>Fresh and salt water flushing?</u>	<u>No</u>
<u>Grey water added?</u>	<u>No</u>
<u>Was the sewage treatment plant tested against the environmental conditions specified in section 5.9 of resolution MEPC.227(64):</u>	
<u>Temperature</u>	<u>Yes</u>
<u>Humidity</u>	<u>Yes</u>
<u>Inclination</u>	<u>Yes</u>
<u>Vibration</u>	<u>Yes</u>
<u>Reliability of Electrical and Electronic Equipment</u>	<u>Yes</u>

APPENDIX II – test data for NX-N

Test results and details of tests conducted on samples from the sewage treatment plant in accordance with resolution MEPC.227(64) including section 4.2:

<u>Sewage treatment plant, Type</u>	<u>NX-N</u>
<u>Manufactured by</u>	<u>Gertsen & Olufsen</u>
<u>Organization conducting the test</u>	<u>PIA</u>
<u>Designed hydraulic loading</u>	<u>2,20 m³/day</u>
<u>Designed organic loading</u>	<u>1,05 kg/day BOD</u>
<u>Number of effluent samples tested</u>	<u>40</u>
<u>Number of influent samples tested</u>	<u>40</u>
<u>Total suspended solids influent quality</u>	<u>605 mg/l</u>
<u>Total nitrogen influent quality</u>	<u>96 mg/l as nitrogen</u>
<u>Total phosphorus influent quality</u>	<u>14 mg/l as phosphorus</u>
<u>BOD5 without nitrification influent quality</u>	<u>425 mg/l</u>
<u>Maximum hydraulic loading</u>	<u>5,28 m³/day</u>
<u>Minimum hydraulic loading</u>	<u>0,24 m³/day</u>
<u>Average hydraulic loading (Q_i)</u>	<u>2,2 m³/day</u>
<u>Effluent flow (Q_e)</u>	<u>2,2 m³/day</u>
<u>Dilution compensation factor (Q_i/Q_e)</u>	<u>1</u>
<u>Geometric mean of total suspended solids</u>	<u>2,8 mg/l</u>
<u>Geometric mean of the thermotolerant coliform count</u>	<u>2,7 coliforms/100 ml</u>
<u>Geometric mean of BOD5 without nitrification</u>	<u>1,6 mg/l</u>
<u>Geometric mean of COD</u>	<u>17,4 mg/l</u>
<u>Geometric mean of total nitrogen</u>	<u>21 mg/l, 77,1 % reduction</u>
<u>Geometric mean of total phosphorus</u>	<u>0,98 mg/l, 92,8 % reduction</u>
<u>Maximum pH:</u>	<u>7,4</u>
<u>Minimum pH:</u>	<u>6,9</u>
<u>Type of disinfectant used</u>	<u>None</u>

Was the sewage treatment plant tested with:

<u>Fresh water flushing?</u>	<u>No</u>
<u>Salt water flushing?</u>	<u>No</u>
<u>Fresh and salt water flushing?</u>	<u>No</u>
<u>Grey water added?</u>	<u>No</u>

Was the sewage treatment plant tested against the environmental conditions specified in section 5.9 of resolution MEPC.227(64):

<u>Temperature</u>	<u>Yes</u>
<u>Humidity</u>	<u>Yes</u>
<u>Inclination</u>	<u>Yes</u>
<u>Vibration</u>	<u>Yes</u>
<u>Reliability of Electrical and Electronic Equipment</u>	<u>Yes</u>

QS - CERTIFICATE OF ASSESSMENT - EC (MODULE E)

Application of: Directive 2014/90/EU of 23 July 2014 on marine equipment (MED), issued as "Forskrift om Skipstyr" by the Norwegian Maritime Authority. This Certificate is issued by DNV GL AS under the authority of the Government of the Kingdom of Norway.

This is to certify:

That the Quality System for the products

with type designation(s) as specified in the Appendix to this Certificate

Issued to

Gertsen & Olufsen AS
Allerød, Denmark

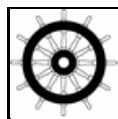
is found to comply with the applicable requirements.

The quality system has been assessed with respect to the procedure of conformity assessment described in Annex II, Module E in the directive 2014/90/EU and regulation (EU) 2017/306.

This Certificate is valid until **2022-08-28**.

Issued at **Høvik** on **2017-08-29**

DNV GL local station:
Copenhagen

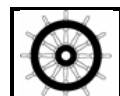


for **DNV GL AS**

Approval Engineer:
Pål Evang Nundal

Notified Body
No.: **0575**

Vidar Dolonen
Head of Notified Body



0575/yyyy

0575: Notified Body number undertaking quality surveillance
yyyy: The year in which the mark is affixed

The product liability rests with the manufacturer or his representative in accordance with Directive 2014/90/EU.
This certificate authorizes the manufacturer in conjunction with the valid EC Type Examination (Module B) Certificate(s) of the equipment listed before to affix the Mark of Conformity (wheelmark) to the product described herein.

This certificate loses its validity if the manufacturer makes any changes to the approved quality system which have not been notified to and agreed with the notified body named on this certificate.

This certificate remains valid unless suspended, withdrawn, recalled or cancelled.

The Manufacturer has to apply for periodical audits to verify the maintenance and application of the quality system every 12 months.



Form code: MED 221.NOR

Revision: 2017-02

www.dnvg.com

Page 1 of 2

© DNV GL 2014. DNV GL and the Horizon Graphic are trademarks of DNV GL AS.

APPENDIX

Item no. MED/2.6 Sewage systems

Type designation	EC Type-Examination Certificate No.	Expiry date	Notified Body No.	USCG approval number
NX10-C/N, NX20-C/N, NX25-C/N, NX30-C/N, NX35-C/N, NX40-C/N, NX45-C/N, NX50-C/N, NX55-C/N, NX60-C/N, NX65-C/N, NX70-C/N, NX75-C/N, NX80-C/N, NX90-C/N ¹	MEDB000017N	2022-03-06	0575	N/A
G&O Bioreactor, Models; BR 014800, BR 018500, BR 023125, BR 027750, BR 037000, BR 046250, BR 055500, BR 064750, BR 074000 ¹	MEDB00001ST	2020-05-29	0575	N/A
G&O Bioreactor, Models; BR 1850BG, BR 3700BG, BR 5550BG, BR 7400BG, BR 9250BG, BR 11100BG ¹	MEDB00002ZC	2020-05-29	0575	N/A

Places of production

1.KSM Poland Sp. z o.o., ul. Złotoryjska 194, Legnica, Poland

SDA-engineering GmbH



Kaiserstr. 100, TPH III

D – 52134 Herzogenrath

Fon +49 - (0) 24 07 – 56 848 -0

Fax +49 - (0) 24 07 - 56 848 -29

e-mail: info@sda-engineering.de

web: www.sda-engineering.de

Report

Analysis of a marine sanitation device according to 33 CFR, §159.105 and §159.107

Project 16-1003.01

Client: Gertsen & Olufsen A/S
Savsvinget 4
DK-2970 Hørsholm
phone: +45 45763600
Fax: +45 45761773

Contractor: SDA-engineering GmbH
Kaiserstr. 100, TPH III
52134 Herzogenrath
phone: +49 (0)2407-56848 0
fax: +49 (0)2407-56848 29

Editors: Dr.-Ing. Britta Holtschoppen
Prof. Dr.-Ing. Christoph Butenweg

Preparation Date: 15.06.2016

Revision: R-0

Number of Pages: 46

Table of Contents

CODES AND LITERATURE	4
TECHNICAL DOCUMENTS ON THE DEVICE.....	4
SOFTWARE	4
1. INTRODUCTION	5
2. SYSTEM / DEVICE.....	5
3. SHOCK TEST.....	7
3.1 General calculation method.....	7
3.2 Calculations on SDof systems.....	9
3.2.1 Material properties	9
3.2.2 Stiffness of the SDof-system.....	9
3.2.3 Eigenperiod of the SDof-system	10
3.2.4 Detailed calculations for the compressor shelf.....	11
3.2.5 Detailed calculations for the permat pump shelf.....	13
3.2.6 Detailed calculations for the dosing pump	14
3.2.7 Detailed calculations for the electrical cabinet.....	14
3.3 Verifications	15
3.3.1 Numerical model.....	16
3.3.2 Verification of the tank shell and the shelf plates.....	17
3.3.3 Verification of welds.....	19
4. ROLLING TEST.....	20
4.1 General calculation method.....	21
4.2 Impulsive rigid response – tangential and radial acceleration due to rolling .	22
4.2.1 Liquid pressure due to resulting acceleration	24
4.2.2 Point loads due to resulting acceleration.....	28
4.3 Numerical model.....	29
4.4 Load cases and load case combinations	29
4.4.1 Load case combination 1: Rolling about x-axis, $\theta = 30^\circ$	30

SDA-engineering GmbH



Kaiserstr. 100, TPH III

D – 52134 Herzogenrath

Fon +49 - (0) 24 07 – 56 848 -0

Fax +49 - (0) 24 07 - 56 848 -29

e-mail: info@sda-engineering.de

web: www.sda-engineering.de

4.4.2 Load case combination 2: Rolling about x-axis, $\theta = 0^\circ$	30
4.4.3 Load case combination 3: Rolling about y-axis, $\theta = 30^\circ$	31
4.4.4 Load case combination 4: Rolling about y-axis, $\theta = 0^\circ$	32
4.5 Results and verifications	33
4.5.1 Equivalent stresses.....	35
5. SUMMARY	45

Codes and Literature

- [1] Code of Federal Regulation (CFR) 33, Chapter I – Coast Guard, Department of Homeland Security, Subchapter O - Pollution, Part 159 - Marine Sanitation Devices; Jan. 30, 1975 with editorial notes of June 19, 2008 = edition valid on April 1, 2016; source: U.S. Government Publishing Office www.ecfr.gov
- [2] Department of Transportation, United States Coast Guard: MSD Laboratory Technical Information Sheet no. 8: Calculations submitted in lieu of Rolling Test; reference: 33 CFR 159.107; 28.03.1978
- [3] Department of Transportation, United States Coast Guard: MSD Laboratory Technical Information Sheet no. 5: Development of Large Equipment Certification Programs; reference: 33 CFR 159.19; 12.04.1976
- [4] DIN EN 1993-1-8; Eurocode 3: Bemessung und Konstruktion von Stahlbauten – Teil 1-8: Bemessung von Anschlüssen; Dez. 2010
- [5] A. K. Chopra: Dynamics of Structures, Prentice Hall, ISBN: 0-13-156174-X, 2007
- [6] K. Meskouris: Structural Dynamics, Ernst & Sohn, ISBN: 3-433-01327-6, 2000

Technical documents on the device

- [7] Isometric view on CAD drawing 1502-001
- [8] Isometric view on CAD drawing 1502-002
- [9] Drawing of the device including plate arrangement; drawing no. 1502-Platearrangement-01
- [10] Drawing of the device including overall dimensions; drawing no. 1502-STATIKMODEL-01
- [11] Three dimensional model of the device as .stp-file; file 1502-STATIKMODEL-01.stp

Software

- [12] InfoCAD, Version 14.50, InfoGraph GmbH, Aachen/Germany

1. Introduction

The code of Federal Regulation (CFR) no. 33 [1] lists requirements for the Certification, Design, Construction and Testing of Marine Sanitation Devices. According to 33 CFR several tests must be performed on each newly developed device type. However, the MSD Laboratory Technical Information Sheet no. 8 [3] describes alternatives to the experimental tests described in 33 CFR §159.103 through §159.131 which may be acceptable to the Coast Guard under 33 CFR §159.19 – Testing equivalency.

The scope of this report is the investigation and verification of the PIA test plant produced by Gertsen & Olufsen, Hørsholm, Denmark regarding shock test and rolling test on a numerical/analytical basis as alternative to the experimental test procedure of 33 CFR § 159.105 and § 159.107.

2. System / Device

The considered device is a rectangular steel tank of dimensions width/depth/height = 1051 / 1006 / 1356 mm with externally attached components (Figure 2-1). Three tank sides and the tank top are stiffened by steel stiffeners of 50 and 60 mm width respectively. The external components are supported by steel shelf constructions that are welded to the tank side (Figure 2-2).

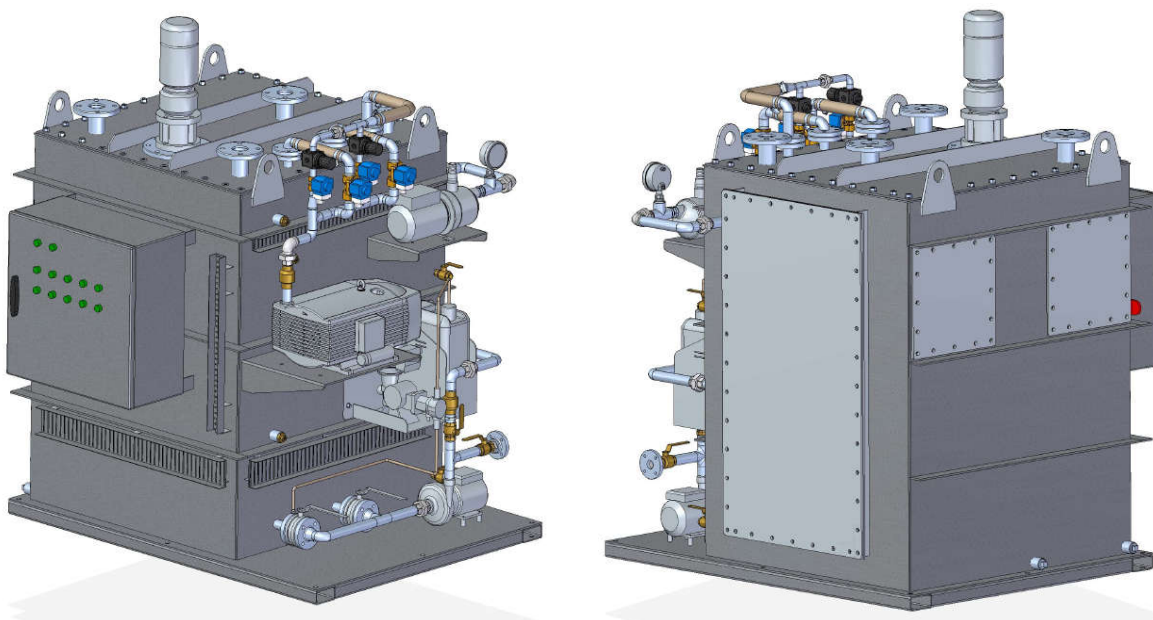


Figure 2-1: CAD drawings of the investigated device [7], [8]

SDA-engineering GmbH



Kaiserstr. 100, TPH III

D – 52134 Herzogenrath

Fon +49 - (0) 24 07 – 56 848 -0

Fax +49 - (0) 24 07 - 56 848 -29

e-mail: info@sda-engineering.de

web: www.sda-engineering.de

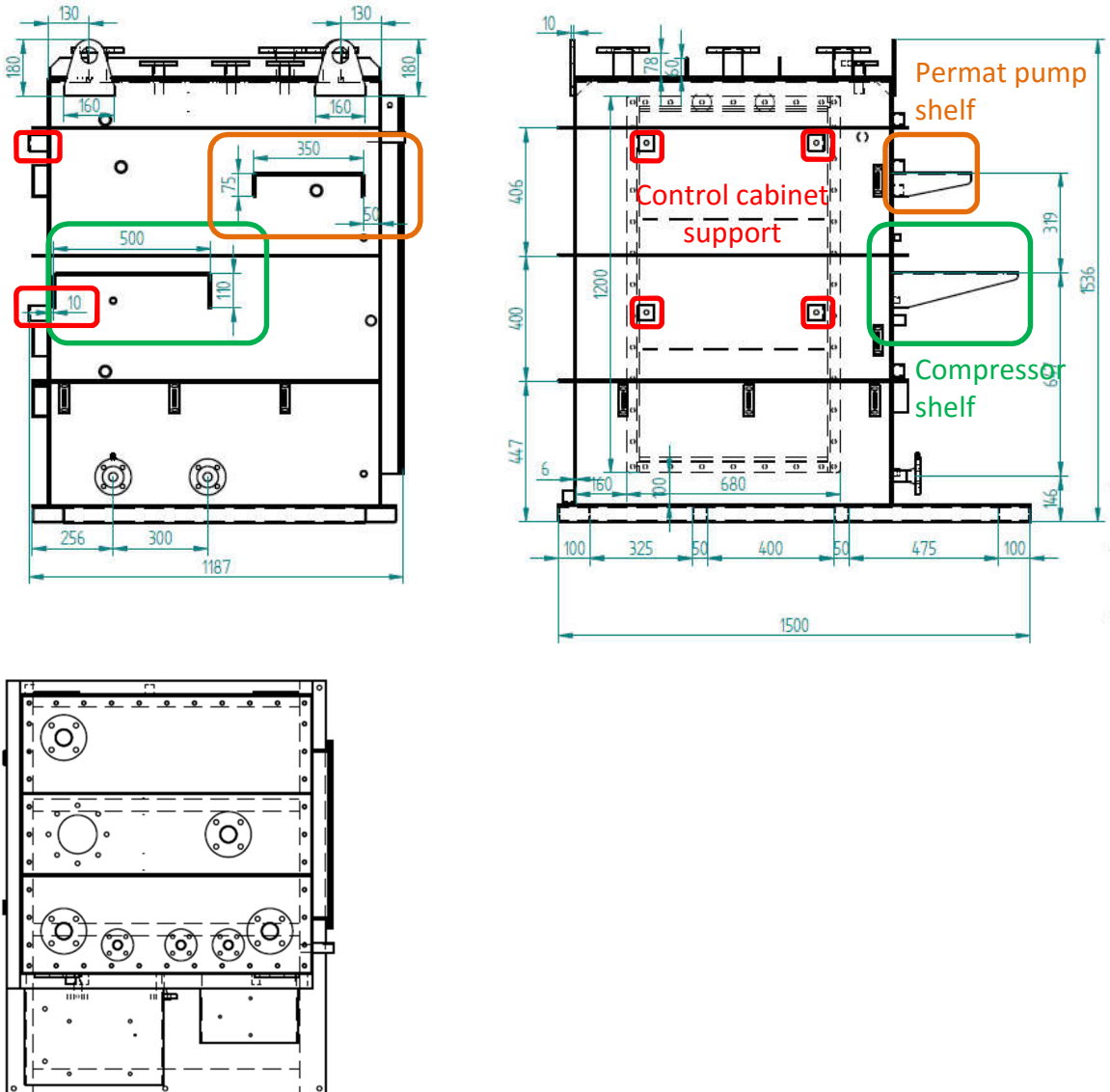


Figure 2-2: Dimensions of the device and auxiliary structural parts [10]

3. Shock test

3.1 General calculation method

In the present investigation the external components depict single degree of freedom systems whose stiffness is given by the shelf structures. Thus, shock spectra can be used to determine the maximum possible dynamic deflection of the shelf and the resulting additional loading to the tank shell.

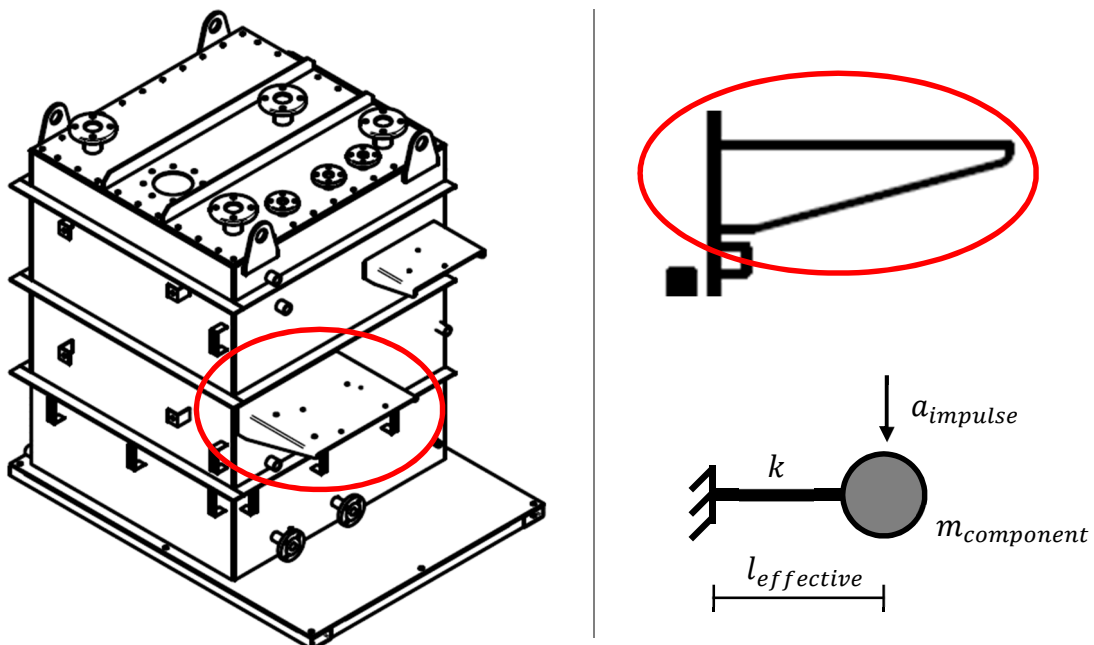


Figure 3-1: Single-degree-of-freedom representation of shelf-structures

Shock spectra depict the amplification in deformation for undamped single-degree-of-freedom systems for typical pulse loads. Depending on the relation between the impulse duration and the eigenperiod of the SDof-system the maximum possible response can be easily read off from the diagram. Figure 3-2 (c) shows the shock spectrum for a half-cycle sine pulse. It is the envelope of the response of the forced vibration phase (Figure 3-2 (a)) and the free vibration phase (Figure 3-2 (b)).

Note: Despite of the substitute analytical verification of the integrity of the device and its components, the operability of the electrical control panel itself must be verified by the shock test procedure described in 33 CFR §159.105 (see [3]) and is, thus, not part of the verifications of this report.

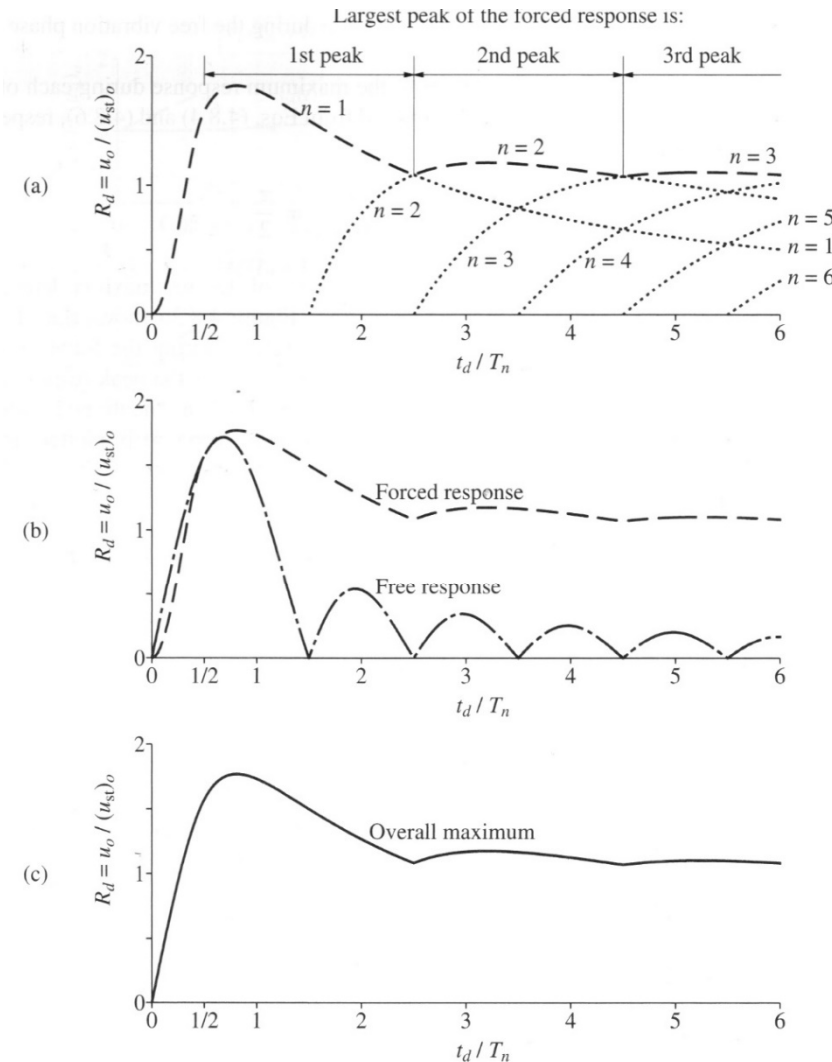


Figure 4.8.3 Response to half-cycle sine pulse force: (a) response maxima during forced vibration phase; (b) maximum responses during each of forced vibration and free vibration phases; (c) shock spectrum.

Figure 3-2: Shock spectrum for a half-cycle sine pulse force [5]

According to 33 CFR §159.105 [1] and MSD Laboratory Technical Information Sheet no. 8 [3] a pulse load (vertical acceleration) of maximum 10 g represented by a half-cycle sine of a duration of 25 milliseconds (Figure 3-3 left) was taken as basis for the calculations regarding the shock test.

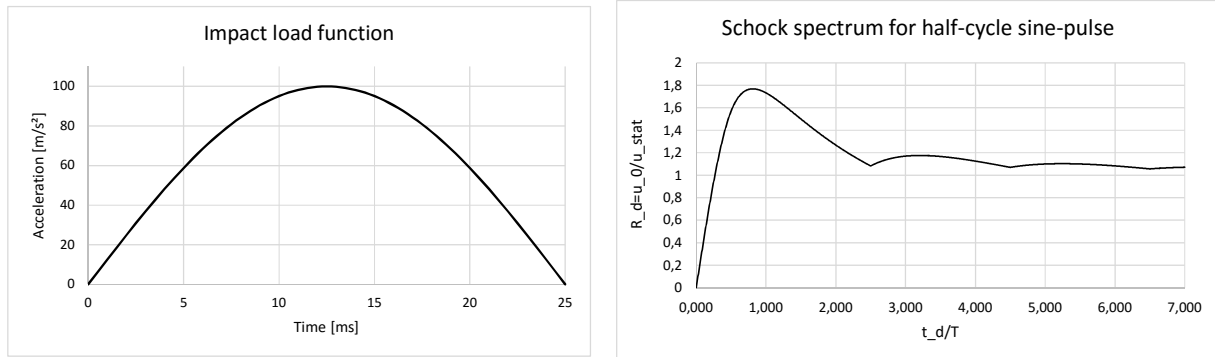


Figure 3-3: left: Half-cycle sine pulse load for shock test
right: Analytically determined shock spectrum for half-cycle sine pulse

In the present study the shock spectrum for the half-cycle sine pulse was set up analytically in order to pick up the exact amplification factor in reference to the calculated period ratio. Figure 3-3 right shows the shock spectrum used for further calculations.

3.2 Calculations on SDof systems

As stated above, the external components and their bearing systems are represented by Single-degree-of-freedom systems. Their parameters (stiffness, eigenperiod) were determined with the help of an auxiliary numerical model because of the complex three-sided bearing behaviour of the shelf plate (see Figure 3-4).

Figure 3-1 serves as reference for the naming of parameters.

3.2.1 Material properties

The shelves as well as the tank itself are made of stainless steel SS316L as stated by Gertsen&Olufson. The corresponding material properties considered in numerical analyses are given as

Material	SS316L
Density	7.9 t/m ³
Elastic modulus	193 000 MN/m ²
Tensile strength	485 MN/m ²
Yield strength @ 0.2%	172 MN/m ²

3.2.2 Stiffness of the SDof-system

In order to determine the stiffness of the equivalent SDof system a 1 N = 0.001 kN vertical load was applied to the shelf beneath the center of mass of the component (Figure 3-4). The resulting vertical deformation δ at the point of load was then employed to calculate the stiffness of the SDof system in terms of $k = 1/\delta$.

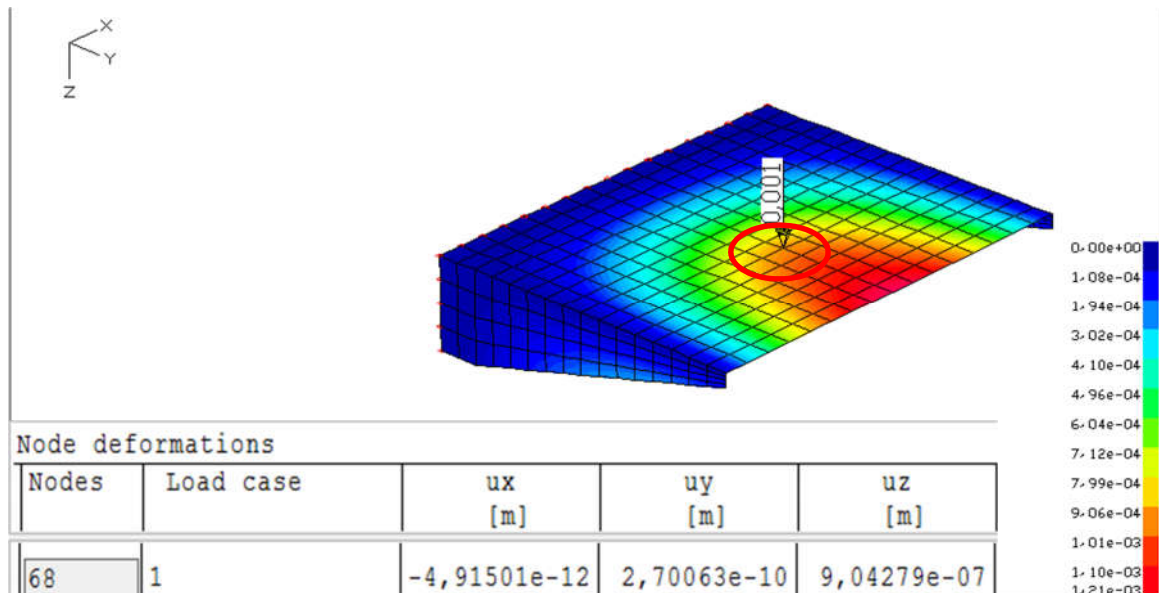


Figure 3-4: Shelf deformation of the compressor unit due to “1”-load beneath center of mass of the unit

3.2.3 Eigenperiod of the SDof-system

The eigenperiod of the system was determined by a modal analysis of the shelf structure including a point mass beneath the center of mass of the component representing the mass of the unit (Figure 3-5). Hand calculations based on the equivalent stiffness k of the SDof-system and the approximate effective mass (including the mass of the component and the vibration effective part of mass of the shelf) resulted in equivalent eigenperiods (see sections 3.2.4 and 3.2.5) verifying the numerical approach.

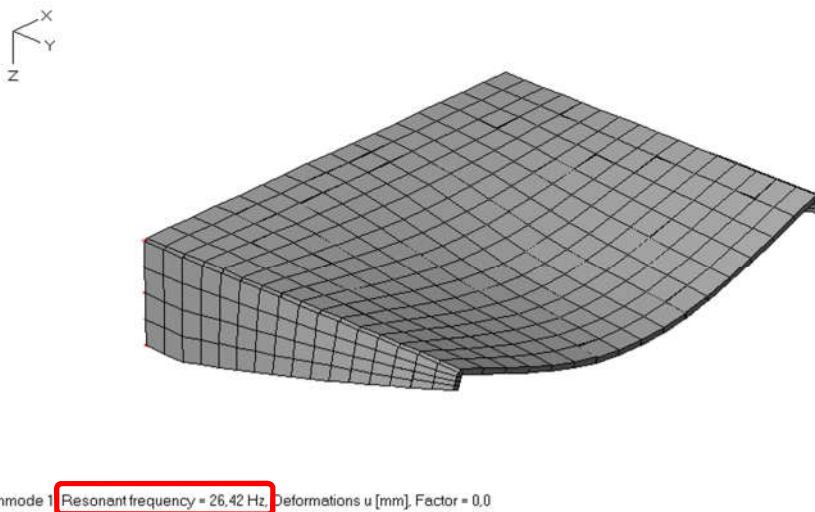


Figure 3-5: 1st eigenform of the compressor shelf and corresponding eigenfrequency

3.2.4 Detailed calculations for the compressor shelf

Evaluation of a half-cycle acceleration sine pulse		
component:	compressor unit	
gravity	g	9,81 m/s ²
SDoF-system		
mass compressor unit given by G&O	m_unit	37 kg
mass of shelf (dead load calculation)	m_shelf	12,33 kg
vibration effective mass of shelf	m_shelf_eff ≈ 1/4*m_shelf	3,08 kg
mass SDoF-system	m = m_unit+m_shelf_eff	40,08 kg
effective length of equiv. SDoF-system	I_eff = distance component - support	0,265 m
calculated deformation due to "1"-load	delta	9,04E-07 m
stiffness of SDoF-system	k = 1/delta	1.105.853 N/m
circular eigenfrequency ("hand calculation")	$\omega = \sqrt{\frac{k}{m}}$	166,10 rad/s
eigenfrequency (from modal analysis of shelf model with unit as point mass)	f	26,42 Hz
circ. eigenfreq. (compare to ω above)	$\omega = 2\pi \cdot f$	166,00 rad/s
Eigenperiod	$T = \frac{1}{f}$	0,0379 s
Pulse load		
duration	t_d [ms]	25 ms
	[s] = t_d [ms] /1000	0,0250 s
max. amplitude	a_max [g]	10 g
	[m/s ²] = a_max [g]*9,81 m/s ²	98,1 m/s ²

SDA-engineering GmbH



Kaiserstr. 100, TPH III

D – 52134 Herzogenrath

Fon +49 - (0) 24 07 – 56 848 -0

Fax +49 - (0) 24 07 - 56 848 -29

e-mail: info@sda-engineering.de

web: www.sda-engineering.de

Evaluation of shock spectrum		
Period ratio	t_d/T	0,6605 [-]
Deformation ratio (from shock spectrum of half-sine pulse)	$R_d = \frac{u_0}{u_{stat,0}} = \text{function of } \left(\frac{t_d}{T} \right)$	1,7320 [-]
static load due to max acc.	$P_{stat} = m \cdot a_{max}$	3932,20 N
calculated deformation due to "1"-load (see above)	delta	9,04E-07 m
static deflection due to P_stat (linear material behaviour assumed)	$u_{stat,0} = \frac{\text{delta}}{1N} \cdot P_{stat}$	3,56E-03 m
maximum dynamic deflection	$u_{0,dyn} = R_d \cdot u_{stat,0}$	0,0062 m
Equivalent dynamic load (vertical)		
	$P_{dyn} = R_d \cdot P_{stat}$	6.810,74 N
width footprint compressor unit in model	b_unit	0,25 m
length footprint compressor unit in model	l_unit	0,4 m
footprint compressor unit in model	A_unit	0,1 m ²
maximum dynamic pressure (vertical)	$p_{dyn} = P_{dyn}/A_{unit}$	68.107,38 N/m²

3.2.5 Detailed calculations for the permat pump shelf

Evaluation of a half-cycle acceleration sine pulse		
component:	permat pump unit	
gravity	g	9,81 m/s ²
SDoF-system		
mass permat pump unit given by G&O	m_unit	9,6 kg
mass of shelf (dead load calculation)	m_shelf	5,71 kg
vibration effective mass of shelf	m_shelf_eff ≈ 1/4*m_shelf	1,43 kg
mass SDoF-system	m = m_unit+m_shelf_eff	11,03 kg
effective length of equiv. SDoF-system	l_eff = distance component - support	0,1535 m
calculated deformation due to "1"-load	delta	3,40E-07 m
stiffness of SDoF-system	k = 1/delta	2.937.997 N/m
circular eigenfrequency ("hand calculation")	$\omega = \sqrt{\frac{k}{m}}$	516,17 rad/s
eigenfrequency (from modal analysis of shelf model with unit as point mass)	f	81,40 Hz
circ. eigenfreq. (compare to ω above)	$\omega = 2\pi \cdot f$	511,45 rad/s
Eigenperiod	$T = \frac{1}{f}$	0,0123 s
Pulse load		
duration	t_d [ms]	25 ms
	[s] = t_d [ms] /1000	0,0250 s
max. amplitude	a_max [g]	10 g
	[m/s ²] = a_max [g]*9,81 m/s ²	98,1 m/s ²

Evaluation of shock spectrum		
Period ratio	t_d/T	2,0350 [-]
Deformation ratio (from shock spectrum of half-sine pulse)	$R_d = \frac{u_0}{u_{stat,0}} = \text{function of } \left(\frac{t_d}{T} \right)$	1,7500 [-]
static load due to max acc.	$P_{stat} = m \cdot a_{max}$	1081,76 N
calculated deformation due to "1"-load (see above)	delta	3,40E-07 m
static deflection due to P_{stat} (linear material behaviour assumed)	$u_{stat,0} = \frac{\text{delta}}{1N} \cdot P_{stat}$	3,68E-04 m
maximum dynamic deflection	$u_{0,dyn} = R_d \cdot u_{stat,0}$	0,0006 m
Equivalent dynamic load (vertical)	$P_{dyn} = R_d \cdot P_{stat}$	1893,08 N
width permat pump unit in model	b_unit	0,15 m
length permat pump unit in model	l_unit	0,25 m
footprint permat pump unit in model	A_unit	0,0375 m ²
maximum dynamic pressure (vertical)	$p_{dyn} = P_{dyn}/A_{unit}$	50.482,13 N/m ²

3.2.6 Detailed calculations for the dosing pump

Since the mass of the dosing pump plus adjacent chemical can is way smaller than the mass of the compressor unit (8+5=13 kg < 38 kg) detailed calculations for the dosing pump and its shelf are not necessary.

It must be assured, however, that the shelf for the dosing pump and the chemical can is constructed similarly to the compressor unit shelf (two vertical webs at the shelf sides welded to the tank attachment plate) and that both, the pump and the can are tightly fastened to the shelf construction. The shelf itself (or its tank attachment plate respectively) must be welded to the tank shell with the boundary conditions given in section 0.

3.2.7 Detailed calculations for the electrical cabinet

The electrical cabinet (dimensions 600 x 600 mm; mass: 38 kg) is mounted on four steel brackets. Due to its configuration it can be regarded as stiff. Thus, the maximum dynamic vertical load due to acceleration impulse is equal to the mass times an acceleration of 10 g. The vertical load must be transferred to the tank shell by the four steel brackets. Additionally, a horizontal force at the upper (tension) and lower (pressure) brackets results from the bending moment due to the eccentric installation.

SDA-engineering GmbH



Kaiserstr. 100, TPH III

D – 52134 Herzogenrath

Fon +49 - (0) 24 07 – 56 848 -0

Fax +49 - (0) 24 07 - 56 848 -29

e-mail: info@sda-engineering.de

web: www.sda-engineering.de

SDoF-system		
mass electrical cabinet given by G&O	m_unit	38 kg
connection to tank		stiff
Pulse load		
max. amplitude	a_max [g]	10 g
	[m/s ²] = a_max [g]*9,81 m/s ²	98,1 m/s ²
Maximum dynamic vertical load		
maximum total vertical load	F_v = m_unit * a_max	3.727,8 N
maximum vertical load per support	F_v,s = 1/4 * F_v	932,0 N
maximum vertical load per node	F_v,n = 1/2 * F_v,s	466,0 N
maximum total horizontal load		
lever arm (approximately)	d = d_support + 1/2 d_cabinet	160 mm
bending moment due to max. vert. load	M = F_v * d	596.448,00 Nmm
height of cabinet	h_cabinet	600 mm
tot. horiz. support force due to bend. mom.	F_h = M/h_cabinet	994,08 N
horizontal force per support	F_h,s = total support force / 2	497,04 N
horizontal force per node	F_h,n = force per support / 2	248,52 N

3.3 Verifications

The maximum dynamic pressure due to acceleration impulse, which were determined in sections 3.2.4 and 3.2.5 were applied to a model of the tank structure (Figure 3-6) in order to identify the maximum resulting stresses in the tank shell and the maximum internal forces for a verification of the welds of the shelves.

3.3.1 Numerical model

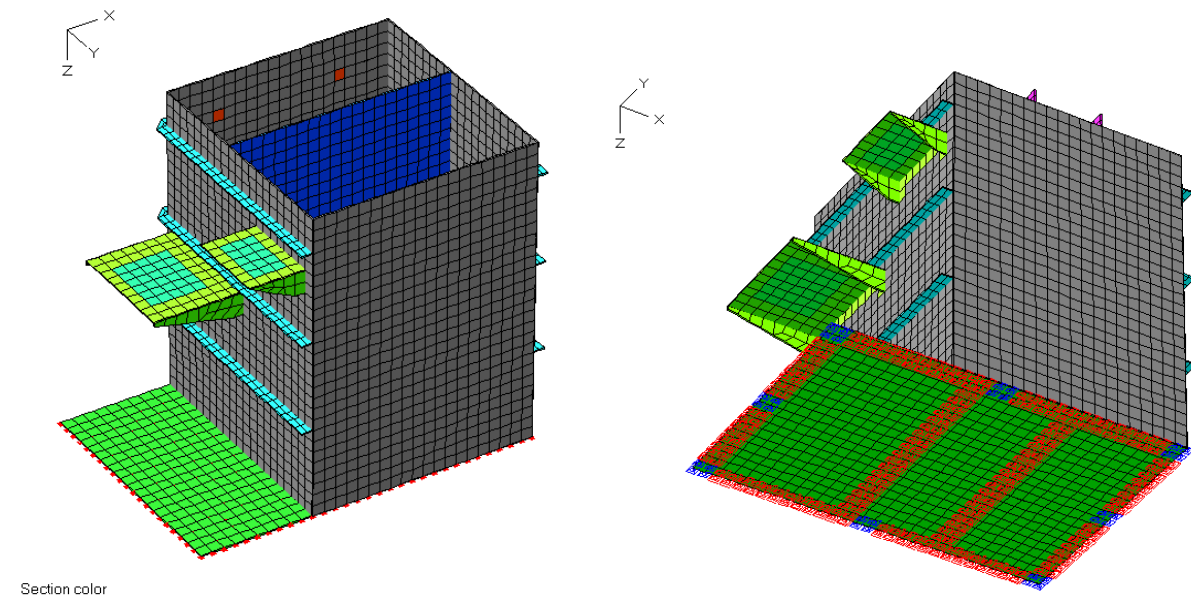


Figure 3-6: FE-model with supports of bottom plate

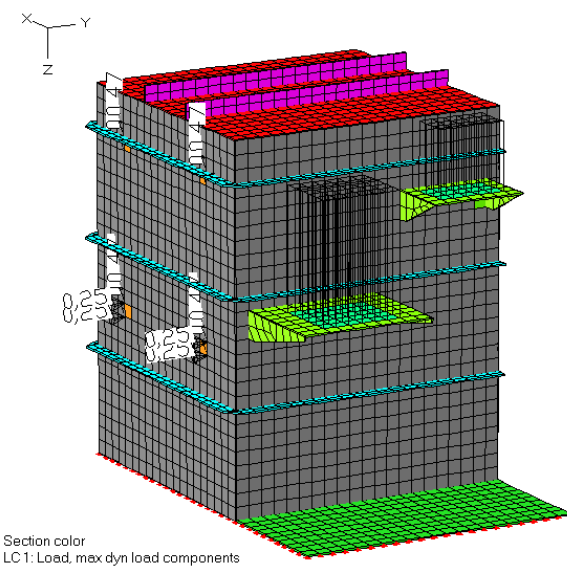


Figure 3-7: FE-model with maximum dynamic loading of components due to sine acceleration impulse

The simulation was done with the FE Software InfoCAD [12] in terms of a static finite element calculation since the dynamic effects are already included in the shock spectra.

The tank shell (sides, top and bottom) and the stiffeners were modelled as 4-node shell elements of 6 mm thickness with nearly quadratic geometry and an element width of approximately 5 cm (elements of stiffeners: rectangular).

Anchorage of the tank was considered by vertical supports (pressure only) at the locations of hollow sections underneath the bottom steel plate (red supports in Figure 3-6 right) and by translational supports in all three directions at the location of bore holes in the bottom steel plate (blue supports in Figure 3-6 right).

The material properties of tank shell and stiffeners are identical to those of the component shelves already given in section 3.2.1 according to Gertsen&Olufson.

3.3.2 Verification of the tank shell and the shelf plates

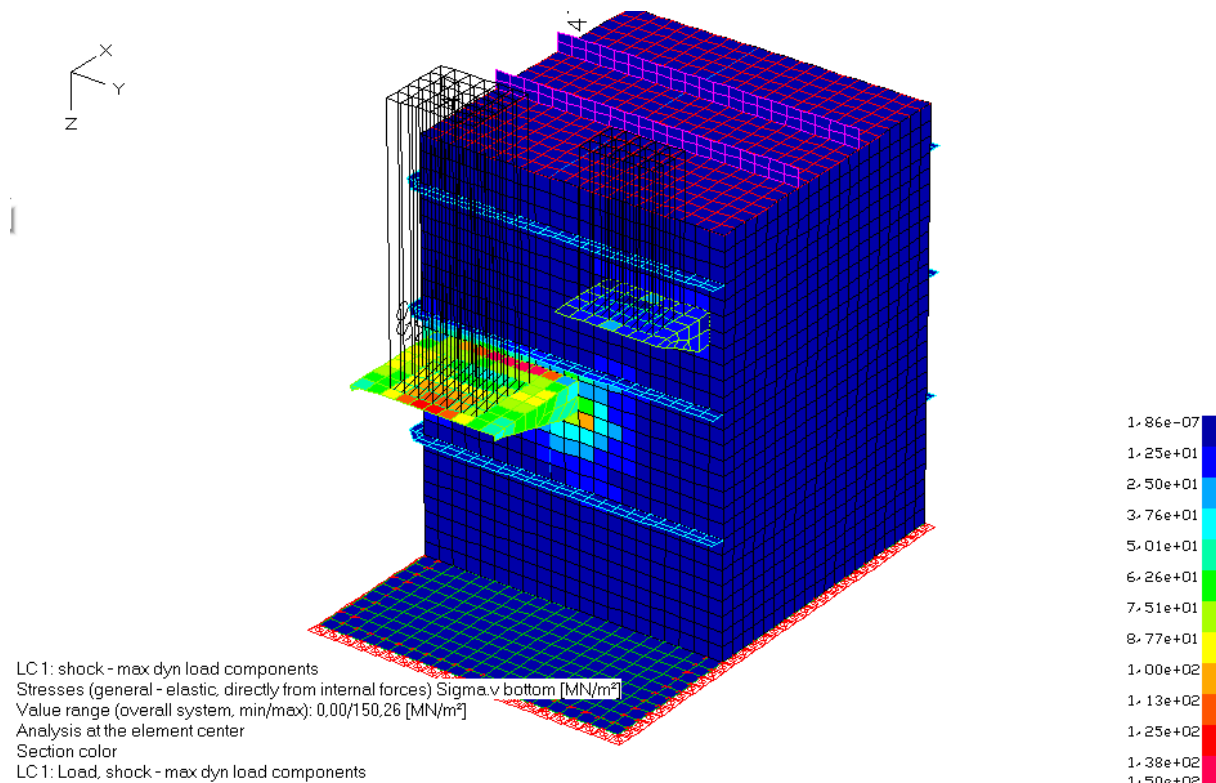


Figure 3-8: Equivalent stresses due to shock load on shelf components 150 MN/m² < 172 MN/m² ✓

The maximum equivalent stresses due to shock load are 150.3 MN/m² which is less than the maximum yield strength of 172 MN/m².

According to DIN EN 1993 the partial safety factor γ_{M0} for the capacity of sections is equal to 1.0, so the yield strength does not have to be reduced.

$$\text{The limit value for shell stresses are met as } \sigma_{v,Ed} = 150 \frac{\text{MN}}{\text{m}^2} < 17 \cdot 2 \frac{\text{MN}}{\text{m}^2} = \frac{f_y}{\gamma_{M0}}$$

The stress values due to the acceleration of the electrical cabinet are much smaller than that (14,5 MN/m²) and thus not relevant for design of the shell.

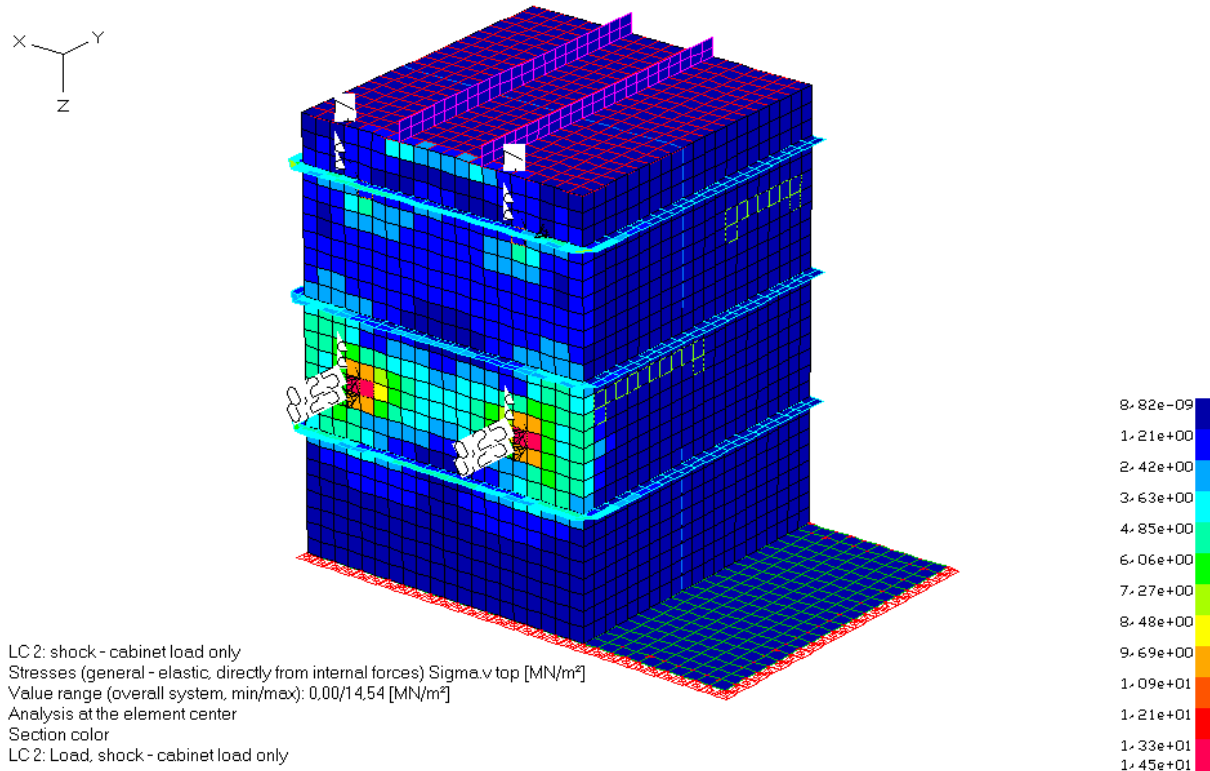


Figure 3-9: Equivalent stresses due to acceleration of electrical cabinet 14,5 MN/m² < 172 MN/m² ✓

3.3.3 Verification of welds

As both shelves are connected to the tank shell with identical welds only the highest loading is considered for weld verification, i.e. the shelf of the compressor unit. The verifications are carried out in accordance with DIN EN 1993-1-8 [4].

Dynamic maximum support reactions		
Vertical force at shelf connection	$F_v = k \cdot u_{0,dyn} = P_{dyn}$	6.810,74 N
Bending moment at shelf connection	$M = F_v \cdot d_{eff}$	1.804,85 Nm
Shear force to be taken up by vertical welds	= F_v	6.810,74 N
lever arm for bending moment	= height of shelf	0,11 m
Tension force to be taken up by horiz. weld	= $M/\text{height of shelf}$	16.407,69 N
weld verification according to DIN EN 1993-1-8		
weld type		fillet weld
shelf thickness	t_shelf	6 mm
shell thickness	t_shell	6 mm
maximum steel thickness	t_max	6 mm
minimum weld thickness	$a_{min} = \max(\sqrt{t_{max}} - 0,5; 3 \text{ mm})$	3,0 mm
chosen weld thickness (assumed)	a	3,0 mm
partial safety factor (material) for connect.	gamma_M2	1,25 -
correlation factor	beta_w	0,8 -
min. tensile strength of the connected parts	f_u	485 N/mm ²
Design value of shear capacity of the weld	$f_{vw,d} = \frac{f_u / \sqrt{3}}{\beta_w \cdot \gamma_{M2}}$	280 N/mm ²
horizontal weld (takes up on horizontal (tension) force due to bending moment)		
shelf length	I_shelf	500 mm
minimum effective weld length	$l_{eff} \geq 6 \cdot a \text{ and } l_{eff} \geq 30 \text{ mm}$	18 mm
effective weld length	$l_{eff} = 2 * (I_{shelf} - 2 * t_{shelf})$	976 mm
effective weld area	$A_w = a * I_{eff}$	2928 mm ²
tension force per unit weld length	$F_{w,Ed} = \text{Tension force} / l_{eff}$	16,81 N/mm
capacity of the weld	$F_{w,Rd} = f_{vw,d} * a$	840,04 N/mm²
safety factor	$F_{w,Rd} / F_{w,Ed}$	49,97 > 1 ok
vertical weld (takes up on shear force due to vertical load)		
shelf height (see above)	h_shelf	110 mm
minimum effective weld length	$l_{eff} \geq 6 \cdot a \text{ and } l_{eff} \geq 30 \text{ mm}$	18 mm
effective weld length	$l_{eff} = 4 * (h_{shelf} - 1 * t_{shelf})$	368 mm
effective weld area	$A_w = a * I_{eff}$	1104 mm ²
shear force per unit weld length	$F_{w,Ed} = \text{Shear force} / h_{eff}$	61,92 N/mm
capacity of the weld	$F_{w,Rd} = f_{vw,d} * a$	840,04 N/mm²
safety factor	$F_{w,Rd} / F_{w,Ed}$	13,57 > 1 ok

4. Rolling test

The MSD Laboratory Technical Information Sheet no. 5 [2] outlines design aspects of marine sanitation devices that should be considered in performing theoretical analyses for submission in lieu of the actual experimental rolling test required by 33 CFR § 159.107.

The Coast Guard's main interests in the rolling test are the system's processing capability (including the prevention of spillover from the device into work spaces or from one chamber into another) and the proof of structural integrity of the device under roll-induced loads.

The following conditions apply:

- The axis of roll should be in the plane of the base of the device and offset from the centerline by $r=1.22$ m.
- The period of the roll should be $T=4$ seconds.
- The angle θ_{max} used should be the maximum for which the device is to be certified.
- The forces to be considered are the weight of the tank and its contents as well as the tangential force due to rolling.
- Stresses should be calculated for the supports, bottom plating, side- and end plating.
- Additionally, if any heavy components are supported by the tank top or sides, the load on the tank plating due to the component's weight and developed tangential force should be considered.

MAXIMUM TANGENTIAL FORCE F_t IS
GIVEN BY

$$F_t = \frac{4\pi^2 r \theta_0 W}{g T^2}$$

WHERE

r = distance from axis to CG

θ_0 = max. roll angle

W = weight of tank and contents

T = period of roll

g = acceleration due to gravity

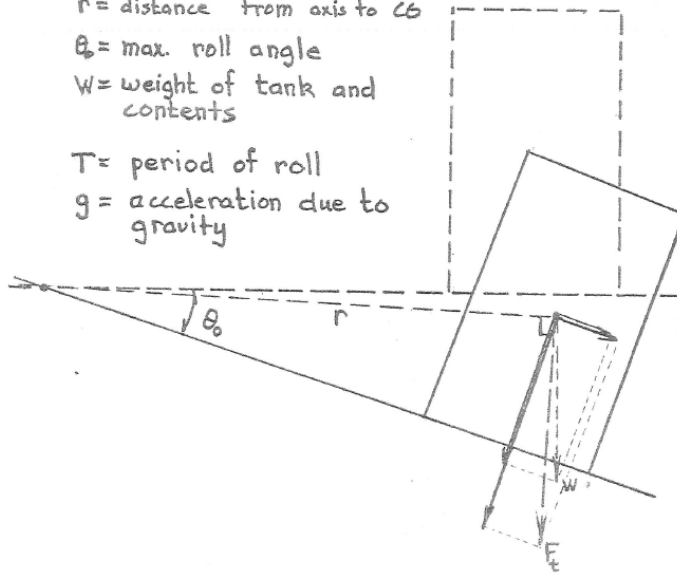


Figure 4-1: Test conditions to be assumed according to MSD Laboratory Technical Information Sheet no. 5 [2]

4.1 General calculation method

Generally, a liquid filled container is exposed to different response components when loaded dynamically:

- The impulsive rigid load component results from a rigid body movement of the liquid together with the tank. **It is pictured by a constant acceleration value that is determined in accordance with the harmonic rolling of the container (see section 4.2).**
- The impulsive flexible load component results from the interaction of the liquid with the deforming thin tank shell. **This is not relevant for the considered case of a sanitation device since the tank is braced by stiffeners and can be regarded as non-deforming when calculating the liquid response.**
- The convective load component results from the sloshing of the liquid. **The additional pressure due to sloshing is very small compared to the impulsive rigid pressure component and can be neglected due to sufficient capacity of the tank. The sloshing height, however, should be taken into account when evaluating the risk of spill over.**

In the following sections the loads to rolling are determined and applied to a numerical model of the device. The resulting stresses in the bottom, side and end plates are calculated and compared to the allowable stresses.

As the sanitation device can be mounted on the ship in either direction, two possible rolling axes are considered in calculation. This is in accordance with the regulations of CFR 33 §159.107 (a) [1].

4.2 Impulsive rigid response due to rolling

4.2.1 Tangential and radial acceleration due to rolling

The impulsive rigid response depends on the rolling angle of the container and leads to a maximum tangential acceleration (at maximum rolling angle) or a maximum radial acceleration (at zero rolling angle). Both are calculated in the following; the maximum tangential acceleration is equal to the value given in MSD Laboratory Technical Information Sheet no. 5 [2]. The direction of action of both accelerations is shown in Figure 4-2.

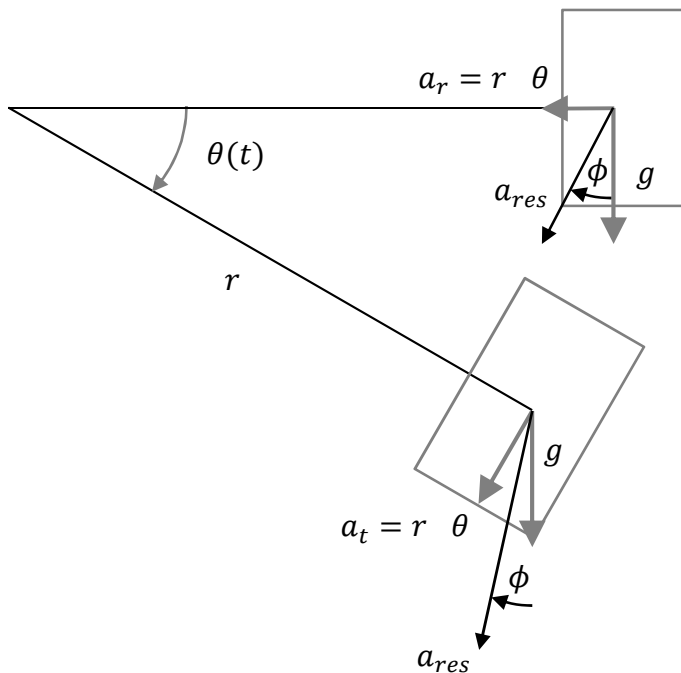


Figure 4-2: Definition of tangential, radial and resulting acceleration

Derivation of maximum acceleration due to rolling:

Circular rolling frequency

$$\omega = \frac{2\pi}{T} = \frac{2\pi}{4s} = 1.571 \frac{\text{rad}}{\text{s}}$$

Maximum rolling angle

$$\theta_{max} = 30^\circ = \pi/6$$

Considered rolling radius

$$r = 1.22 \text{ m}$$

Time dependent rolling angle

$$\theta(t) = \theta_{max} \sin(\omega t)$$

Time dependent rolling velocity

$$\theta(t) = \theta_{max} \omega \cos(\omega t)$$

Time dependent rolling acceleration

$$\theta(t) = \theta_{max} \omega^2 \sin(\omega t)$$

If $\theta(t) = \theta_{max}$:

$$\theta(t) = 0$$

$$\theta(t) = \theta_{max} = \theta_{max} \frac{4\pi^2}{T^2}$$

radial acceleration:

$$a_{r,max} = r \theta^2 = 0$$

tangential acceleration:

$$a_{t,max} = r \theta_{max} = \frac{4\pi^2}{(4s)^2} 1.22 \text{ m} \frac{\pi}{6} = 1.58 \text{ m/s}^2$$

If $\theta(t) = 0$:

$$\theta(t) = \theta_{max} = \theta_{max} \frac{2\pi}{T}$$

$$\theta(t) = 0$$

radial acceleration:

$$a_{r,max} = r \theta^2 = 1.22 \text{ m} \left(\frac{\pi}{6} \frac{2\pi}{4s} \right) = 1.0 \text{ m/s}^2$$

tangential acceleration:

$$a_{t,max} = r \theta = 0$$

The tangential and radial acceleration act on both the liquid and the components attached to the container. It can be combined with gravity to determine a resulting global acceleration:

Resulting acceleration on liquid and components and its global direction:

If $\theta(t) = \theta_{max} = 30^\circ$:

$$g = 9.81 \text{ m/s}^2 @ 0^\circ \text{ (= z-direction)}$$

$$a_{t,max} = 1.58 \text{ m/s}^2 @ 150^\circ$$

resulting acceleration:

$$a_{res} = \sqrt{9.81^2 + 1.58^2 - 2 \cdot 9.81 \cdot 1.58 \cos(150^\circ)} \\ = 11.21 \text{ m/s}^2$$

angle of resulting acc.:

$$\phi = \arcsin \left(\frac{a_{t,max} \sin 30^\circ}{a_{res}} \right) = 4.04^\circ \text{ off the vertical}$$

global acceleration in z:

$$a_z = a_{res} \cos \phi = 11.18 \text{ m/s}^2$$

global gravity factor in z:

$$a_{z,factor} = \frac{a_z}{g} = \frac{11.18}{9.81} = 1.14$$

global acceleration in x or y:

$$a_y = a_{res} \sin \phi = 0.80 \text{ m/s}^2$$

global gravity factor in x or y:

$$a_{y,factor} = \frac{a_y}{g} = \frac{0.80}{9.81} = 0.08$$

If $\theta(t) = 0$:	$g = 9.81 \text{ m/s}^2$	@ 0° (= z-direction)
	$a_{r,max} = 1.0 \text{ m/s}^2$	@ 90°
resulting acceleration:	$a_{res} = \sqrt{9.81^2 + 1.0^2} = 9.86 \text{ m/s}^2$	
angle of resulting acc.:	$\phi = \arctan\left(\frac{1.0}{9.81}\right) = 5.82^\circ$ off the vertical	
global acceleration in z:	$g = 9.81 \text{ m/s}^2$	
global gravity factor in z:	$a_{z,factor} = \frac{g}{g} = 1.0$	
global acceleration in x or y:	$a_{r,max} = 1.0 \text{ m/s}^2$	
global gravity factor in x or y:	$a_{y,factor} = \frac{1.0}{g} = 0.1$	

4.2.2 Liquid pressure due to resulting acceleration

The liquid pressure due to the rigid-body acceleration can be determined analogously to the hydrostatic pressure where the gravity component is replaced by the resulting impulsive rigid acceleration (Figure 4-3 and calculation in section 4.2.1). The maximum height h_{liquid} for the calculation of liquid pressure depends on the rolling angle θ and the width of the tank b . It is calculated by

$$h_{liquid} = h_{filling} \cos \theta \pm \frac{b_{tank}}{2} \sin \theta$$

The resulting triangle-shaped pressure is distributed over the wetted surface, which refers to the inclined fluid surface and is calculated by

$$h_{wetted\ surface} = h_{liquid} \pm \frac{b}{2} \tan \theta$$

In the case of maximum radial acceleration (which occurs at an angle of $\theta = 0^\circ$) the values of h_{liquid} and $h_{wetted\ surface}$ are obviously identical and equal to the filling height $h_{filling}$ (Figure 4-3 right).

The maximum filling height was specified by Gertsen&Olufson as $h_{filling} = 1150 \text{ mm}$ for tank 1 and $h_{filling} = 1225 \text{ mm}$ for tank 2.

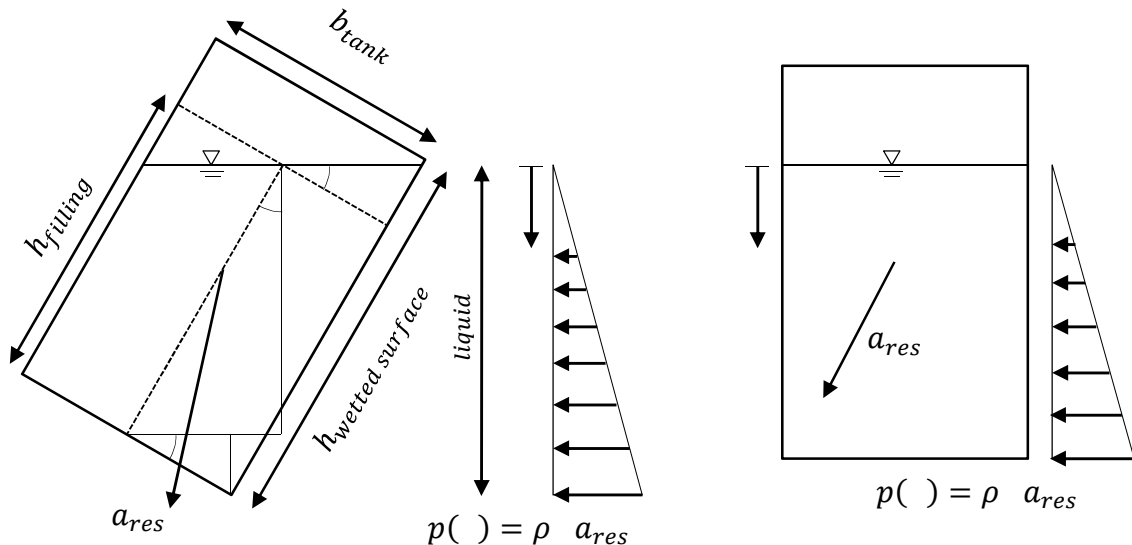


Figure 4-3: Impulsive rigid pressure component at maximum rolling angle (left) and at 0° rolling angle (right)

The following tables summarise the relevant heights and the resulting pressure components for the individual load case combinations. The pressures are calculated with reference to the flat liquid surface at a roll angle of 30°. The effect of sloshing (waves) additional to the surface inclination is not relevant for stress analysis and, thus, not considered in the determination of the liquid pressures.

Please note, though, that in the case of rolling about the y-axis (30° max; LCC 3) the calculative maximum height of the liquid surface will be higher than the height of the tank walls (see underlined values below). That means that the liquid will slosh to the tank top leading to a potential spill over if tank top and walls are not sealed.

Sloshing above the maximum wall height is also expected in the case of rolling about the x-axis (LCC 1) since the values given in the tables below only refer to the flat liquid surface in case of 30° rolling angle. Wave height due to sloshing must be added to these values.

In order to comply with CFR 33 [1], the manufacturer must in particular prevent spill over between the two tanks by sealing the gap between internal wall and tank top. Tank top and outer walls of the device must be tightly bolted together to prevent spill over to the outside.

SDA-engineering GmbH



Kaiserstr. 100, TPH III

D – 52134 Herzogenrath

Fon +49 - (0) 24 07 – 56 848 -0

Fax +49 - (0) 24 07 - 56 848 -29

e-mail: info@sda-engineering.de

web: www.sda-engineering.de

For load case combination 1 ($\theta(t) = \theta_{max} = 30^\circ$, rolling about the x-axis)

tank no.	filling height	width	$h_{min,wet\ sur}$	$h_{liquid,left}$	$h_{max,wet\ sur}$	$h_{liquid,right}$
1 (big)	1150 mm	604 mm	976 mm	845 mm	1324 mm	1147 mm
2 (small)	1225 mm	435 mm	1099 mm	952 mm	<u>1351 mm</u>	1170 mm

$$\text{Specific weight of the water (see 4.2.1): } \rho \quad a_{res} = 1 \frac{t}{m^3} \quad 11.21 \frac{m}{s^2} = 11.21 \frac{kN}{m^3}$$

→ loads on tank 2 (small)

$$\begin{aligned}
 p_{max,left} &= 11.21 \cdot 0.952 = 10.7 \frac{kN}{m^2} \text{ up to 1099 mm} & = 11.21 \cdot 0.845 = 9.5 \frac{kN}{m^2} \text{ up to 976 mm} \\
 p_{max,right} &= 11.21 \cdot 1.170 = 13.1 \frac{kN}{m^2} \text{ up to 1350 mm} & = 11.21 \cdot 1.147 = 12.9 \frac{kN}{m^2} \text{ up to 1324 mm} \\
 p_{min,bottom} &= p_{max,left} = 10.7 \frac{kN}{m^2} & = p_{max,left} = 9.5 \frac{kN}{m^2} \\
 p_{max,bottom} &= p_{max,right} = 13.1 \frac{kN}{m^2} & = p_{max,right} = 12.9 \frac{kN}{m^2}
 \end{aligned}$$

→ loads on tank 1 (big)

For load case combination 2 ($\theta(t) = \theta_{max} = 0^\circ$, rolling about the x-axis)

tank no.	filling height	width	$h_{min,wet\ sur}$	$h_{liquid,left}$	$h_{max,wet\ sur}$	$h_{liquid,right}$
1 (big)	1150 mm	604 mm	1150 mm	1150 mm	1150 mm	1150 mm
2 (small)	1225 mm	435 mm	1225 mm	1225 mm	1225 mm	1225 mm

$$\text{Specific weight of the water (see 4.2.1): } \rho \quad a_{res} = 1 \frac{t}{m^3} \quad 9.86 \frac{m}{s^2} = 9.86 \frac{kN}{m^3}$$

→ loads on tank 2 (small)

$$\begin{aligned}
 p_{max} &= 9.86 \cdot 1.225 = 12.1 \frac{kN}{m^2} \text{ up to 1225 mm} & = 9.86 \cdot 1.15 = 11.3 \frac{kN}{m^2} \text{ up to 1150 mm}
 \end{aligned}$$

→ loads on tank 1 (big)

For load case combination 3 ($\theta(t) = \theta_{max} = 30^\circ$, rolling about the y-axis)

tank no.	filling height	width	$h_{min,wet\ sur}$	$h_{liquid,front}$	$h_{max,wet\ sur}$	$h_{liquid,back}$
1 (big)	1150 mm	1000 mm	861 mm	746 mm	<u>1439 mm</u>	1246 mm
2 (small)	1225 mm	1000 mm	936 mm	811 mm	<u>1514 mm</u>	1311 mm

$$\text{Specific weight of the water (see 4.2.1): } \rho \quad a_{res} = 1 \frac{t}{m^3} \quad 11.21 \frac{m}{s^2} = 11.21 \frac{kN}{m^3}$$

➔ loads on tank 2 (small)

$$p_{max,back} = 11.21 \cdot 0.746 = 8.4 \frac{kN}{m^2} \text{ up to 861 mm} \quad = 11.21 \cdot 0.811 = 9.1 \frac{kN}{m^2} \text{ up to 936 mm}$$

$$p_{max,front} = 11.21 \cdot 1.246 = 14.0 \frac{kN}{m^2} \text{ up to 1350 mm} \quad = 11.21 \cdot 1.311 = 14.7 \frac{kN}{m^2} \text{ up to 1350 mm}$$

$$p_{min,bottom} = p_{max,back} = 8.4 \frac{kN}{m^2} \quad = p_{max,back} = 9.1 \frac{kN}{m^2}$$

$$p_{max,bottom} = p_{max,front} = 14.0 \frac{kN}{m^2} \quad = p_{max,front} = 14.7 \frac{kN}{m^2}$$

The small loading of the top shell is negligible for stress and buckling verifications.

➔ loads on tank 1 (big)

For load case combination 4 ($\theta(t) = \theta_{max} = 0^\circ$, rolling about the y-axis)

➔ Calculation of liquid pressure equal to load case combination 2

$$\text{Specific weight of the water (see 4.2.1): } \rho \quad a_{res} = 1 \frac{t}{m^3} \quad 9.86 \frac{m}{s^2} = 9.86 \frac{kN}{m^3}$$

➔ loads on tank 2 (small)

$$p_{max} = 9.86 \cdot 1.225 = 12.1 \frac{kN}{m^2} \text{ up to 1225 mm} \quad = 9.86 \cdot 1.15 = 11.3 \frac{kN}{m^2} \text{ up to 1150 mm}$$

➔ loads on tank 1 (big)

For load case combination 5 (uneven filling; $\theta(t) = \theta_{max} = 30^\circ$, rolling about the x-axis)

- ➔ Calculation of liquid pressure equal to load case combination 1, but liquid pressure is only considered in the smaller tank (higher maximum filling); the bigger tank is considered empty.

4.2.3 Point loads due to resulting acceleration

The following point loads are applied to the FE-model of the tank representing the external components:

For load case combination 1 ($\theta(t) = \theta_{max} = 30^\circ$, rolling about the x-axis)

- ➔ global acceleration in z: $a_z = 11.18 \text{ m/s}^2$ acceleration factor: 1.14
- ➔ global acceleration in y: $a_y = 0.80 \text{ m/s}^2$ acceleration factor: 0.08

Component	mass	load in z-dir.	load in y-dir.
compressor	37.0 kg	414 N = 4*103.5 N	30 N = 4*7.5 N
permat pump	9.6 kg	107 N = 2*53.5 N	8 N = 2*4.0 N
circulation pump	8.3 kg	not relevant (set on base)	not relevant
dosing pump & chemical can	13.0 kg	145 N = 4*36 N	10 N = 4*2.5 N
electrical cabinet	38.0 kg	425 N = 4*106 N	30 N = 4*7.5 N

For load case combination 2 ($\theta(t) = \theta_{max} = 0^\circ$, rolling about the x-axis)

- ➔ global acceleration in z: $a_z = 9,81 \text{ m/s}^2$ acceleration factor: 1.0
- ➔ global acceleration in y: $a_y = 1,0 \text{ m/s}^2$ acceleration factor: 0.1

Component	mass	load in z-dir.	load in y-dir.
compressor	37.0 kg	363 N = 4*91 N	30 N = 4*9,3 N
permat pump	9.6 kg	94 N = 2*47 N	10 N = 2*5.0 N
circulation pump	8.3 kg	not relevant (set on base)	not relevant
dosing pump & chemical can	13.0 kg	128 N = 4*32 N	13 N = 4*3,3 N
electrical cabinet	38.0 kg	373 N = 4*93.6 N	38 N = 4*10 N

For load case combination 3 ($\theta(t) = \theta_{max} = 30^\circ$, rolling about the y-axis)

- ➔ global acceleration in z: $a_z = 11.18 \text{ m/s}^2$ acceleration factor: 1.14
- ➔ global acceleration in x: $a_x = 0.80 \text{ m/s}^2$ acceleration factor: 0.08

Component	mass	load in z-dir.	load in x-dir.
compressor	37.0 kg	414 N = 4*103.5 N	30 N = 4*7.5 N
permat pump	9.6 kg	107 N = 2*53.5 N	8 N = 2*4.0 N
circulation pump	8.3 kg	not relevant (set on base)	not relevant
dosing pump & chemical can	13.0 kg	145 N = 4*36 N	10 N = 4*2.5 N
electrical cabinet	38.0 kg	425 N = 4*106 N	30 N = 4*7.5 N

For load case combination 4 ($\theta(t) = \theta_{max} = 0^\circ$, rolling about the y-axis)

- ➔ global acceleration in z: $a_z = 9,81 \text{ m/s}^2$ acceleration factor: 1.0
- ➔ global acceleration in x: $a_x = 1,0 \text{ m/s}^2$ acceleration factor: 0.1

Component	mass	load in z-dir.	load in x-dir.
compressor	37.0 kg	363 N = 4*91 N	30 N = 4*9,3 N
permat pump	9.6 kg	94 N = 2*47 N	10 N = 2*5.0 N
circulation pump	8.3 kg	not relevant (set on base)	not relevant
dosing pump & chemical can	13.0 kg	128 N = 4*32 N	13 N = 4*3,3 N
electrical cabinet	38.0 kg	373 N = 4*93.6 N	38 N = 4*10 N

For load case combination 5 (uneven filling; $\theta(t) = \theta_{max} = 30^\circ$, rolling about the x-axis)

- ➔ Dead load of components equal to load case combination 1

4.3 Numerical model

The employed numerical model is described in section 3.3.1.

4.4 Load cases and load case combinations; safety factors

In stress and stability analyses the situation of maximum filling height is relevant for verifications. Thus, the case of half-filled tanks was not considered.

However, the effect of uneven filling of the two tanks was investigated by assuming the smaller tank (higher filling level) fully filled and the bigger tank empty (LCC 5).

In all load case combinations, a safety factor of 1.35 for dead load and of 1.5 for liquid pressure was taken into account.

Five load case combinations were considered for the simulation of the roll test:

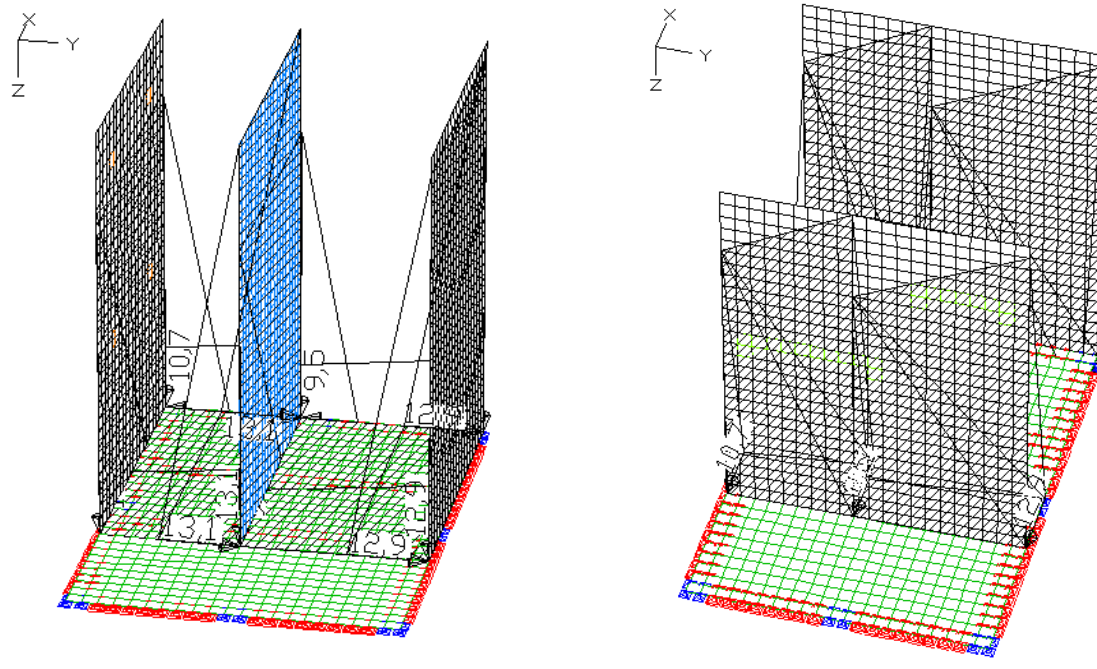
- | | | |
|-------------------------------|----------------------|---------------------|
| LCC 1: maximum filling height | rolling about x-axis | $\theta = 30^\circ$ |
| LCC 2: maximum filling height | Rolling about x-axis | $\theta = 0^\circ$ |
| LCC 3: maximum filling height | Rolling about y-axis | $\theta = 30^\circ$ |
| LCC 4: maximum filling height | Rolling about y-axis | $\theta = 0^\circ$ |
| LCC 5: uneven filling | Rolling about x-axis | $\theta = 30^\circ$ |

For all load case combinations, the resulting deformations and equivalent stresses were determined and a linear buckling analysis was carried out.

4.4.1 Load case combination 1: Rolling about x-axis, $\theta = 30^\circ$

Dead load of components is considered as point loads on the component supports according to section 4.2.3.

Liquid pressure on the tank walls is considered according to section 4.2.2 (see Figure 4-4).



left and right side + internal wall + bottom

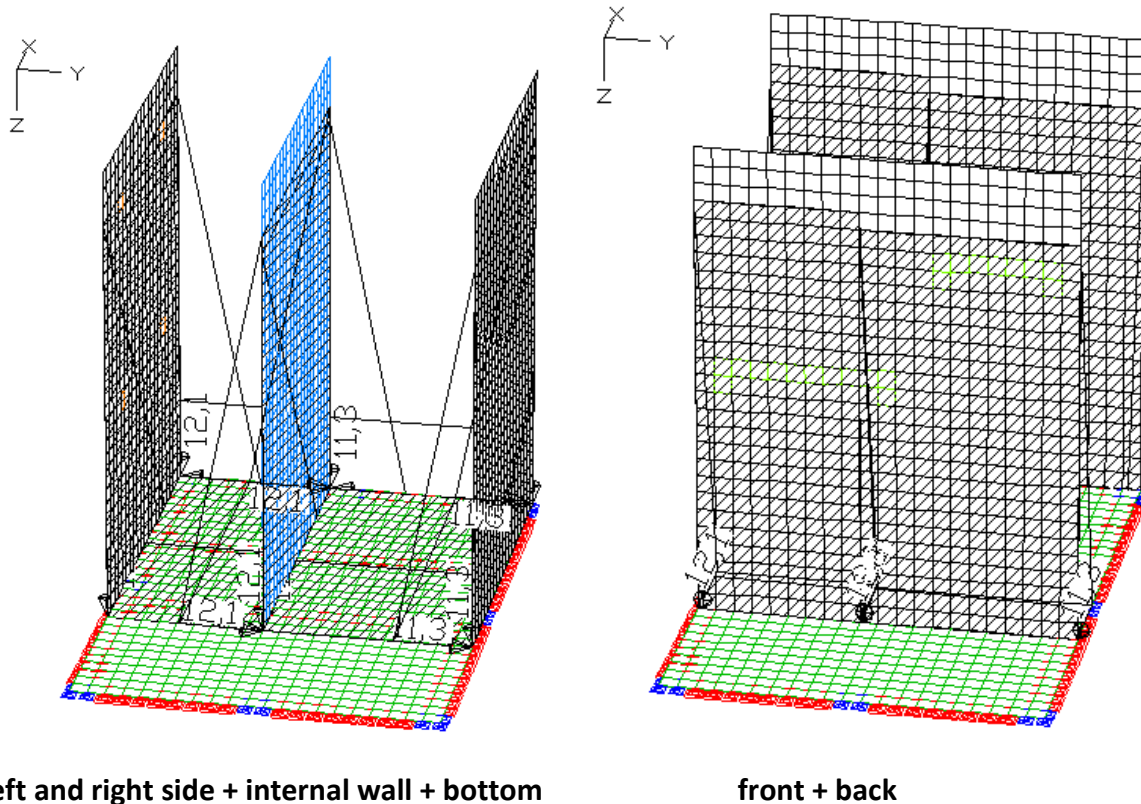
front + back

Figure 4-4: Liquid pressure in load case combination 1

4.4.2 Load case combination 2: Rolling about x-axis, $\theta = 0^\circ$

Dead load of components is considered as point loads on the component supports according to section 4.2.3.

Liquid pressure on the tank walls is considered according to section 4.2.2 (see Figure 4-5).



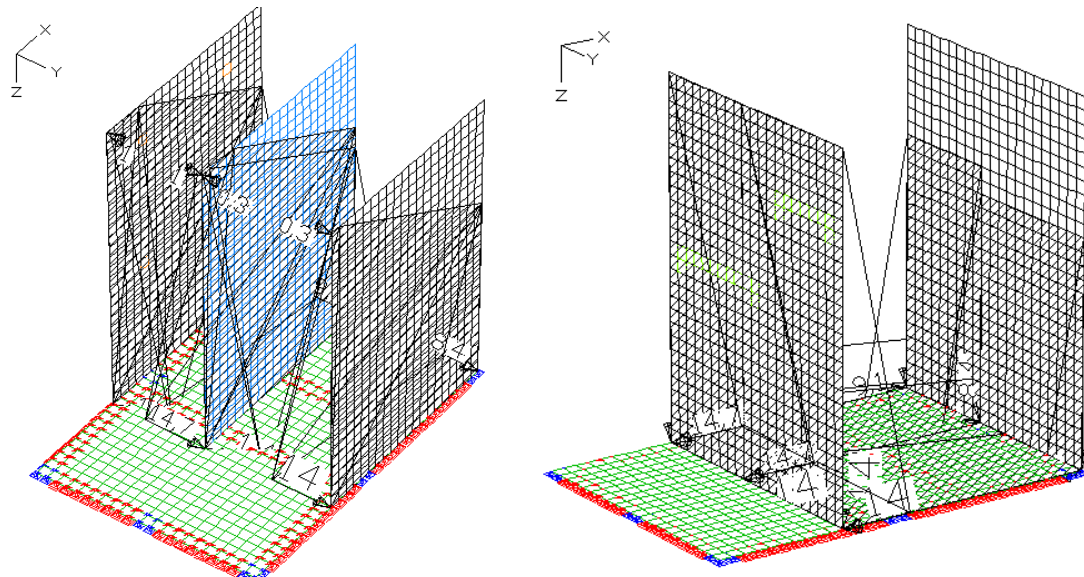
left and right side + internal wall + bottom **front + back**

Figure 4-5: Liquid pressure in load case combination 2

4.4.3 Load case combination 3: Rolling about y-axis, $\theta = 30^\circ$

Dead load of components is considered as point loads on the component supports according to section 4.2.3.

Liquid pressure on the tank walls is considered according to section 4.2.2 (see Figure 4-6). The small liquid pressure on the tank top is not applied to the FE-model as it is not relevant for the stress verifications.



left and right side + internal wall

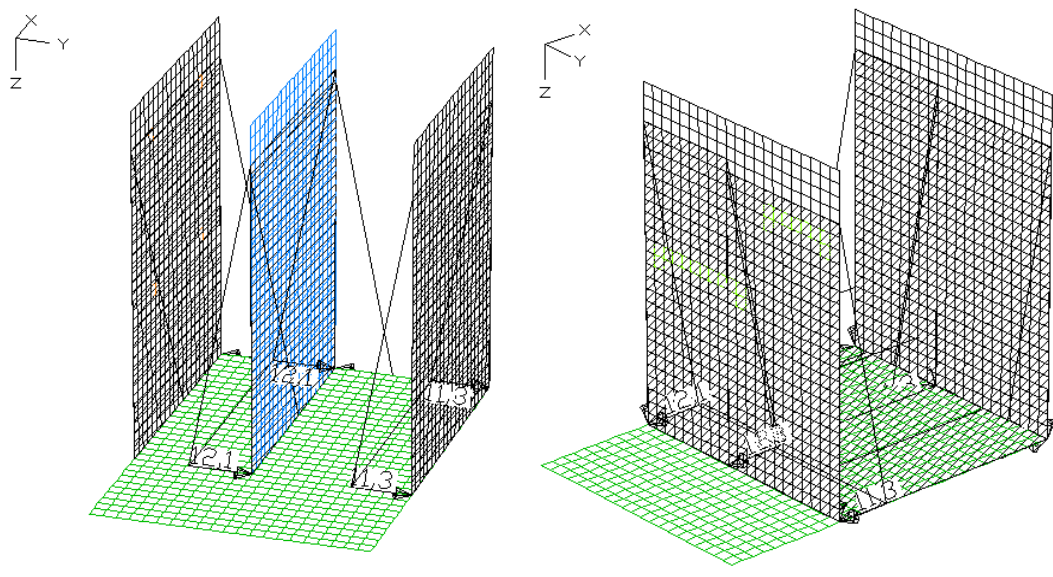
front + back + bottom

Figure 4-6: Liquid pressure in load case combination 3

4.4.4 Load case combination 4: Rolling about y-axis, $\theta = 0^\circ$

Dead load of components is considered according to section 4.2.3.

Liquid pressure on the tank walls is considered according to section 4.2.2 (see Figure 4-7).



left and right side + internal wall

front + back + bottom

Figure 4-7: Liquid pressure in load case combination 4

4.4.5 Load case combination 5: Uneven filling; rolling about x-axis, $\theta = 30^\circ$

Dead load of components is considered according to section 4.2.3.

Liquid pressure on the tank walls is considered according to section 4.2.2 (see Figure 4-8).

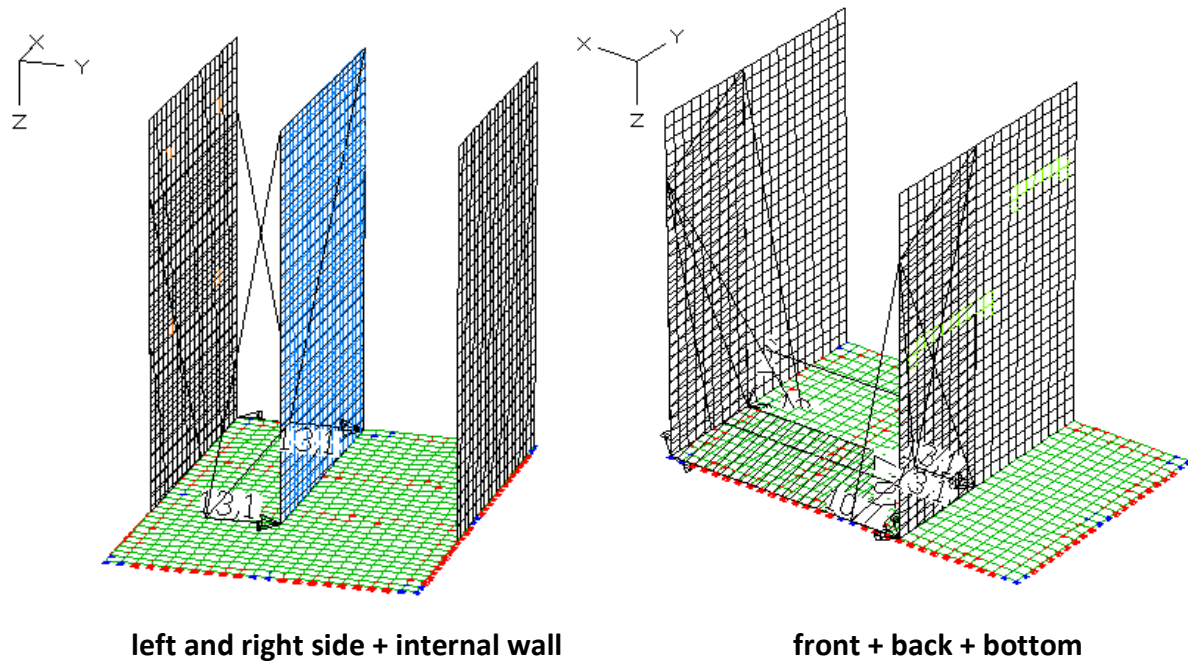


Figure 4-8: Liquid pressure in load case combination 5

4.5 Results and verifications

As expected, the decisive load case combinations are rolling about the x-axis at the maximum roll angle of 30° (LCC 1) and uneven filling of the tanks (LCC 5). The first one leads to a maximum loading of the side shell without stiffeners, the second one to the maximum loading of the internal wall.

Figure 4-9 and Figure 4-10 in section 4.5.1 show the maximum deformations due to LCC 1 and LCC 5 respectively.

Section 4.5.2 highlights the maximum equivalent stresses in all load case combinations.

Section 4.5.3 deals with the anchorage of the device to the ship.

4.5.1 Maximum deformations

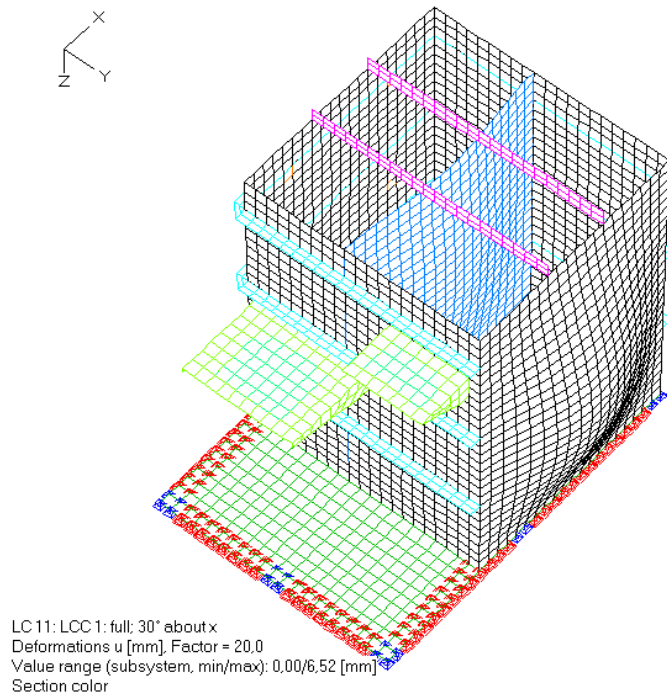


Figure 4-9: Maximum shell deformation due to roll angle 30° about the x-axis: 6,5 mm

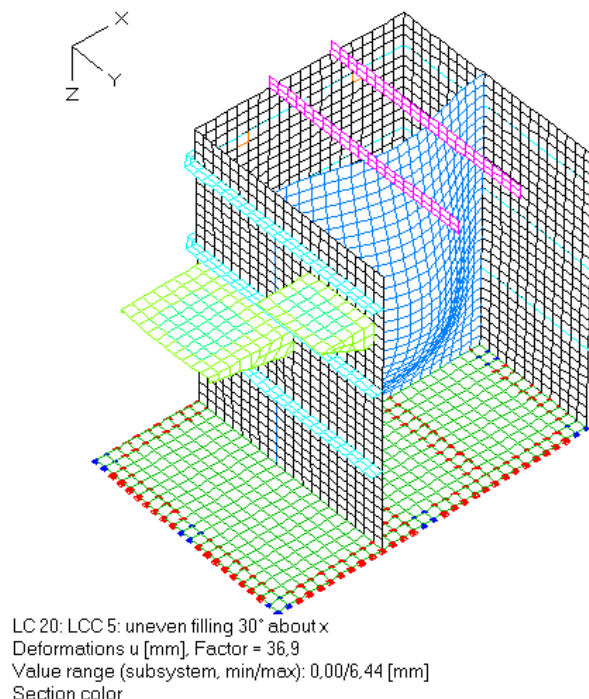


Figure 4-10: Maximum shell deformation due to roll angle 30° about the x-axis at uneven filling of the tanks: 6,4 mm

4.5.2 Equivalent stresses

Due to all load case combinations the maximum allowable stress is met.

Maximum equivalent stresses in a fully filled tank constellation occur on the right side of the device (outer wall of tank 2) at the connections of the right side to the front, back and bottom. It results from the deformation of the non-stiffened outer tank wall (Figure 4-11 to Figure 4-14).

In the unevenly filled situation, maximum equivalent stresses occur on the interior wall at the connections to the front and the back (Figure 4-15).

The effect of tangential acceleration and gravity on the attached component is small compared to the effect of the accelerated liquid.

Equivalent stresses due to all five load case combinations are shown in the following figures.

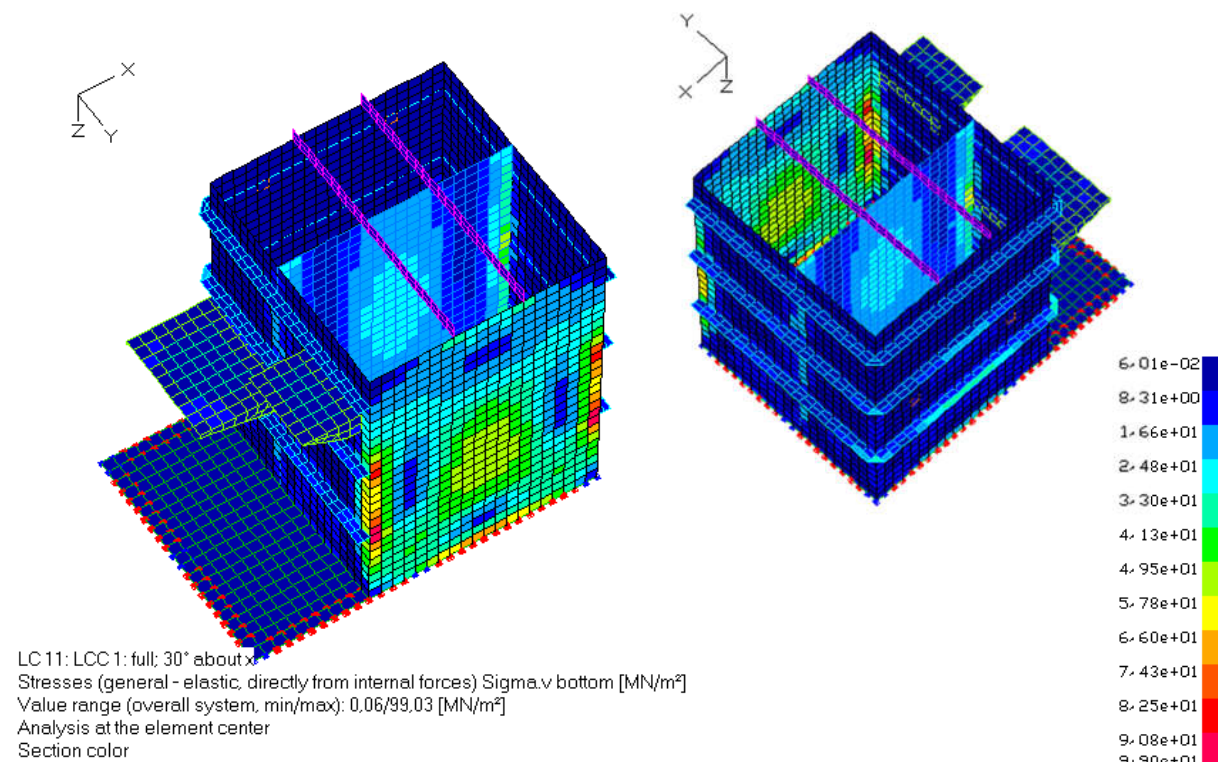
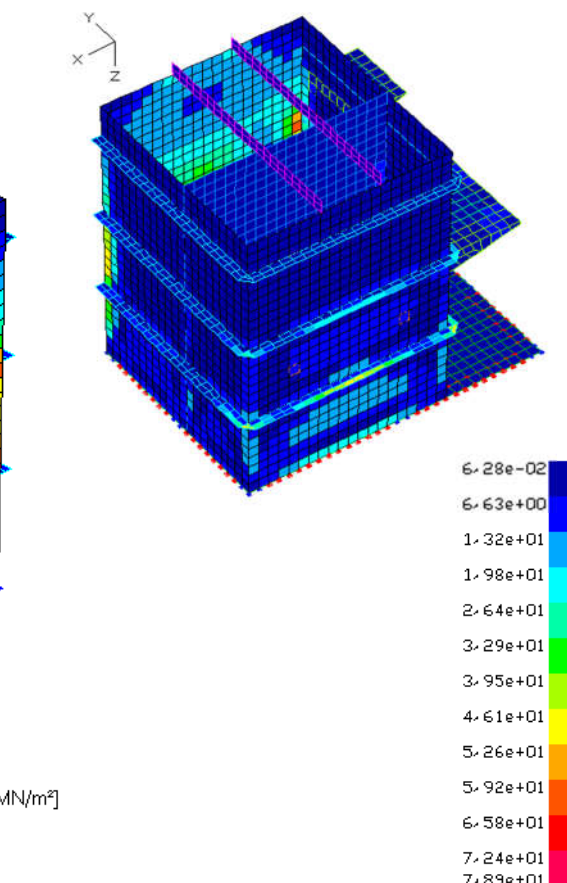


Figure 4-11: LCC 1: Maximum equivalent stresses due to liquid pressure and dead load at roll angle 30° about the x-axis: 99 MN/m² < 172 MN/m² ✓



LC 12: LCC 2: full; 0° about x

Stresses (general - elastic, directly from internal forces) Sigma.v bottom [MN/m²]

Value range (overall system, min/max): 0,06/78,93 [MN/m²]

Analysis at the element center

Section color

Figure 4-12: LCC 2: Maximum equivalent stresses due to liquid pressure and dead load at roll angle 0° about the x-axis: 79 MN/m² < 172 MN/m² ✓

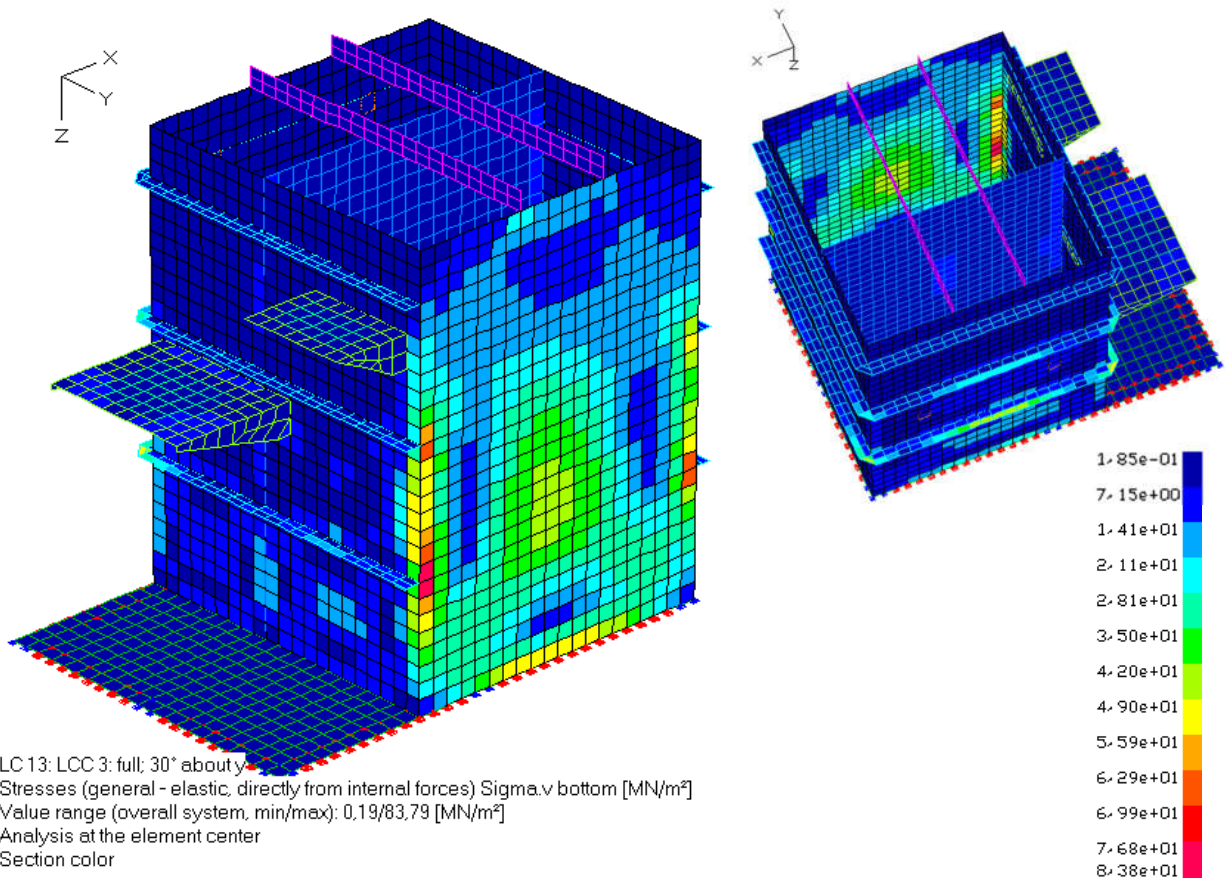


Figure 4-13: LCC 3: Maximum equivalent stresses due to liquid pressure and dead load at roll angle 30° about the y-axis: 84 MN/m² < 172 MN/m² ✓

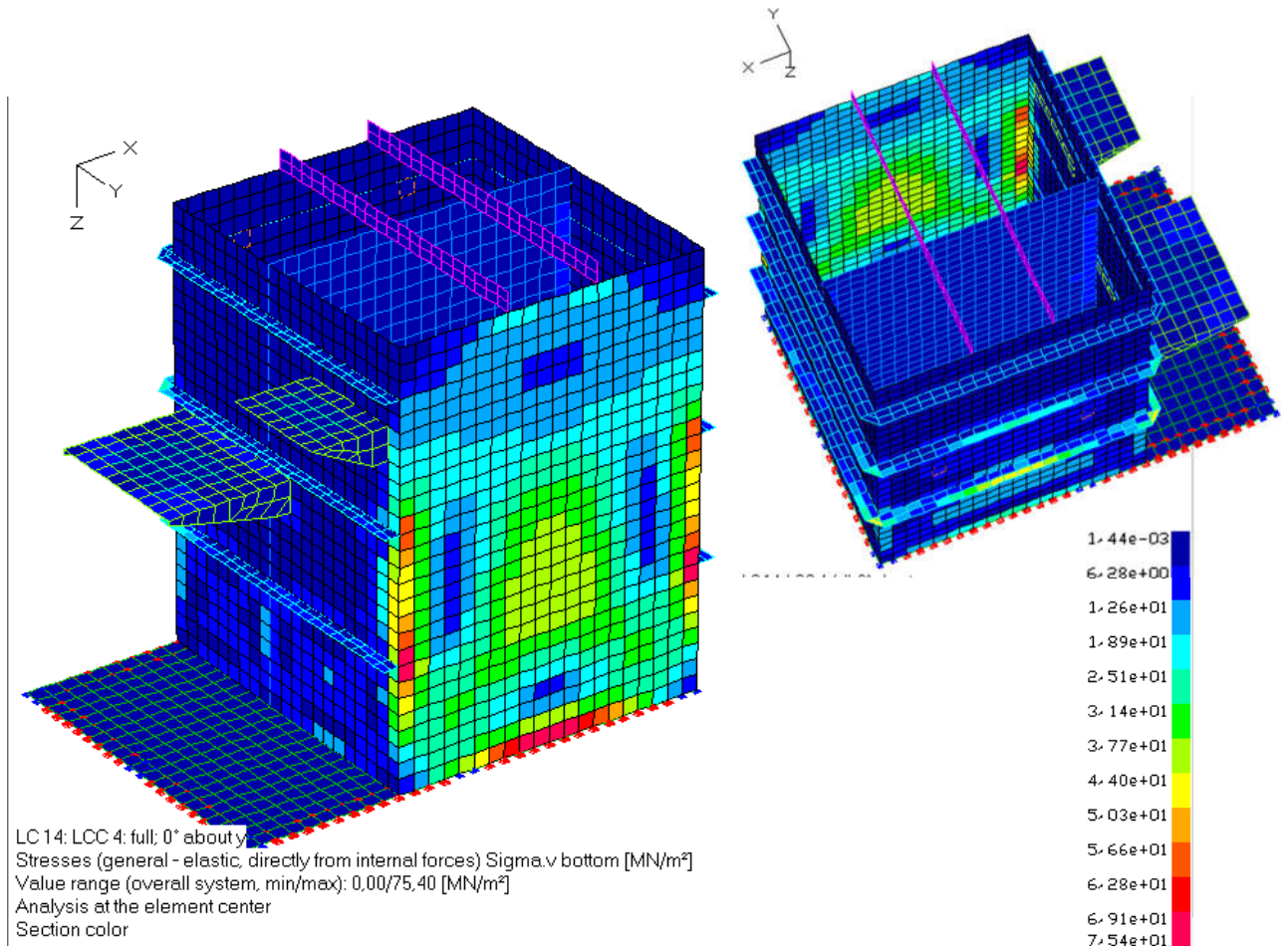


Figure 4-14: LCC 4: Maximum equivalent stresses due to liquid pressure and dead load at roll angle 0° about the y-axis: 78,5 MN/m² < 172 MN/m² ✓

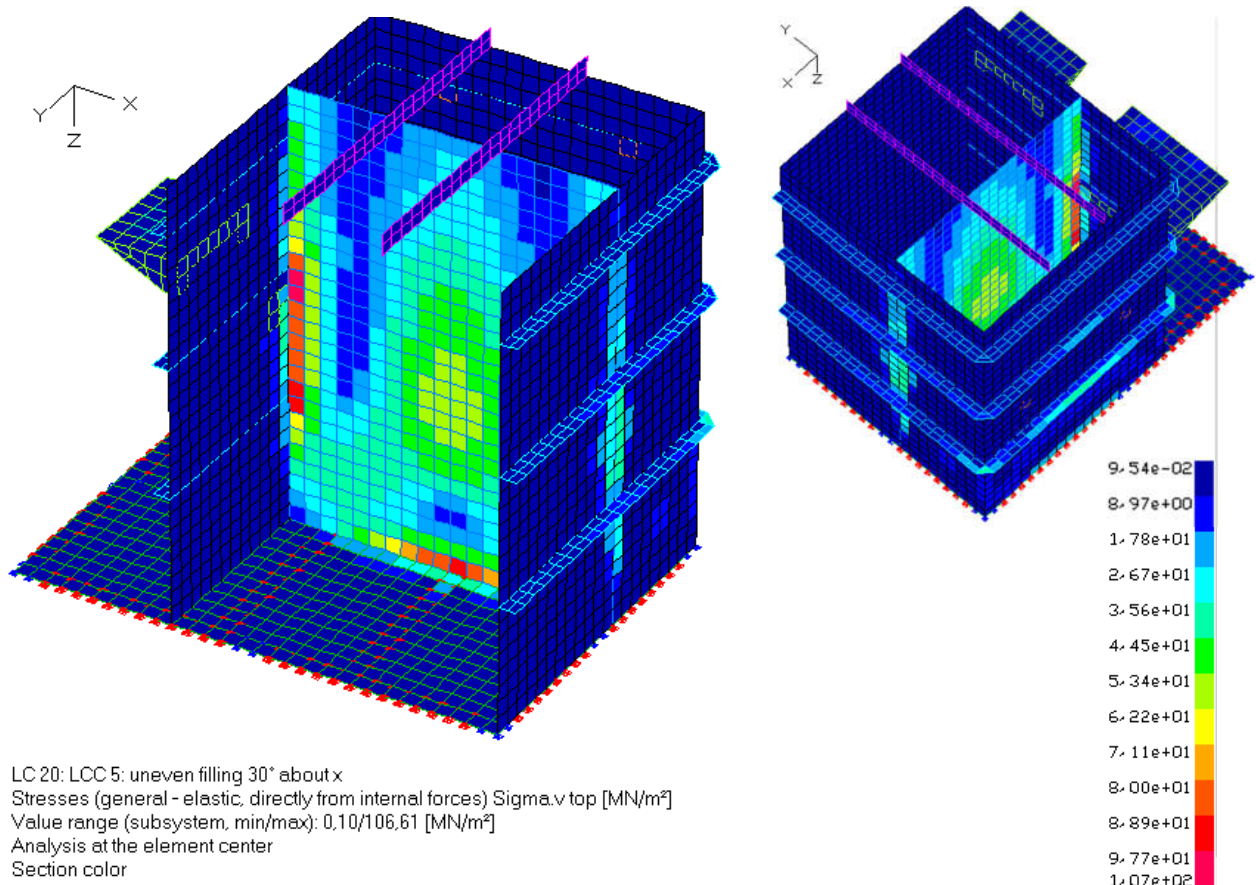
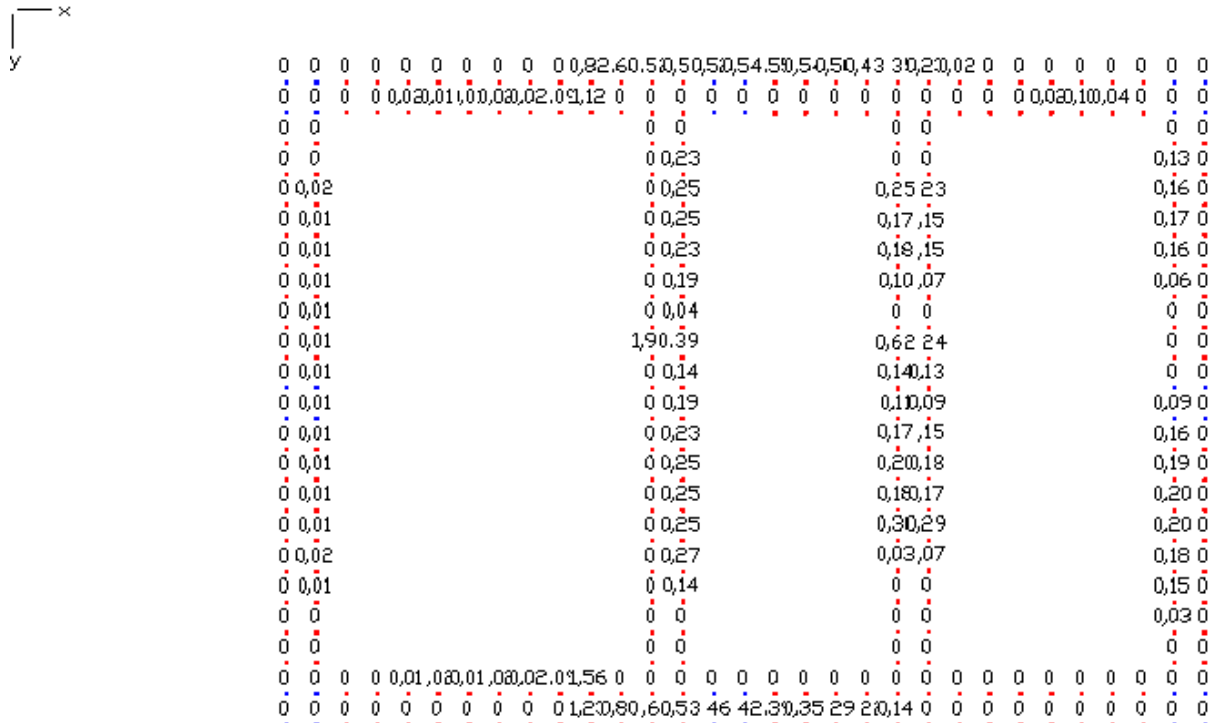


Figure 4-15: LCC 5: Maximum equivalent stresses due to liquid pressure (uneven filling) & dead load at roll angle 30° about the x-axis: 107 MN/m² < 172 MN/m² ✓

4.5.3 Anchorage

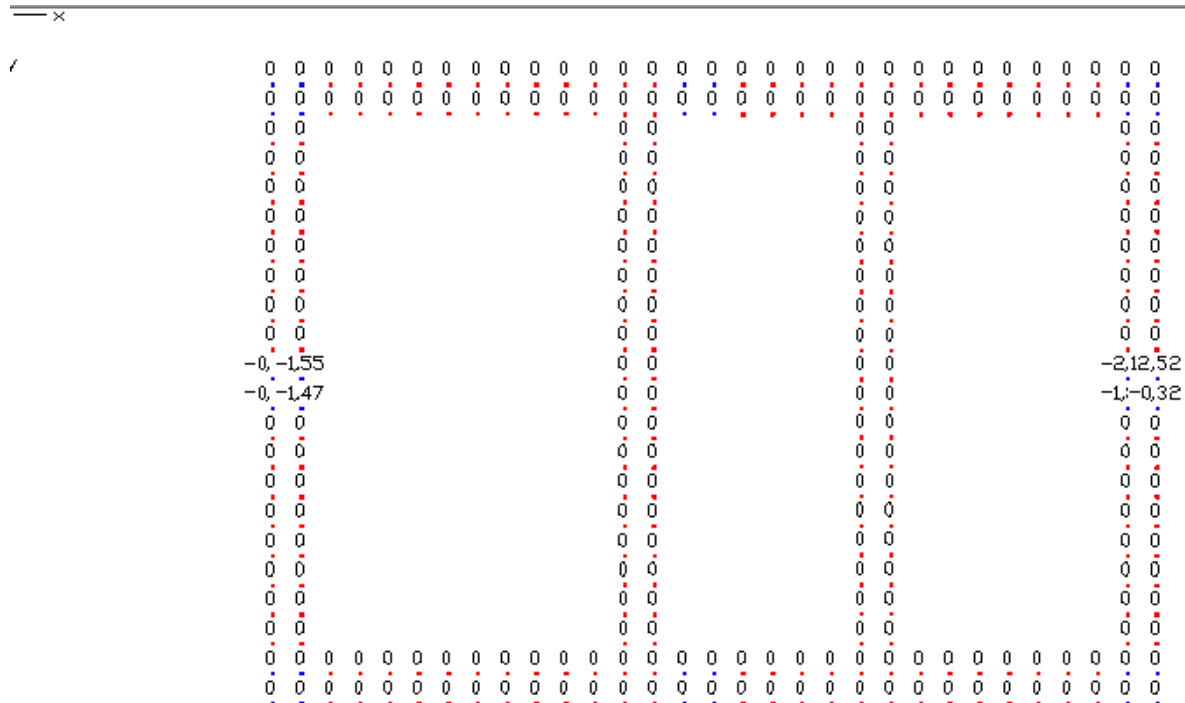


LC 13: LCC 3: full; 30° about y-axis

Support reactions in the local system Rz(l) [kN]

Sum in the global system Rz(g) = 27,42 [kN]

**Figure 4-16: Maximum vertical reaction force
(load case combination 3: full; 30° about y-axis)
No vertical tension forces; this results from vertical (downward) liquid pressure that is higher than the tension force due to overturning moment**

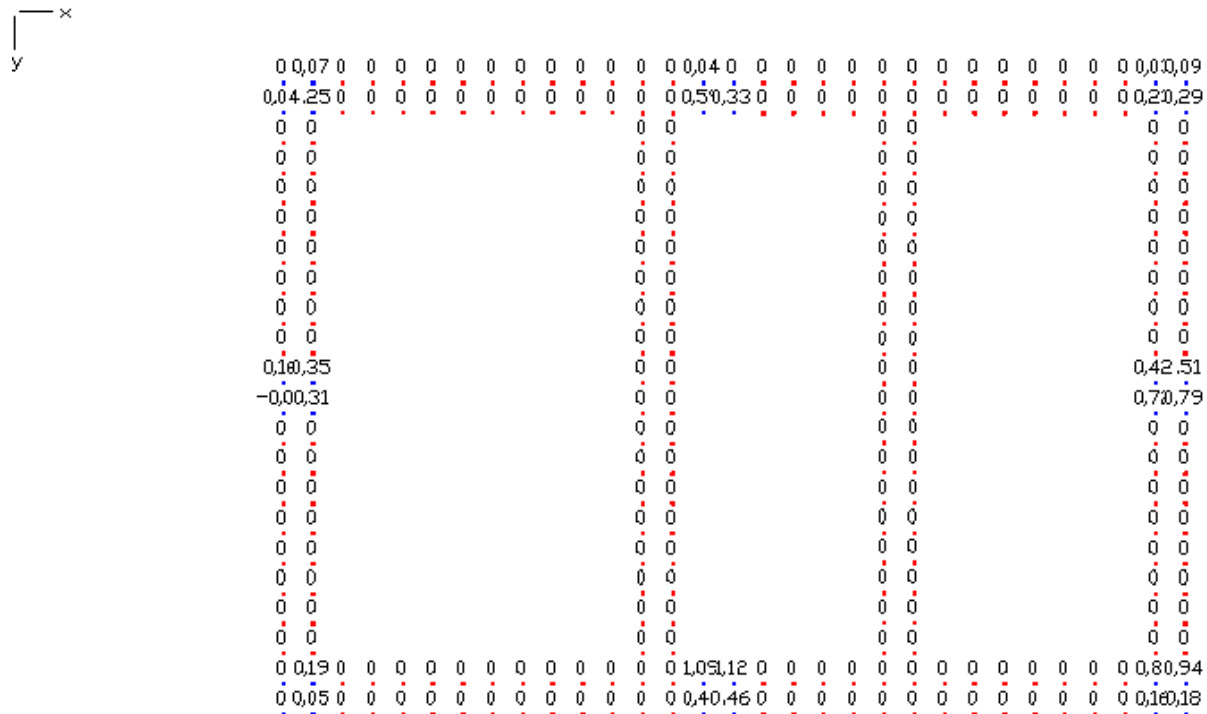


LC13: LCC 3: full; 30° about y

Support reactions in the local system $P_x(l)$ [kN]

Sum in the global system Px(g) = -8,52 [kN]

Figure 4-17: Maximum horizontal reaction force in global x-direction
 (load case combination 3: full; 30° about y-axis)
 Maximum horizontal load on screw: 4,8 kN



LC11:LCC1:full; 30° about x

Support reactions in the local system Ry(l) [kN]

Sum in the global system Ry(g) = 10,58 [kN]

Figure 4-18: Maximum horizontal reaction force in global y-direction
 (load case combination 1: full; 30° about x-axis)
 Maximum horizontal load on screw: 2.4 kN

The maximum horizontal (shear) force to be taken on by screw (conservative combination of maximum forces in x- and y-direction regardless of load case combination) results to:

$$F_{h,max} = \sqrt{4,8^2 + 2,4^2} = 5,4 \text{ kN}$$

Additionally, a minimum vertical tension force of 10 kN per screw / bolt should be considered for the dimensioning of the anchorage.

4.5.4 Stability

Additionally to the requirements of CFR 33 §59.107, linear buckling analyses were carried out for all load cases to determine the stability safety of the device. In all cases the buckling load factor was determined to be far beyond the limit value of 1.0. The following figures show the relevant buckling eigenmodes and the corresponding load factors.

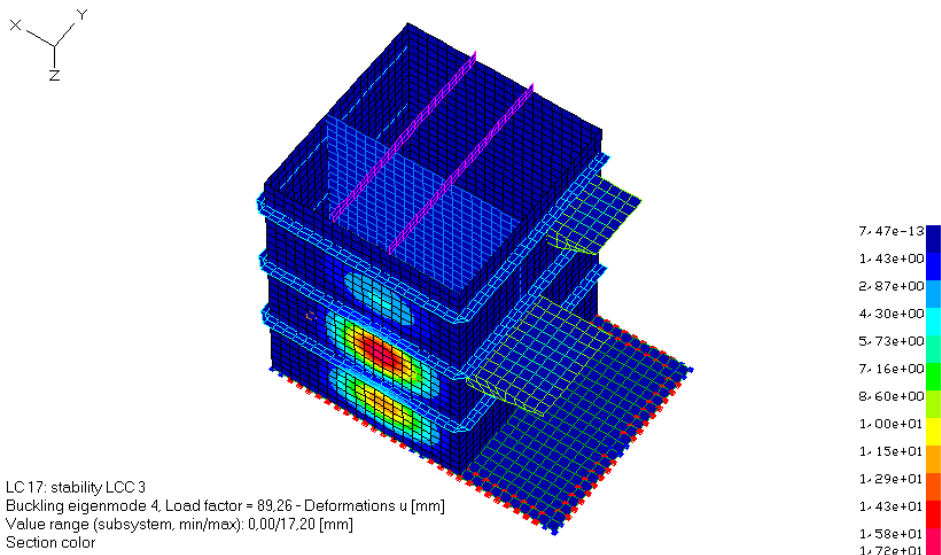


**Figure 4-19: Relevant buckling eigenmode for left wall
loading according to load case combination 3: full; roll 30° about y-axis
load factor 89 > 1 ✓**

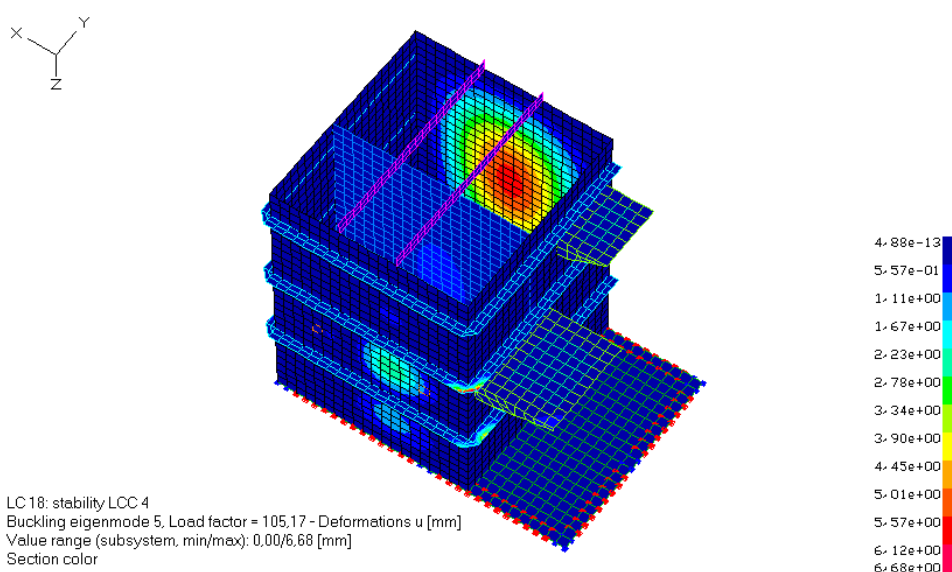


**Figure 4-20: Relevant buckling eigenmode for right wall
loading according to load case combination 4: full; roll 0° about y-axis
load factor 105 > 1 ✓**

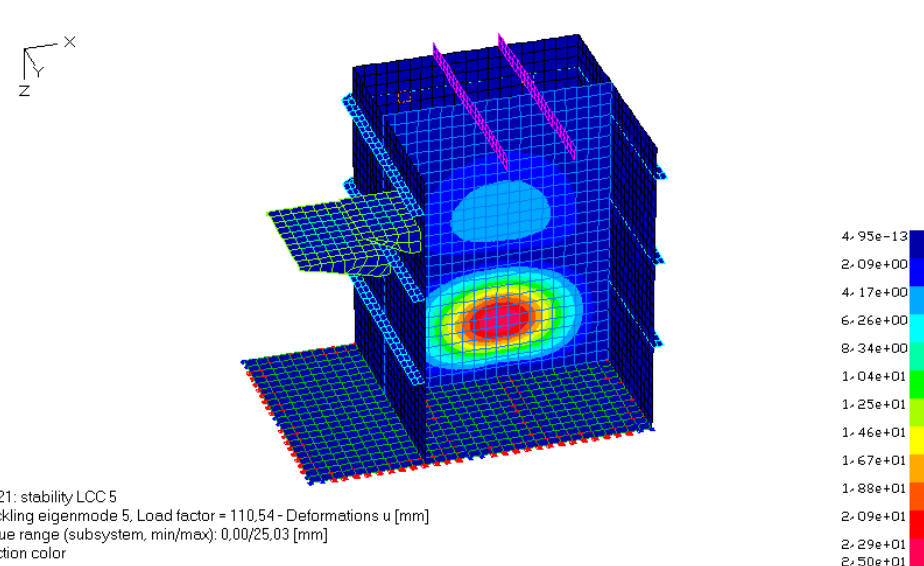


Figure 4-21: Relevant buckling eigenmode for internal wall loading according to load case combination 5: uneven filling; roll 30° about x-axis; load factor 111 > 1 ✓

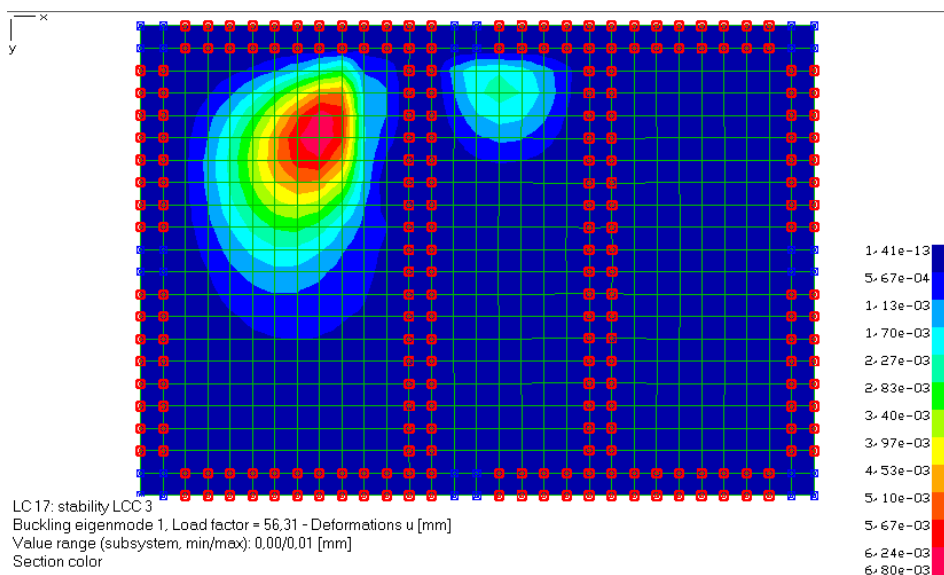


Figure 4-22: Relevant buckling eigenmode for bottom shell loading according to load case combination 3: full; roll 30° about y-axis load factor 56 > 1 ✓

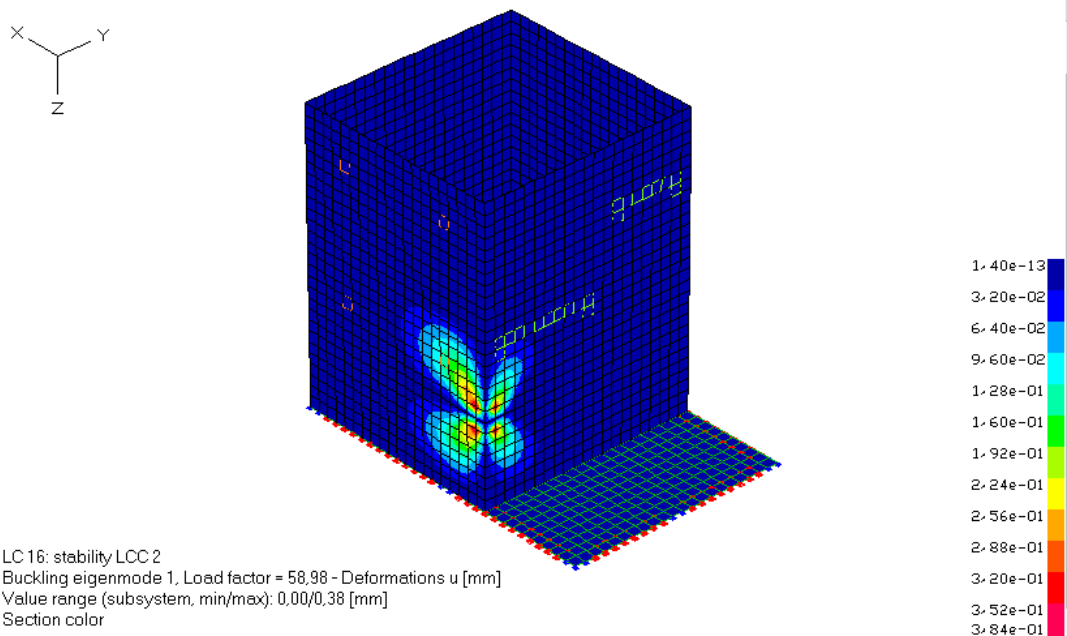


Figure 4-23: Relevant buckling eigenmode for front shell loading according to load case combination 2: full; roll 0° about x-axis load factor 59 > 1 ✓

5. Summary

The scope of this report was the investigation and verification of the PIA test plant produced by Gertsen&Olufsen, Hørsholm, Denmark regarding shock test and rolling test on a numerical/ analytical basis as alternative to the experimental test procedure of 33 CFR §159.105 and §159.107.

Conclusion on shock test

The relevant loading and the equivalent stresses due to a sinusoidal acceleration of 10 g within a duration of 25 ms were determined combining shock spectra analyses on single degree of freedom systems (depicting the externally mounted heavy components) and finite element analyses of the tank shell (see section 3).

It was proven that the resulting equivalent stresses due to shock loading are smaller than the allowable stresses (see section 3.3.2).

Further, it was verified that occurring loads onto the component shelves are safely transferred to the tank shell provided that the shelves are welded to the shell with a continuous weld of at least 3mm on both sides of the shelves (see section 0). The manufacturer is responsible for executing a minimum weld thickness of 3mm on both sides of the shelves.

Conclusion on roll test

The relevant loading and the equivalent stresses due to rolling action of the device were determined based on kinematic considerations and in accordance with the MSD Laboratory Technical Information Sheet no. 5 [2] (see section 4.2).

Five load case combinations were considered to investigate the response to rolling about the x-axis (30° angle + 0° angle) and the y-axis (30° angle + 0° angle) as well as the effect of uneven filling (30° about the x-axis; one tank empty) (see section 4.4).

It was proven that the resulting equivalent stresses due to rolling action are smaller than the allowable stresses (see section 4.5.2).

The maximum loading of the anchorage of the device was determined for all load cases and must be safely transferred to the ground / ship by adequately dimensioned and tightly fastened screws.

Additionally to the requirements of CFR 33 §59.107, the safety against buckling was proven by linear buckling analyses (see section 4.5.4).

General remarks

According to Gertsen&Olufson the internal wall between the two containers is not structurally connected to the top of the tank. In order to assure leak tightness in case of rolling the gap between internal wall and top should be sealed. The maximum horizontal deformation of the upper edge of the internal wall was calculated to 2,35 mm (in load case combination 1 – 30° roll about x-axis). The seal must be able to bear such deformations.

The shelf for the dosing pump and the chemical can was not specified by the manufacturer. It was assumed rigid for the transfer of shock and roll loads. The manufacturer must ensure that the shelf is able to bear and safely transfer shock acceleration of the supported components and that pump and can are tightly attached to the shelf.

The entire device must be safely anchored at the floor / ship. Minimum anchor forces for each screw / bolt are given in section 4.5.3.

Fatigue due to continuous loading was not within the scope of this investigation.

The operability of the electrical control panel itself must be confirmed by the producer of the panel or verified by the shock test procedure described in 33 CFR §159.105 and is not within the scope of this investigation.

Herzogenrath, 15.06.2016



Dr.-Ing. B. Holtschoppen



Prof. Dr.-Ing. C. Butenweg

Udvikling af bedre og mere energieffektive renseanlæg med næringsstoffjernelse

Formålet med projektet er at undersøge markedet for avanceret spildevandsrensning off-shore og bringe ny teknologi ind i det nuværende Gertsen og Olufsen produkt til off-shore spildevandsrensning, for derigennem at kunne opfylde de skærpede krav til spildevandsrensning, som træder i kraft fra 2016. De nye krav vil, foruden de eksisterende krav til organiskstof og mikroorganismer, også stille krav til næringssaltsfjernelse.



Miljøstyrelsen
Haraldsgade 53
2100 København Ø

www.mst.dk